

This is to certify that the

thesis entitled

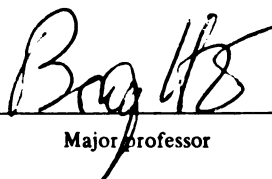
DISPERSION AND INSTABILITY CHARACTERISTICS OF SOLID-  
STATE CARRIER WAVES IN MICROWAVE INTEGRATED SYSTEMS

presented by

Chang Eon Kang

has been accepted towards fulfillment  
of the requirements for

Ph.D. degree in Electrical Engineering

  
Major professor

Date February 5, 1974

DISPERSION  
CARRIER

The in  
is studied in  
characteristic  
Maxwell's, co  
in a general  
investigated  
interaction i  
the slow circ  
of interaction  
two adjacent  
the carrier e  
in solids are

In the  
a hydrodynam  
motion. The  
thickness, ar  
general dispe  
finite semico  
non-trivial s

## ABSTRACT

### DISPERSION AND INSTABILITY CHARACTERISTICS OF SOLID-STATE CARRIER WAVES IN MICROWAVE INTEGRATED SYSTEMS

by

Chang Eon Kang

The interaction of solid-state carrier waves in semiconductors is studied in order to predict the wave instabilities and wave characteristics of propagating modes. The analysis is based on the Maxwell's, continuity, and Boltzmann transport equations, and is developed in a general manner. Here, two models of wave interactions are mainly investigated in the frequency range of  $1 \sim 10$  GHz: the first model of interaction is obtained between a carrier stream in semiconductors and the slow circuit waves guided by meander-tape line, and the second model of interaction is obtained due to velocity-modulated carrier waves in two adjacent streams propagated in the same direction. By introducing the carrier effective mass and collision frequency, the scattering effects in solids are taken into account.

In the interaction of the carrier stream with rf circuit waves, a hydrodynamic model is adopted to describe the behavior of the carrier motion. The effects of diffusion, insulator thickness, semiconductor thickness, and the substrate material are included in the analysis. A general dispersion expression of the coupled waves traveling along a finite semiconductor slab is developed in a formal way so that for a non-trivial solution of the fields the determinant of the fields matrix



must vanish. The  
net gain for ma  
continuous mean  
circuit. The i  
for a range of  
collision frequ  
Judging from th  
and the practi  
does not heavi  
fabrication an  
shows that the  
ratio play an

The fea  
is investigate  
Two stream ins  
transmission l  
equations for  
instability ch  
and doping lev  
results, which

must vanish. This analysis aims to evaluate the possibility of obtaining net gain for materials such as InSb, GaAs, Si and Ge by choosing the continuous meander-tape circuit and capacitively-coupled meander-tape circuit. The instability characteristics of the growing wave are analyzed for a range of material parameters in terms of frequency, circuit velocity, collision frequency, carrier drift velocity and actual layer thickness. Judging from the theoretical analysis varied by the material constants and the practical point of view, the best result of this type of device does not heavily depend upon materials themselves but proper design, fabrication and maximization of their drift velocities. The result shows that the collision frequency and the drift to thermal velocity ratio play an important role in the nature of the carrier wave.

The feasibility of wave amplification in the two-valley model is investigated, leading to a clearer description of Gunn instability. Two stream instability is analyzed first by establishing an equivalent transmission line and then by writing the appropriate partial differential equations for the interactions between two valleys. The dispersion and instability characteristics are obtained as a function of frequencies and doping levels. The analysis is in agreement with the experimental results, which confirm the validity of this approach.

DISPERSI

CARTE

DISPERSION AND INSTABILITY CHARACTERISTICS OF SOLID-STATE  
CARRIER WAVES IN MICROWAVE INTEGRATED SYSTEMS

By

Chang Eon Kang

A THESIS

Submitted to  
Michigan State University  
in partial fulfillment of the requirements  
for the degree of

DOCTOR OF PHILOSOPHY

Department of Electrical Engineering

1974

200

WHO D

G87902.

TO MY PARENTS

MR. AND MRS. BYUNG HYU KANG

WHO DID SO MUCH TOWARD THE COMPLETION OF THIS PROJECT

The author  
Professor, Dr.  
through his teaching  
stimulating discussion  
and research.  
Dr. J. Asmusse  
suggestions throughout

The author  
Electrical Engineering  
Division at Michigan  
Dr. G. Haddad,  
of Michigan, for  
facilities in the  
Financial support  
and the Division  
acknowledged.

Finally,  
parents for encouragement  
wife, Jung Hee for  
live and good character  
been a source of

## ACKNOWLEDGMENTS

The author would like to express his heartfelt appreciation to Professor, Dr. B. Ho for bringing the topic to the author's attention through his teaching, his interest, good humor, invaluable guidance, stimulating discussions and encouragement during this period of study and research. Thanks are also due to committee members, Dr. S. Frame, Dr. J. Asmussen, Dr. D. Nyquist and Dr. K. Chen for their guidance and suggestions through all phases of the project.

The author wants to extend thanks to Dr. D. Fisher, Professor of Electrical Engineering and Mr. J. Hoffman, Director of the Engineering Division at Michigan State University, for helpful assistance, and to Dr. G. Haddad, Director of Electron Physics Laboratory at the University of Michigan, for the permission of the use of the integrated circuit facilities in the course of the preparation of this investigation. Financial support was granted by the Department of Electrical Engineering and the Division of Engineering Research. This support is gratefully acknowledged.

Finally, an expression of immeasurable gratitude is given to his parents for encouraging him to undertake a life long education, to his wife, Jung Hee for her continuous encouragement, patience, understanding, live and good cheer, and to his children, Jeannie and Joseph for having been a source of joy.



ABSTRACT

ACKNOWLEDGMENTS

LIST OF FIGURES

LIST OF TABLES

Chapter

I. INTRODUCTION

II. PRELIMINARY CONCEPTS

2.1 Introduction

2.2 History

2.3 Physical Principles

2.4 Fundamental Concepts

2.5 Linear and Nonlinear

2.6 Negative and Positive

III. FIELD DISTRIBUTION

3.1 Introduction

3.2 Methods

3.3 Wave Equations

3.4 Boundary Conditions

3.5 Field Equations

3.6 Field Equations

3.7 Electromagnetic

IV. FIELD ANALYSIS  
OF LINEAR SYSTEMS

4.1 Introduction

4.2 Boundary

4.3 Electromagnetic

4.4 Two-Dimensional

4.5 Generalized

4.6 Formulation

4.7 Determination

4.8 Comparison

V. DISPERSION  
RELATIONS

## TABLE OF CONTENTS

	Page
ABSTRACT	
ACKNOWLEDGMENTS	iii
LIST OF FIGURES	vi
LIST OF TABLES	ix
Chapter	
I. INTRODUCTION	1
II. PRELIMINARY ANALYSIS AND THEORETICAL BACKGROUND	4
2.1 Introduction	4
2.2 Historical Observation of Wave Interaction Phenomena in Semiconductors	5
2.3 Physical Description of Mathematical Model	8
2.4 Fundamental Equations	10
2.5 Linearized Small Signal Analysis and Wave Theorems Relevant to Slow-wave Circuit	14
2.6 Negative Resistance Effects and Two Valley Instability in Solids	17
III. FIELD DISTRIBUTION IN SOLID-STATE MATERIALS	22
3.1 Introduction	22
3.2 Method of Solution and Configuration of Sample	23
3.3 Wave Equation of Charged Carriers in Solids	28
3.4 Boundary Conditions in Semiconductors	31
3.5 Field Interpretation in the Solid-State	33
3.6 Field Analysis in the Influence of Collision Effect	38
3.7 Electromagnetic Field Description for Streaming Carriers in the Absence of Collisions	40
IV. FIELD ANALYSIS OF SLOW WAVE CIRCUIT AND FORMULATION OF LINEAR EQUATIONS FOR THE COMPLETE SYSTEM	43
4.1 Introduction	44
4.2 Boundary Conditions about a Slow-wave Circuit Structure	45
4.3 Electromagnetic Field Solutions in the Slow- wave Circuit Region when the Permittivities of Two Insulating Layers are the Same	46
4.4 General Field Analysis in the Circuit Region	48
4.5 Formulation of Linear Equations and Determination of Unknown Coefficients for the Coupled System	49
V. DISPERSION AND GAIN CHARACTERISTICS OF INTERACTION BETWEEN CARRIER WAVES AND SLOW CIRCUIT WAVES	55

Chapter

- 5.1 Int
- 5.2 Dis
- 5.2
- 5.2
- 5.3 Rel
- 5.4 Wav
- 5.5 Sol
- 5.5
- 5.5
- 5.6 Gai
- 5.7 The

VI. TWO STRE

- 6.1 Int
- 6.2 For
- 6.3 Pop
- 6.4 Car
- 6.5 Cir
- 6.6 The
- 6.7 The
- 6.8 Sol
- 6.8
- 6.8

VII. DESIGN AN  
DEVICES

- 7.1 Intr
- 7.2 Effe
- 7.3 Sele
- 7.4 Desi
- 7.5 Fabr

VIII. CONCLUSIO  
MENT

BIBLIOGRAPHY  
APPENDICES

Chapter	Page
5.1 Introduction	55
5.2 Dispersion Relations for Carrier Wave Interactions	56
5.2.1 General Dispersion Relation	56
5.2.2 Dispersion Relation in a Collision Dominated Stream	61
5.3 Relations of Dispersion Characteristics and Gain	63
5.4 Wave Interaction Analysis with Numerical Method	65
5.5 Solution of Dispersion Equations for Different Materials	69
5.5.1 Continuous Type of Tape-Circuit Model	69
5.5.2 Capacitively Coupled Tape-circuit Model	74
5.6 Gain Characteristics as a Function of Collision Frequency, Circuit Velocity and Carrier Drift Velocity	77
5.7 The Functional Dependence of Device Gain Upon the Variation of Insulating-layer Thickness	82
VI. TWO STREAM INSTABILITY IN SOLIDS	85
6.1 Introduction	85
6.2 Formation of Two-valley Model	88
6.3 Population Densities of Carriers in Two-valley Model	91
6.4 Carrier Interaction in a Two-valley Semiconductor	93
6.5 Circuit Equation of Carriers in the Upper Valley	96
6.6 The Electronic Equation of the Lower Valley Carriers	96
6.7 The Dispersion Characteristic Equation in Carrier Wave Interaction	98
6.8 Solution of the Dispersion Characteristic Equation for Gunn Devices	100
6.8.1 Collisionless Analysis	100
6.8.2 General Analysis	104
VII. DESIGN AND FABRICATION CONSIDERATIONS OF PRACTICAL DEVICES	116
7.1 Introduction	116
7.2 Effect of the Insulating Layer Between Circuit and Semiconductor	117
7.3 Selection of Solid-state Materials	118
7.4 Design of Slow-wave Circuit Structure	120
7.5 Fabrication Considerations of Devices	122
VIII. CONCLUSIONS AND SUGGESTIONS FOR FURTHER DEVELOPMENT	127
BIBLIOGRAPHY	130
APPENDICES	137

## Figure

- 2.6.1 Ener  
numb
- 2.6.2 Velo  
for
- 2.6.3 Two v  
diff
- 3.2.1 One p  
wave
- 4.1.1 Sever
- 4.3.1 Geomo  
diele
- 5.2.1 Field  
confi
- 5.5.1  $f$ - $\beta$  d
- 5.5.2 Varia  
InSh
- 5.5.3  $f$ - $\alpha$  d  
mater
- 5.5.4 Compar  
insula  
semico
- 5.6.1 Gain c  
normal  
solid-
- 5.6.2 Gain c  
normal  
state
- 5.6.3 Gain vs  
solid-s
- 5.7.1 Gain ch  
insulat
- 6.1.1 A possib  
instabil

## LIST OF FIGURES

Figure		Page
2.6.1	Energy, velocity and effective mass vs. wave number for electrons in conduction band.	18
2.6.2	Velocity (or current density) vs. energy curve for voltage controlled negative resistance.	19
2.6.3	Two valley model separated by an energy difference $\Delta E$ .	20
3.2.1	One possible structure for solid-state traveling-wave amplifier	26
4.1.1	Several typical tape slow-wave structures	44
4.3.1	Geometry of the device structure with the same dielectric constant around the circuit	46
5.2.1	Field coefficients matrix of the structure configuration.	57
5.5.1	$f$ - $\beta$ diagram for a $n = 10^{14}/\text{cm}^3$ InSb sample	70
5.5.2	Variation of attenuation with frequency for a InSb sample	72
5.5.3	$f$ - $\alpha$ diagram of the growing mode for four different materials	75
5.5.4	Comparison of attenuation constants when the insulating layer between the circuit and the semiconductor exists and not exists	76
5.6.1	Gain characteristics with respect to the normalized collision frequency for several solid-state materials	79
5.6.2	Gain characteristics with respect to the normalized circuit velocity for several solid-state materials	80
5.6.3	Gain vs. normalized drift velocity for various solid-state materials	81
5.7.1	Gain characteristics for various values of an insulating layer thickness ( $d$ )	83
6.1.1	A possible configuration for two-stream instability devices	87

Figure

- 6.2.1 Simplified model of GaAs
- 6.2.2 Theoretical results with
- 6.4.1 An overview of the valley to the
- 6.8.1 f- $\beta$  of GaAs upper
- 6.8.2 f- $\beta$  of GaAs upper
- 6.8.3 f- $\beta$  of sample stream
- 6.8.4 Variation of four v. sec cm<sup>3</sup>
- 6.8.5 Attenuation where
- 6.8.6 Attenuation  $\epsilon_r =$
- 6.8.7 f- $\beta$  of sample constant
- 6.8.8 f- $\beta$  of sample
- 6.8.9 f- $\beta$  of sample
- 6.8.10 Variation of n=10 constant
- 6.8.11 Variation of n=10 valley

Figure		Page
6.2.1	Simplified energy band structure of two valley model. The numerical values are taken from a GaAs sample	89
6.2.2	Theoretical and experimental drift velocity with electric field of GaAs sample	92
6.4.1	An over-all equivalent representation of two-valley models. A displacement current is flown to the circuit	95
6.8.1	f- $\beta$ diagram of four waves for a $n=10^{13}/\text{cm}^3$ GaAs sample when the collision frequency of an upper stream is neglected	101
6.8.2	f- $\beta$ diagram of four waves for a $n=10^{14}/\text{cm}^3$ GaAs sample when the collision frequency of an upper stream is neglected	102
6.8.3	f- $\beta$ diagram of four waves for a $n=10^{15}/\text{cm}^3$ GaAs sample when the collision frequency of an upper stream is neglected	103
6.8.4	Variation of attenuation with frequency for four waves where $v_u=0$ , $E=7 \text{ KV/cm}$ , $\mu_l=5000 \text{ cm}^2/\text{v.sec}$ , $\mu_u=100 \text{ cm}^2/\text{v.sec}$ , $\epsilon_r=12.5$ , and $n=10^{13}/\text{cm}^3$	105
6.8.5	Attenuation vs. frequency curves of four waves where $\epsilon_r=12.5$ , $v_u=0$ , and $n=10^{14}/\text{cm}^3$ .	106
6.8.6	Attenuation vs. frequency of four waves where $\epsilon_r=12.5$ , $v_u=0$ , and $n=10^{15}/\text{cm}^3$ .	107
6.8.7	f- $\beta$ curves of four waves for a $n=10^{13}/\text{cm}^3$ GaAs sample when all collision frequencies are considered	108
6.8.8	f- $\beta$ curves of four waves for a $n=10^{14}/\text{cm}^3$ GaAs sample when collision frequencies are considered.	109
6.8.9	f- $\beta$ curves of four waves for a $n=10^{15}/\text{cm}^3$ GaAs sample when collision frequencies are considered.	110
6.8.10	Variation of attenuation with frequency for a $n=10^{13}/\text{cm}^3$ GaAs device when collisions are considered.	111
6.8.11	Variation of attenuation with frequency for a $n=10^{14}/\text{cm}^3$ GaAs sample when the lower and upper valley collision are considered.	112



Figure

6.8.12 Vari  
a n=  
are c

7.4.1 A me

7.5.1 Slow  
stat

D.1 Flow

Figure		Page
6.8.12	Variation of attenuation with frequency for a $n=10^{15}/\text{cm}^3$ GaAs device when all collisions are considered	113
7.4.1	A meander-tape line	118
7.5.1	Slow-wave circuit and test structure of a solid-state traveling-wave amplifier	121
D.1	Flow chart for computer solutions of a polynomial	149

Table

5.4.1 Typi  
mater

7.2.1 Diele

Appendix B

## LIST OF TABLES

Table	Page
5.4.1 Typical numerical values for several solid-state materials	67
7.2.1 Dielectric permittivity	118
Appendix B Table of electromagnetic field solutions for all regions	141

The cla  
amplification  
interelectrode  
In order to c  
brothers prop  
electron bunc  
operation the  
cavity gap, h  
modulation an

The sch  
wave amplifie  
a great deal  
to potential  
devices. At p  
generation or  
because it sho  
although the e  
power operatio  
consideration,  
stage of taking  
future are expe  
In this t  
several solid-s

## CHAPTER I

### INTRODUCTION

The classical electron vacuum device in the generation or amplification of high frequency signals has many drawbacks, such as the interelectrode capacitance and long transit time between electrodes. In order to overcome such deleterious effects the Heils and the Varian brothers proposed the scheme of velocity modulation, in which the electron bunching process produces the signal. However, in the klystron operation the electron beam interacts with the rf field over a short cavity gap, hence the electric field must be intense to provide proper modulation and the frequency band is rather narrow.

The scheme, extended interaction space, is the wellknown traveling-wave amplifier or backward-wave oscillator. In the past several years, a great deal of research effort in solid-state physics has been devoted to potential application between electron beam devices and solid-state devices. At present the solid-state device has some merits in the generation or amplification of microwave and millimeter-wave signals because it shows excellent noise figure and high frequency response, although the electron beam device has no competition in considering high power operation. Furthermore, especially due to cost, weight and space consideration, some solid-state sources for applications are in the stage of taking over. Besides, many potential applications in the future are expected in various aspects.

In this thesis the properties of carrier-wave interactions in several solid-state materials will be investigated — mainly concerning

two types of  
carrier wave

Two st  
which explai  
some similar  
beams in a v  
physical ins  
coupling, th  
in electron  
instability

Anothe  
to a driftin  
line on the  
solid-state  
meander type  
stream of a  
relation is  
are determin  
some crucial  
and the way  
explored, nor  
surface charg  
its finite di  
dispersion re

Wave pro  
theoretically,  
possibly some

two types of interactions, namely, the two stream instability and carrier wave interaction with the circuit.

Two stream instability in solids could cause wave amplification, which explains the Gunn instability mechanism. Possibly there exist some similarities between the streams of carriers in solids and electron beams in a vacuum. Therefore, in order to understand the important physical insights of the phenomena such as energy conversion and wave coupling, the concept of wave interaction, which has been successful in electron beam devices, will be used in describing the various instability characteristics in solid-state materials.

Another interaction is when a slow electromagnetic wave is coupled to a drifting stream of carriers by depositing the slow-wave meander line on the semiconductor slab with integrated circuit technology. The solid-state traveling-wave amplifier is based on the principle that a meander type of slow-wave circuit is suitably coupled to the carrier stream of a negative kinetic power. Conventionally, the dispersion relation is first formulated and then the instability characteristics are determined by examining its propagation constant. In such approaches, some crucial aspects of the interactions such as the limiting conditions and the way of finding the dispersion relation were neither fully explored, nor rigorous enough. For example, the reflected waves and surface charges on the semiconductor were totally ignored in spite of its finite dimension. A formal and straightforward way of deriving the dispersion relation is presented here.

Wave propagation in solid-state materials will be examined theoretically, then solved by a computer technique. From the solutions, possibly some instabilities can be obtained.



In CH  
preliminary  
device stru  
in semicond  
V presents  
computer so  
function of  
collision f  
instability  
experimental

Chapte  
devices. Th

Finall  
Chapter VIII

In Chapter II, the literature survey for solid-state devices and preliminary analysis are presented with descriptive explanations of the device structure. Electromagnetic field solutions of wave propagation in semiconductor and circuit are derived in Chapter III and IV. Chapter V presents the characteristic equations and gain expressions, and the computer solution of gain and dispersion solution are plotted, as a function of the carrier drift velocity, circuit wave velocity and collision frequency. Chapter VI is devoted to investigating two stream instability and the theoretical results of gain are compared with the experimental results.

Chapter VII presents the design criteria of solid-state microwave devices. The design data of experimental devices are illustrated.

Finally, a discussion of results and conclusions is given in Chapter VIII, together with suggestions for further study.

## 2.1 Intro

Before

might be v

background

This chapter

required b

matical mod

Section 2.2

action theo

is concerne

the problem

will be treat

equations an

small signal

equations ca

structures an

significantly

Finally

two valley mo

phenomena, bu

intense inter

from junction

power output f

## CHAPTER II

### PRELIMINARY ANALYSIS AND THEORETICAL BACKGROUND

#### 2.1 Introduction

Before getting started with the development of the main theory it might be well not only to understand the theoretical and historical background of the study but also to establish directions for the research. This chapter contains what is believed to be the most fundamental details required by the following chapters. Some basic equations and a mathematical model that will be used in subsequent studies are discussed. Section 2.2 is mainly devoted to the literature review of wave interaction theory in the solid-state and semi-metal materials. Section 2.3 is concerned with the mathematical description of our model in attacking the problem. Descriptive explanations and developments of the model will be treated within the context of this model configuration. Maxwell's equations and Boltzmann's equation are introduced in Section 2.4 and small signal analysis is employed in Section 2.5 so that the nonlinear equations can be linearized. Several theorems pertaining to periodic structures and wave propagation are also explained; these will be significantly helpful in understanding the main problem.

Finally, the basic theory of negative resistance effects and the two valley model are reviewed in Section 2.6. Of several physical phenomena, bulk effects within solid-state materials have received intense interest. Devices employing these phenomena are quite different from junction devices, such as transistors, and one would expect greater power output from bulk effect devices since the interaction regions are

one or two  
are two ty  
instabilit  
cal work o  
analysis a  
bulk effec

## 2.2 Historical conduct

In the  
suggested t  
ogously be  
was not the  
semimetals  
confined to  
prediction t  
solids with  
Konstantinov  
magnetic fie

After  
experimental  
1961 by Bower  
fore, is not  
plasma from t  
convective an

In 1963  
periodic osci  
This was compl

one or two orders of magnitude larger in dimension. In solids there are two types of bulk effects, negative resistance and two valley instability which are explained in Section 2.6. However, the theoretical work on these effects has not been well developed. Two stream analysis and a new type of wave interaction mechanism based on these bulk effects will be investigated utilizing the contents of this chapter.

## 2.2 Historical Observation of Wave Interaction Phenomena in Semiconductors

In the 1960's a great deal of interest in solid-state plasma suggested the possibility that the gaseous plasma theory could analogously be applied to the solid-state materials but a clear description was not then possible. The solid-state plasma exists in semiconductors, semimetals and metals commonly — being a gas of conduction electrons confined to the volume of the specimen. Interest began with the prediction that certain electromagnetic waves would be propagated in solids with relatively little attenuation. The idea was proposed by Konstantinov [K01] and independently by Aigrain [AI1] in applying dc magnetic fields to certain semiconductors.

After first reports of wave propagation in semiconductors, an experimental observation was successfully carried out with sodium in 1961 by Bowers, et al [B01]. The problem in solid-state plasma, therefore, is not how to generate a plasma but how to disturb the existing plasma from thermal equilibrium and induce instabilities, both convective and absolute.

In 1963 Gunn [GU1], [GU2] observed that, with GaAs and InP, a periodic oscillation could be obtained at a threshold electric field. This was completely different from previous negative resistance effects

which occur  
measured by  
capacitive  
moving high

Kromer  
properties  
differentia  
also insist  
differentia  
field on wh  
states. Th  
incremental  
been propos

Ridley  
negative mol  
dynamic argu  
single layer  
discontinuit  
controlled r  
another type  
junction and  
had verified  
responsible  
GaAs [BL2],  
[BE2] treat  
McCumb  
relevant tra

which occurred in p-n junction semiconductor devices. The velocity was measured by a heterodyne detection system, removing any possibility that capacitive probe experiments [GU2] measured something other than a moving high field region in bulk GaAs devices.

Kromer [KR4], [KR5] proposed in late 1964 that the observed properties of the Gunn effect [GU1], [GU2] could be explained by a differential negative conductivity. The negative mass amplifier was also insisted upon earlier by Kromer [KR2], [KR3] in 1959. The differential negative mobility changes sign at the critical electric field on which sufficient electrons are transferred to low mobility states. This is caused by a decrease in carrier drift velocity with an incremental increase in electric field. Actually this mechanism had been proposed three years earlier by Ridley and Watkins [RI1].

Ridley [RI2] extended the earlier analysis [RI1] of differential negative mobility of the voltage controlled type by general thermodynamic arguments. He neglected carrier diffusion and assumed that a single layer of mobile charge would accumulate or be removed from the discontinuity in the longitudinal electric field. While the voltage controlled negative resistance occurs in bulk Gunn effect devices, another type of current controlled negative resistance may occur in p-n junction and impact ionization devices [GU1], [GU2]. Several workers had verified experimentally that the transferred electron mechanism is responsible for the voltage controlled negative conductance observed in GaAs [BL2], [FO1], [GI1], [HI2], [HU4], [RO1]. Additionally, Betjemann [BE2] treated temporal effects on carrier mobility.

McCumber and Chynoweth [MC1] undertook the solution of the relevant transport nonlinear equations for bulk GaAs by numerical



methods.

satellit

Maxwelli

amplifica

and exper

several a

[K03], [K

[T01]. N

mechanism

that an e

conduction

conduction

In t

Pierce [PI

interactio

requiremen

model.

Thim

stable, lin

GaAs device

carrier den

Recent

instabilitie

which has be

[ST1] — ana

transmission

methods. They assumed that the relative population of the central and satellite conduction band valleys was given instantaneously by a Maxwellian distribution with a single electron temperature. Microwave amplification and negative conductance have been discussed theoretically and experimentally for materials such as GaAs, InP, InSb, and CdTe by several authors — [BL3], [BL4], [HA2], [HA3], [HA5], [HE1], [HI2], [KO3], [KR5], [LA1], [LO1], [MA1], [NA1], [PE1], [PI1], [RI3], [SA2], [TO1]. No one, however, has clearly justified the transferred electron mechanism in semiconductors. It is very obvious quantum mechanically that an electron is transferred from a high mobility, low mass, conduction sub-band of low energy valley to a low mobility, high mass, conduction sub-band of high energy valley when the excitation is given.

In this work we adopt a similar approach to the method used by Pierce [PI2] for the traveling-wave tube amplifier where the mutual interactions between beam and circuit are subjected to a self consistency requirement to explain the new interaction mechanism of the two valley model.

Thim and Barber [TH1] demonstrated that it is possible to achieve stable, linear and comparatively high microwave amplification in bulk GaAs devices. The devices tested had  $n\ell = 2 \times 10^{12} / \text{cm}^2$  where  $n$  is carrier density and  $\ell$  active length.

Recently Ho [HO1], [HO2], [HO3] attempted to describe the various instabilities in solid-state plasmas by the concept of wave interaction, which has been successfully used in electron beam devices [RA1], [SE1], [ST1] — analyzing the problem by both the coupled mode approach and transmission line analog [FU1].

The  
conductors  
[CO1], [GA1]  
power carrier

Soly  
substituting  
carrier in  
explanation  
ultrasonic  
industry has  
[DE2], [ED1]  
[SA1], [SA2]  
transverse s  
of dc longitud

### 2.3 Physical

In des  
microscopic o  
scopic treatme  
Boltzmann equa  
mechanically.  
particle syste  
be dealt with  
transport equat

Although  
long wavelength  
mathematically  
model to make t

The amplification of acoustic waves in piezoelectric semi-conductors such as CdS has been analyzed by many research workers [BU4], [CO1], [GAL], [HA1], [HU1], [HU2], [IN1], [KR1], [LO1], [MI1]. Kinetic power carried by carrier waves was given by Vural and Bloom [VU2].

Solymer and Ash developed [SO1] a one dimensional analysis by substituting the electron beam in a traveling-wave tube for the drifting carrier in a semiconductor. Sumi [SU1], [SU2] treated the theoretical explanation of solid-state traveling-wave amplifier by comparing it to ultrasonic wave amplification. Even though the growth of semiconductor industry has many workers concentrating on this type of research [DE1], [DE2], [ED1], [EN1], [ET1], [FU2], [HI1], [KO1], [MU1], [NE2], [PI1], [SA1], [SA2], [VU1], a successful result has not been reported. The transverse solid-state device has also been studied with the application of dc longitudinal magnetic fields [BA1], [BO2], [HU3], [TU1].

### 2.3 Physical Description of Mathematical Model

In describing any physical phenomenon on some object, either a microscopic or a macroscopic approach is in general used. The microscopic treatment, which uses Maxwell's equations with the microscopic Boltzmann equation, puts emphasis on each individual particle quantum mechanically. On the other hand, the macroscopic approach treats the particle system collectively. That is, a large number of particles can be dealt with statistically, using the same Maxwell's equation with the transport equation.

Although the same result from both treatments is obtained in the long wavelength range, the first approach is usually much more difficult mathematically and requires serious physical restriction be placed on the model to make the problem tractable.

In a  
self-create  
characteris  
determined  
appropriate  
should be in  
scopic attac

The b  
parameters,  
collision fr  
phenomenolog  
wave and elec  
the charged s  
Also, in the  
excitations w

The int  
solids is take  
effect of carr  
carrier effect  
that the semic  
carriers due to  
"source" or "si

Furtherm  
larger than the  
hydrodynamically

In a semiconductor a large number of carriers interact with their self-created or externally applied electromagnetic field or both. The characteristics and behavior of such a system are experimentally determined by the average behavior of the ensemble. Therefore, the appropriate theoretical model description may be statistical and it should be in general a quantum-statistical description. The macroscopic attack of the hydrodynamic model will be used throughout.

The behavior of the hydrodynamic model is characterized by several parameters, such as mean velocity  $v$ , mean plasma frequency  $\omega_p$ , mean collision frequency  $\nu$  and pressure  $p$  (or mean thermal velocity  $v_t$ ). The phenomenological expressions describing the interaction of the circuit wave and electromagnetic wave can be obtained combining the equation of the charged stream of Maxwell's equations, with boundary conditions. Also, in the model the dispersion relations of the medium for different excitations will be derived.

The interaction of carriers with lattice and thermal vibration in solids is taken into account in the model by including the collision effect of carriers,  $\nu = \frac{1}{\tau}$ , and the environmental effect by considering carrier effective mass,  $m^* = \hbar^2 \left( \frac{d^2 E}{dk^2} \right)^{-1}$ , in the model. It is assumed that the semiconductor is heavily doped such that the change in number of carriers due to generation of recombination, usually referred to as "source" or "sink" terms, can be neglected.

Furthermore, the wave length of any disturbance is comparatively larger than the Debye length,  $\lambda_D$  so that one may treat the electron stream hydrodynamically.

## 2.4 Fun

W

field  $\vec{B}$

and time

through.

Si

density  $\rho$

intensity

it is nec

the solid-

equations,

are needed

all chapte

dimensions

Maxw

$\nabla \times$

$\nabla \times$

$\nabla \cdot \vec{E}$

$\nabla \cdot \vec{B}$

If th

where  $\mu$  is t.

all vector qu

In add

continuity eq

and charge den

## 2.4 Fundamental Equations

When the electric field  $\vec{E}(\vec{r}, t)$  is applied, it builds a magnetic field  $\vec{B}(\vec{r}, t)$  and charge density  $\rho(\vec{r}, t)$  which are functions of position and time. Simultaneously, a current with density  $\vec{J}(\vec{r}, t)$  will flow through.

Similarly, a charged carrier in solid-state possesses a charge density  $\rho(\vec{r}, t)$ . These densities will produce an electric field intensity  $\vec{E}(\vec{r}, t)$  and a magnetic field intensity  $\vec{H}(\vec{r}, t)$ . Therefore, it is necessary to interrelate all quantities in the rf circuit and in the solid-state. In order to describe the relationship, Maxwell's equations, continuity equation, force equation and Boltzmann's equation are needed. Conveniently, M.K.S. rationalized units are used throughout all chapters except for describing carrier densities and small sample dimensions.

Maxwell's equations are given by:

$$\nabla \times \vec{E} = - \frac{\partial \vec{B}}{\partial t} \quad (2.4.1)$$

$$\nabla \times \vec{H} = \vec{J} + \frac{\partial \vec{D}}{\partial t} \quad (2.4.2)$$

$$\nabla \cdot \vec{D} = 0 \quad (2.4.3)$$

$$\nabla \cdot \vec{B} = 0 \quad (2.4.4)$$

If the medium is isotropic, the B and E field vectors become:

$$\vec{B} = \mu \vec{H} \quad (2.4.5)$$

$$\vec{D} = \epsilon \vec{E} \quad (2.4.6)$$

where  $\mu$  is the permeability and  $\epsilon$  is the permittivity of the medium and all vector quantities are functions of space and time.

In addition, the carrier and rf waves are related by the continuity equation and the equation relating current density, velocity, and charge density:



where  $\vec{v}$  is

Not

due to den

however, w

(electrons

The

where  $q$  and

Performing

are veloci

electron s

In

by:

Therefore,

devices as

provided t

The

to the equa

where  $v_i$ ,  $v$

attachment

which reduc

$$\nabla \cdot \vec{J} + \frac{\partial \rho}{\partial t} = 0 \quad (2.4.7)$$

$$\vec{J} = \rho \vec{v} \quad (2.4.8)$$

where  $\vec{v}$  is velocity of particle.

Note that charge density  $\rho$  and current density  $\vec{J}$  generally are due to densities of electrons and holes. Only heavily doped semiconductors, however, will be used for the devices here, therefore one type of carrier (electrons here) will be considered.

The Lorentz force equation is:

$$\frac{d\vec{v}}{dt} = \frac{q}{m^*} (\vec{E} + \vec{v} \times \vec{B}) \quad (2.4.9)$$

where  $q$  and  $m^*$  are the charge and effective mass of a particle respectively. Performing the analysis in Eulerian variables, the dependent variables are velocity, charge and current density at a fixed position within the electron stream [B03].

In Eulerian variables the operator,  $d/dt$  in Eq. (2.4.9), is given by:

$$\frac{d\vec{v}}{dt} = \left( \frac{\partial}{\partial t} + \vec{v} \cdot \nabla \right) \vec{v} \quad (2.4.10)$$

Therefore, the Lorentz force equation can be rewritten for most microwave devices as:

$$\left( \frac{\partial}{\partial t} + \vec{v} \cdot \nabla \right) \vec{v} = \frac{q}{m^*} (\vec{E} + \vec{v} \times \vec{B}) \quad (2.4.11)$$

provided that collision and pressure terms are not involved.

The zeroth moment of the Boltzmann equation (i.e.,  $\phi = 1$ ) leads to the equation of continuity for carriers

$$\frac{\partial n}{\partial t} + \nabla_r \cdot (n\vec{v}) = n (v_i - v_a - v_r) \quad (2.4.12)$$

where  $v_i$ ,  $v_a$ ,  $v_r$  represent the collision frequency due to ionization, attachment and recombination. Usually one assumes  $v_i - v_a - v_r = 0$  which reduces Eq. (2.4.12) to a simple continuity equation.

How  
in the ga  
state and  
results i  
impuritie  
another i  
will usua  
create an  
can act t  
depends u  
and the w  
scatterin  
or even i

An  
the atoms  
aperiodic  
scatter t  
they migh  
to the th  
is, the s  
of scatte  
is the do  
perfect c

On  
permittiv

where  $R$  is

However, the collision effect in solids is more complicated than in the gas. That is one of the most important differences between solid-state and gaseous plasmas. The collision mechanism in solids which results in randomizing the carrier distribution must be associated with impurities, structural imperfections or aperiodicities of one sort or another in the crystal. The presence of an impurity atom in a crystal will usually alter the electrostatic potential in the neighborhood and create an aperiodicity in the potential field within the crystal which can act to scatter conduction electrons. This impurity scattering process depends upon the nature of the impurity atom, its ionic size, its valence, and the way it is bonded into the crystal lattice. The impurity scattering mechanism is dominant in crystals which are relatively impure, or even in very pure samples at very low temperatures.

Another scattering mechanism is due to the thermal vibrations of the atoms in a very pure material. At any given time, a slight aperiodicity of the potential exists within the crystal which serves to scatter the conduction electrons, dissipating whatever drift velocity they might have acquired from externally applied fields and retaining them to the thermal equilibrium state. Obviously the higher the temperature is, the stronger the lattice vibrations and the higher the probability of scattering per unit time become. This lattice scattering mechanism is the dominant scattering process in relatively pure and structurally perfect crystals, especially in the higher temperature ranges.

One more important scattering parameter due to the material permittivity is the dielectric relaxation frequency which is defined by

$$\nu_d = \frac{1}{\epsilon R} \quad (2.4.13)$$

where  $R$  is the resistivity of the material.

Of :

(i.e., lat

to thermal

three colli

the impurit

respectivel

equation be

$$\left(\frac{\partial f}{\partial t}\right)_c$$

where  $v = v_y$

and  $f_0$  repre

If mo

effective co

frequency  $v$

The f

where  $\langle \vec{v} \rangle =$

and  $\vec{p} =$

Assumi

where  $k$  is Bo

carriers ( $^{\circ}\text{K}$ )

$\nabla$

One may rewrit

applying Eq. (

$$\left(\frac{\partial}{\partial t}\right)$$

Of several scattering mechanisms, if three scattering factors (i.e., lattice, impurity and dielectric relaxation) operate simultaneously to thermalize the carrier distribution function, then there will be three collision frequencies,  $\nu_t$ ,  $\nu_p$ ,  $\nu_d$ , associated with the lattice, the impurity, the dielectric relaxation, scattering mechanism respectively. Under these conditions the collision term of the Boltzmann equation becomes

$$\left(\frac{\partial f}{\partial t}\right)_{\text{coll}} = (-\nu_t - \nu_p - \nu_d) (f - f_0) = -\nu (f - f_0) \quad (2.4.14)$$

$$\text{where } \nu = \nu_t + \nu_p + \nu_d \quad (2.4.15)$$

and  $f_0$  represents the equilibrium state of the distribution function  $f$ .

If more than three scattering mechanisms are involved, the effective collision frequency can be written by a single collision frequency  $\nu$  given by

$$\nu = \sum_n \nu_n \quad (2.4.16)$$

The first moment of the Boltzmann equation becomes

$$\frac{d\langle \vec{v} \rangle}{dt} = \frac{q}{m^*} (\vec{E} + \langle \vec{v} \rangle \times \vec{B}) - \nu \langle \vec{v} \rangle - \frac{1}{nm^*} \nabla_r \cdot \vec{p} \quad (2.4.17)$$

where  $\langle \vec{v} \rangle$  = average velocity of carriers

and  $\vec{p}$  = intrinsic pressure tensor

$$= nm^* \int_V (\langle \vec{v} \rangle - \vec{v}) \cdot (\langle \vec{v} \rangle - \vec{v}) f dV_x dV_y dV_z$$

Assuming that  $\vec{p}$  is isotropic and can be expressed as  $p = n\gamma kT$  where  $k$  is Boltzmann's constant,  $T$  is the absolute temperature of the carriers ( $^{\circ}\text{K}$ ) and  $\gamma = 1 \sim 3$ , then

$$\nabla \cdot \vec{p} = \nabla p = \nabla(n\gamma kT) = \gamma kT \nabla n \quad (2.4.18)$$

One may rewrite Eq. (2.4.17) by conveniently dropping the bracket  $\langle \rangle$  and applying Eq. (2.4.10).

$$\left(\frac{\partial}{\partial t} + \vec{v} \cdot \nabla + \nu\right) \vec{v} = \frac{q}{m^*} (\vec{E} + \vec{v} \times \vec{B}) - \frac{\nu_t}{n} \nabla n \quad (2.4.19)$$

where  $v_t = \sqrt{\dots}$

If an electron

$\gamma = 1$ . For  $\hbar$

appears in the

In series

the electron

where

## 2.5 Linearized Slow-wave

Uniform

exact solution

equations, a

system. All

part) and an

assumed to be

all products

Only one free

problem can be

According

quantities can

where the sub

component.

When the

in Section 2.

where  $v_t = \sqrt{\frac{\gamma kT}{m^*}}$  = mean thermal velocity of carrier.

If an electron stream is considered to be under an isothermal condition,  $\gamma = 1$ . For higher frequencies  $\gamma = 3$  since the environmental circumstance appears in the adiabatic state.

In semiconductors the resistivity can be expressed in terms of the electron charge density  $n$  and the mobility  $\mu$ .

$$R = -\frac{1}{n\mu e} \quad (2.4.20)$$

where  $\mu = \frac{e}{vm^*} \quad (2.4.21)$

## 2.5 Linearized Small Signal Analysis and Wave Theorems Relevant to Slow-wave Circuit

Unfortunately most equations are nonlinear in nature and hence, exact solutions are very difficult to obtain. In order to simplify the equations, a small signal analysis is introduced in linearizing a given system. All quantities are broken up into a dc part (or time average part) and an ac part (or time varying part). Further the ac part is assumed to be very small in magnitude compared with the dc part, so that all products of second or higher order in ac quantities can be neglected. Only one frequency needs be considered, and the general time varying problem can be solved using the Fourier transform technique.

According to the small signal simplification, all various quantities can be written in the following form:

$$\vec{A}(\vec{r}, t) = \vec{A}_0(\vec{r}) + \vec{A}_1(\vec{r}, t) = \vec{A}_0(\vec{r}) + \vec{A}_1(\vec{r}) e^{j\omega t} \quad (2.5.1)$$

where the subscript "0" refers to the dc component and "1" to the ac component.

When the above equation is substituted into the equations given in Section 2.4, one obtains the dc equations:



$$\nabla \times \vec{E}_0$$

$$\nabla \times \vec{H}_0$$

$$\nabla \cdot \vec{D}_0$$

$$\nabla \cdot \vec{B}_0$$

$$\nabla \cdot \vec{J}_0$$

$$\vec{J}_0 = \rho_0$$

$$\vec{v}_0 \cdot \nabla$$

and ac equat

$$\nabla \times \vec{E}_1$$

$$\nabla \times \vec{H}_1$$

$$\nabla \cdot \vec{D}_1$$

$$\nabla \cdot \vec{E}_1$$

$$\nabla \cdot \vec{J}_1$$

$$\vec{J}_1 = \rho_1$$

$$j\omega \vec{v}_1 + (\vec{v}_1 \times \vec{B}_0)$$

$$\vec{v}_1 \times \vec{B}_0)$$

All p

equations; t

are still no

must first b

linear natur

cases. For

$\vec{v}_0$  and  $\rho_0$  ar

point on, in

interest.

The w

described by

$$\nabla \times \vec{E}_0 = 0 \quad (2.5.2)$$

$$\nabla \times \vec{H}_0 = \vec{J}_0 \quad (2.5.3)$$

$$\nabla \cdot \vec{D}_0 = \rho_0 \quad (2.5.4)$$

$$\nabla \cdot \vec{B}_0 = 0 \quad (2.5.5)$$

$$\nabla \cdot \vec{J}_0 = 0 \quad (2.5.6)$$

$$\vec{J}_0 = \rho_0 \vec{v}_0 \quad (2.5.7)$$

$$\vec{v}_0 \cdot \nabla \vec{v}_0 = \frac{q}{m^*} (\vec{E}_0 + \vec{v}_0 \times \vec{B}_0) - \frac{v_t^2}{n} \nabla n_0 - \nabla \vec{v}_0 \quad (2.5.8)$$

and ac equations

$$\nabla \times \vec{E}_1 = -j\omega\mu\vec{H}_1 \quad (2.5.9)$$

$$\nabla \times \vec{H}_1 = \vec{J}_1 + j\omega\epsilon\vec{E}_1 \quad (2.5.10)$$

$$\nabla \cdot \vec{D}_1 = \rho_1 \quad (2.5.11)$$

$$\nabla \cdot \vec{B}_1 = 0 \quad (2.5.12)$$

$$\nabla \cdot \vec{J}_1 = -j\omega\rho_1 \quad (2.5.13)$$

$$\vec{J}_1 = \rho_0 \vec{v}_1 + \rho_1 \vec{v}_0 \quad (2.5.14)$$

$$j\omega\vec{v}_1 + (\vec{v}_0 \cdot \nabla)\vec{v}_1 + (\vec{v}_1 \cdot \nabla)\vec{v}_0 + \nabla \vec{v}_1 = \frac{q}{m^*} (\vec{E}_1 + \vec{v}_0 \times \vec{B}_1 + \vec{v}_1 \times \vec{B}_0) - \frac{v_t^2}{n} \nabla n_1 \quad (2.5.15)$$

All products of ac quantities have been neglected in the ac equations; thus, the ac equations are linearized. However, the dc equations are still nonlinear. To solve the linear ac equations, the dc equations must first be solved. Various artifices are used to circumvent the nonlinear nature of the dc equations. These will be cleared later in specific cases. For the moment, merely assume that they have been solved so that  $\vec{v}_0$  and  $\rho_0$  are known functions to be used in the ac equations. From this point on, in most cases, one needs only be concerned with ac equations of interest.

The wave form traveling along an axially periodic structure is described by the concept of space harmonic functions commonly known as

Floquet's  
to linear  
different  
French ma  
out by Bl  
are often  
waves tha

Floquet's

[T

p

a

p

In other

period to

proof of

Th

as the fu

correspon

attenuati

$g + \frac{2\pi n}{p} w$

harmonic.

where  $\beta_n$

To

media, a

one by Br

ship betw

diagramma

Floquet's theorem. This theorem actually constitutes a generalization to linear partial differential equations of a theorem in ordinary linear differential equations with periodic coefficients established by the French mathematician Floquet. Such a generalization has been carried out by Bloch. Accordingly, waves that propagate along a periodic structure are often called Bloch waves by analogy to the quantum-mechanical electron waves that propagate through a periodic crystal lattice in solids.

Floquet's theorem is stated as follows:

[Theorem 2.5.1] Floquet's Theorem: "For a given mode of propagation and at a given steady state frequency, the fields at two points on a transmission system, separated by one period, differ by a complex constant."

In other words, the waves regardless of the choice of origin differ from period to period only in phase and not in wave-form or magnitude. The proof of the theorem is shown in Appendix A.

The general complex Floquet wave number  $k = \beta - j\alpha$  is referred to as the fundamental propagation constant where  $\beta$  and  $\alpha$  represent the corresponding phase and attenuation constants. For lossless circuits the attenuation constant  $\alpha$  is zero. The wave propagates with a phase constant  $\beta + \frac{2\pi n}{p}$  where the  $n$ 'th term is called the  $n$ 'th space harmonic or Hartree harmonic. For a lossless system, since  $k = \beta_0$  we define

$$\beta_n = \beta_0 + \frac{2\pi n}{p} \quad (2.5.16)$$

where  $\beta_n$  is termed the phase constant for the  $n$ 'th space harmonic.

To understand the wave characteristics of slow waves in given media, a diagrammatic representation of their properties, similar to the one by Brillouin, is required. This plot shows the functional relationship between the operating frequency  $\omega$  and the phase constant  $\beta$ . The diagrammatic representation is called a Brillouin diagram or  $\omega$ - $\beta$  diagram.

If a Brillouin  
either experi  
to predict the  
except for a  
give similar  
used. Another  
as a function  
be derived for  
interaction.

dispersion curve  
In re  
[Theor  
"The  
the  
and

The proof of

## 2.6 Negative

It is  
lead to osci  
with negativ  
to traveling  
with separat  
converted to  
voltage-cont

The e  
effective ma  
k curve in t

If a Brillouin diagram for any specified medium or circuit can be prepared, either experimentally or theoretically, then there is enough information to predict the possible outcome of the interaction with carrier streams, except for a knowledge of field distribution and power. Many other forms give similar information, but the Brillouin form is the most commonly used. Another common diagram is the dispersion curve which is plotted as a function of frequency or wavelength. The dispersion equation will be derived for the given problem and utilized in the analysis of wave interaction. The Brillouin diagram is sometimes referred to as a dispersion curve.

In regard to power flow there is a theorem pertaining to systems.

[Theorem 2.5.2] Power Flow Theorem:

"The time average power flow in the passband is equal to the group velocity times the time average stored electrical and magnetic energy per period divided by the period."

The proof of this statement is shown in Appendix A.

## 2.6 Negative Resistance Effects and Two Valley Instability in Solids

It is well known that nonconvective (or absolute) instabilities lead to oscillator devices which can be represented as one-port devices with negative internal resistance, and that convective instabilities lead to traveling wave amplifiers which are generally used as two port devices with separate input and output ports. However, any amplifier can be converted to an oscillator by applying positive feedback. First, look at voltage-controlled negative effects due to negative effective mass.

The earliest proposal for such an effect involved negative effective masses for electrons. In solids, the energy  $E$  vs. wave number  $k$  curve in the conduction band is shown in Figure 2.6.1 (a). The energy

(a)

(b)

(c)

(d)

Figure 2.6.

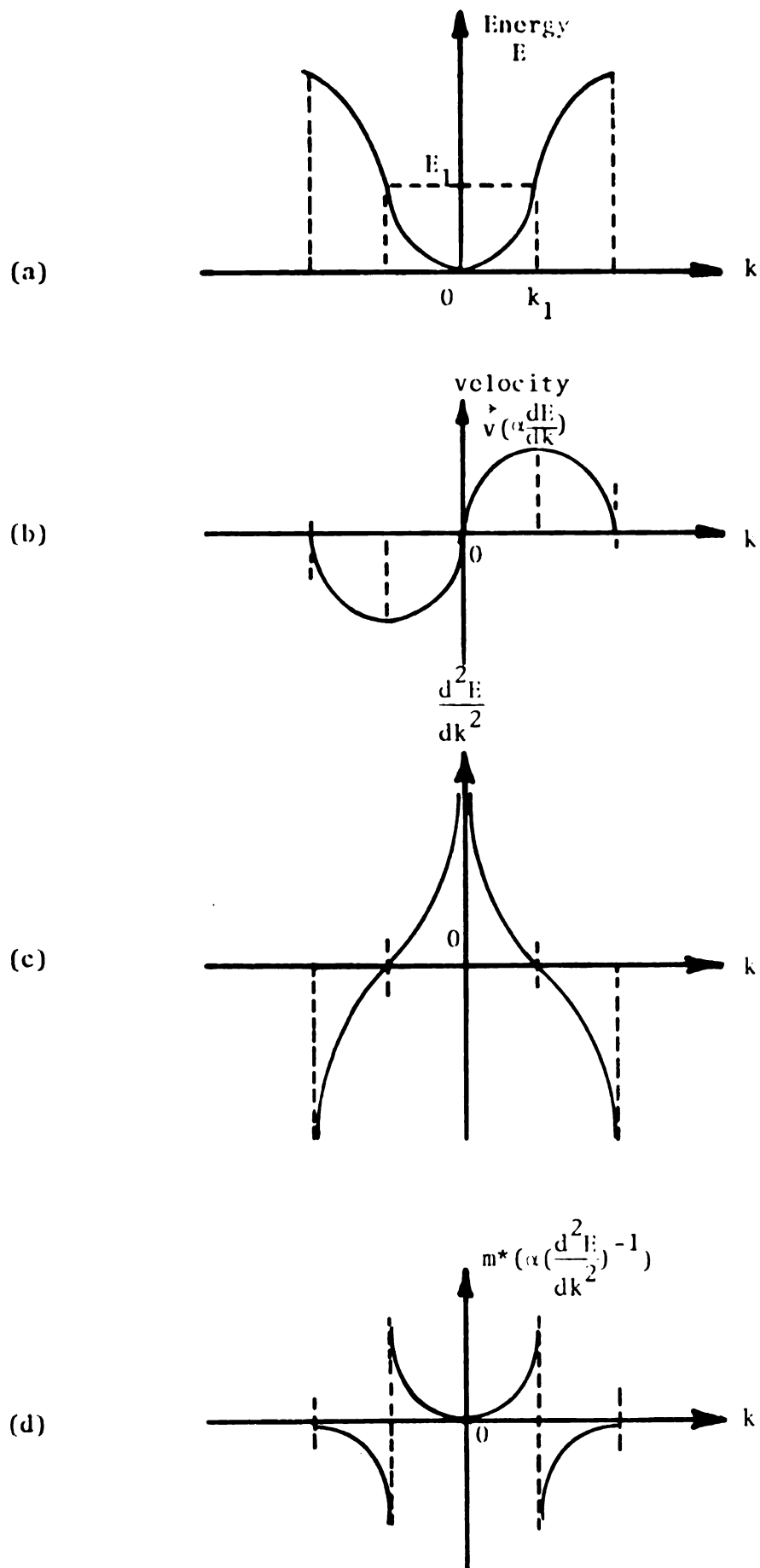


Figure 2.6.1 Energy, velocity and effective mass vs. wave number for electrons in conduction band.



of the elec

where  $p = 1$

Sim

above equa

where  $\tilde{h} =$

First and

and effect

or

or

The electri

and 2.6.1

velocity  $c$

driven in

a velocity

one shown

device ext

Figure 2.6

of the electron is given by

$$E = \frac{1}{2} mv^2 = \frac{1}{2} \frac{p^2}{m} \quad (2.6.1)$$

where  $p = mv$

Since the electron momentum is related to the wave number  $k$ , the above equation can be rewritten as

$$E = \frac{\hbar^2 k^2}{2m} \quad (2.6.2)$$

where  $\hbar = 2\pi\hbar = \text{Planck's constant}$

First and second differentiations of Eq. (2.6.2) yield electron velocity and effective mass respectively as follows:

$$\frac{dE}{dk} = \frac{\hbar^2 k}{m} = \frac{\hbar p}{m} = \hbar v$$

or

$$v = \frac{1}{\hbar} \frac{dE}{dk} \quad (2.6.3)$$

or

$$\frac{d^2 E}{dk^2} = \frac{\hbar^2}{m}$$

$$m^* = \hbar^2 \left( \frac{d^2 E}{dk^2} \right)^{-1} \quad (2.6.4)$$

The electron velocity and effective mass are plotted in Figures 2.6.1 (b) and 2.6.1 (d). For energies greater than  $E_1$ ,  $m^*$  is negative, and the velocity decreased with increasing energy. If enough electrons can be driven in energy levels with the application of external electric field, a velocity versus electric field intensity curve is obtained, like the one shown in Figure 2.6.2. Therefore, for energy greater than  $E'$ , the device exhibits negative resistance effects.

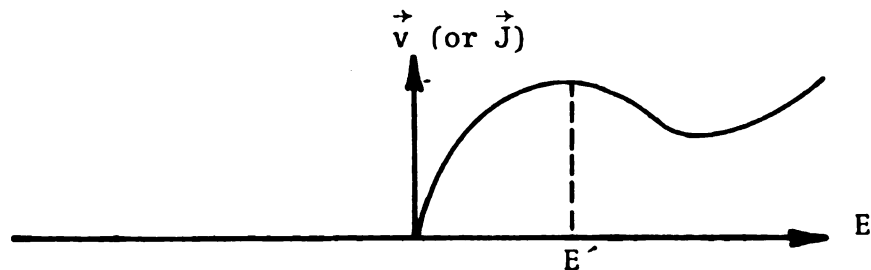


Figure 2.6.2 Velocity (or current density) vs. energy curve for voltage controlled negative resistance.

In  
as [H45]

where  $m_0^*$   
The average  
Eq. (2.6.5)

And  
Watkins [R  
experiment

Con  
separated  
lower val.

$(\vec{v} = \mu \vec{E})$ ,  
low mobil

As the el  
the upper  
than  $\mu E$ .

valley de  
current f  
negative

Figure 2.

In bulk semiconductor material the effective mass may be expressed as [HA5]

$$m^* = m_o^* + \frac{dm^*}{dE} E_1 \quad (2.6.5)$$

where  $m_o^*$  is effective average carrier mass at the dc bias field  $E_o$ .

The average carrier mass  $m^*$  varies with ac electric field  $E_1$  as shown in Eq. (2.6.5).

Another type of instability in solids was predicted by Ridley and Watkins [RI1] and Hilsun [HI2] theoretically and was demonstrated experimentally in 1963 by Gunn [GU2], as indicated in Section 2.2.

Consider a semiconductor having a conductive band with two minima separated by an energy difference  $\Delta E$  as shown in Figure 2.6.3. The lower valley has electrons with a low effective mass and high mobility ( $\vec{v} = \mu \vec{E}$ ), while the upper valley electrons have large effective mass and low mobility. Initially all electrons occupy the lower state, in L valley. As the electric field increases, some electrons gain energy and get into the upper valley if the energy supplied to the lower valley is greater than  $\Delta E$ . When this situation happens, the electron velocity in the U valley decreases sharply due to the low mobility there. This reduces current flow in the U valley, and hence the semiconductor exhibits a negative resistance in the bulk material.

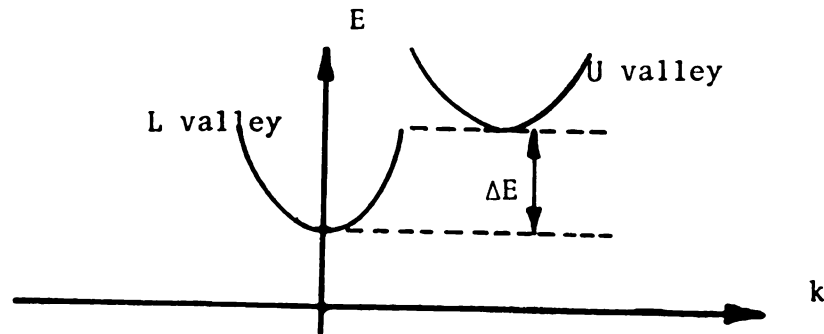


Figure 2.6.3 Two valley model separated by an energy difference  $\Delta E$ .

The  
explained

From

The

where  $\tau =$

It

the charge

amplifica

In

The maxim

device.

by elect.

For a gr

greater

defined

For a ty

than  $10^1$

The instability induced by the negative conductance effect can be explained as follows:

From the continuity equation and Poisson's equation, we have

$$\frac{\partial \rho}{\partial t} = - \nabla \cdot \vec{J} = - \nabla \cdot (\sigma \vec{E}) = - \sigma \frac{\rho}{\epsilon} \quad (2.6.6)$$

The solution of  $\rho(\vec{r}, t)$  has the following form:

$$\rho(\vec{r}, t) = \rho_0(\vec{r}, 0) e^{\frac{1}{\tau} t} \quad (2.6.7)$$

where  $\tau = \frac{\epsilon}{-\sigma}$  and  $\rho_0(\vec{r}, 0)$  is the initial charge density.

It can be seen from Eq. (2.6.7) that a negative conductance makes the charge density  $\rho$  grow exponentially. This growth can lead to amplification, and with the proper feedback, to oscillators.

In solids the conductivity  $\sigma$  can be expressed as

$$\sigma = qn\mu \quad (2.6.8)$$

The maximum growth of  $\rho$  is at  $t = T$  where  $T$  is the transit time of the device. The growth factor is equivalent to the sample length  $\ell$  divided by electron velocity  $v_0$ .

$$\frac{T}{\tau} = \frac{\frac{\ell}{v_0}}{\frac{\epsilon}{qn\mu}} = \frac{\ell qn\mu}{\epsilon v_0} \quad (2.6.9)$$

For a group of charge to form and grow, the growth factor should be greater than unity, i.e.,  $\frac{T}{\tau} > 1$ . In other words, the  $nl$  product is defined for fixed constants  $n$ ,  $\mu$ ,  $\epsilon$ ,  $q$  and  $v_0$  as:

$$nl > \frac{\epsilon v_0}{q\mu} \quad (2.6.10)$$

For a typical Gunn device material such as GaAs, the  $nl$  product is greater than  $10^{12}/\text{cm}^2$ .

### 3.1 Intro

This  
interpreta  
dominated  
to figure  
is require  
range of p

Th  
concentra  
with a te  
is order  
the dopin  
and Si, a  
( $\omega_p$ ) is a  
material  
 $10^{14}$  c/s  
( $\nu$ ) play  
temperat  
(300°K).  
the soli  
of any s  
16. For

## CHAPTER III

### FIELD DISTRIBUTION IN SOLID-STATE MATERIALS

#### 3.1 Introduction

This chapter deals with the general sample configuration, wave interpretation, wave equation and field analysis in general, collision dominated and collisionless cases. Every field solution is too complicated to figure out the wave picture at a glance. Appropriate approximation is required to understand the propagating wave — keeping the typical range of parameters in mind.

The electron density ( $n$ ) in solids is determined by doping concentration and limited by materials, though the density can be varied with a technical manner. The density of typical solids, GaAs and InSb, is order of magnitude  $10^{13} \sim 10^{16}$  electrons/cm<sup>3</sup>. For other materials the doping concentration is over the range of  $10^{14}$  electrons/cm<sup>3</sup> for Ge and Si, and in the range of  $10^{22}$  electrons for Cu. The plasma frequency ( $\omega_p$ ) is a function of the dielectric constant and effective mass of a material with a range of  $10^5 \sim 10^{12}$  c/sec for typical semiconductor and  $10^{14}$  c/sec for materials. Besides microwave frequency, collision frequency ( $\nu$ ) plays an important role in solids, ranging over  $10^7 \sim 10^{13}$  c/sec as temperature increases from liquid nitrogen (77°K) to room temperature (300°K). Because the crystal lattice is polarizable the permittivity of the solid is determined by the constituents and the lattice configuration of any specific materials. The relative dielectric constant range is  $4 \sim 16$ . For SiO<sub>2</sub>  $\epsilon_r = 4$ , for mica  $\epsilon_r = 6$  for InSb  $\epsilon_r = 15$ , and for GaAs  $\epsilon_r =$



12.5.

are inc

is cons

$10^{-3} \sim$

defined

times t

most pa

grows b

instabi

and in c

system h

support

used as

### 3.2 Met

R

to the c

solid-st

many imp

for wave

relation

oversimp

mechanis

clearly

on the s

dimensio

12.5. Since the bunching and debunching effects in most microwave devices are indispensable, whenever these effects occur, the diffusion effect (D) is consequently involved. For typical materials its magnitude is  $D = 10^{-3} \sim 10^{-1} \text{ m}^2/\text{sec}$ . Another factor for solids is debye length ( $\lambda_D$ ), defined as  $\lambda_D = 10^{-8} \sim 10^{-5} \text{ m}$  and for metals,  $\lambda_D = 10^{-10} \sim 10^{-6} \text{ m}$ . Sometimes the  $\lambda_D$  can be replaced by  $\beta_v = \omega_p/v_t$  (/ m) in semiconductors, since most parameters for solids are interrelated functions.

If a propagating system is unstable such that the disturbance grows but is propagated away from the origin, this system has convective instability. On the other hand, if the disturbance grows in amplitude and in extent but always embraces the original point of origin, this system has nonconvective instability. The convective instability can support amplifying waves while the nonconvective instability can only be used as an oscillator, as mentioned earlier.

### 3.2 Method of Solution and Configuration of Sample

Recently several authors investigated the wave amplification due to the coupling between the space charge wave and the circuit wave in solid-state materials, as was mentioned in Section 2.2. In most cases many important aspects of the analysis such as the limiting conditions for wave interaction and the way of finding roots of the dispersion relations are not clearly justified. The approaches used were either oversimplified or theoretically unfounded. Furthermore, the physical mechanism of wave interaction and the energy conversion scheme were not clearly revealed. For instance, the reflected waves and surface charges on the semiconductor were totally ignored in spite of the finite dimensions of the slab. In a simple one-dimensional analysis, these

approaches  
propagation

The  
the slow-wave  
physical di  
problem mor  
of the prin  
action a tw

As w  
as InSb, Ga  
voltage. I  
types of se  
physical st  
arises from  
to generate

The  
ultrasonic w  
1960's, espe  
amplificatio  
[HUI] in 196

The c  
amplifiers h  
agreement wi  
sional analy  
justifiable.  
magnetic fiel  
motion of cha

approaches are adequate as far as the transverse direction for wave propagation is neglected.

The difficulty lies in the fact that for any practical devices the slow-wave structure and the semiconductor active region have finite physical dimensions, i.e., finite boundary conditions which make the problem more complicated. Consequently, to obtain a better understanding of the principle of operation and the physical insight of a given interaction a two or three dimensional analysis should be carried out.

As was previously mentioned, the n-type bulk semiconductor such as InSb, GaAs, InP, and CdTe, have negative conductances above threshold voltage. It was verified theoretically and experimentally that different types of semiconductors have different threshold potentials due to the physical structure of the material. This kind of convective instability arises from the negative differential conductance and has been utilized to generate or amplify microwave signals in the past few years.

The solid-state traveling-wave amplification is similar to the ultrasonic wave amplification which has been developed in the early 1960's, especially in the wave coupling mechanism. The ultrasonic amplification in CdS observed for the first time by Hutson and McFee [HU1] in 1961 was an example of traveling-wave amplifications in solids.

The one dimensional analysis of the ultrasonic and traveling-wave amplifiers has been developed, and the results are in satisfactory agreement with experimental work. In most cases the use of one dimensional analysis in traveling-wave and ultrasonic wave amplifiers are justifiable. The former device generally uses a strong focusing static magnetic field and as a result there exists a negligible transverse motion of charged particles. In the latter device, if the wave propagates

longitudi  
remain la  
coupling  
types of  
dimension

On  
deposited  
two or th  
analysis

A  
analyzed  
is shown  
to obtain  
microwave  
slow wave  
and semic

Th  
the adjac  
If the ca  
insulation  
The more

Us  
the insul  
an insula  
propagati  
charged ca  
are approx

longitudinally, a variation in the transverse dimensions — where they remain larger than the acoustic wavelength — makes no change in the coupling of carrier waves with the rf circuit waves. Therefore, both types of wave interaction mechanism were essentially treated as a one dimensional problem.

On the other hand, the coupling through a slow wave circuit deposited on semiconductor by the integrated circuit technology is of two or three dimensional nature, and requires two or three dimensional analysis for the right solution of wave interaction phenomena.

A two dimensional problem of wave interaction in solids will be analyzed through this chapter. The two dimensional structure considered is shown in Figure 3.2.1. This is one of the possible structures used to obtain coupling between semiconductor space charge wave and external microwave. The device configuration consists of mainly four parts: slow wave circuit, two insulating layers at top and bottom of the circuit, and semiconductor.

The meander line is adopted for the slow wave circuit in which the adjacent tape elements are coupled capacitively or continuously. If the capacitively coupled type of slow wave circuit is used, one insulating layer between solid-state and meander line may be excluded. The more descriptive detail will be given in design consideration.

Using integrated circuit technology the circuit is deposited on the insulating layer or directly on the semiconductor. The exclusion of an insulating layer in capacitively coupled circuit, might give slowly propagating-waves a better chance to interact strongly with moving charged carriers if the rf wave propagation and carrier drift velocities are approximately synchronous. Energy is also easily transferred from

rf input

slow-wave  
structure

Y

Figure 3.2.

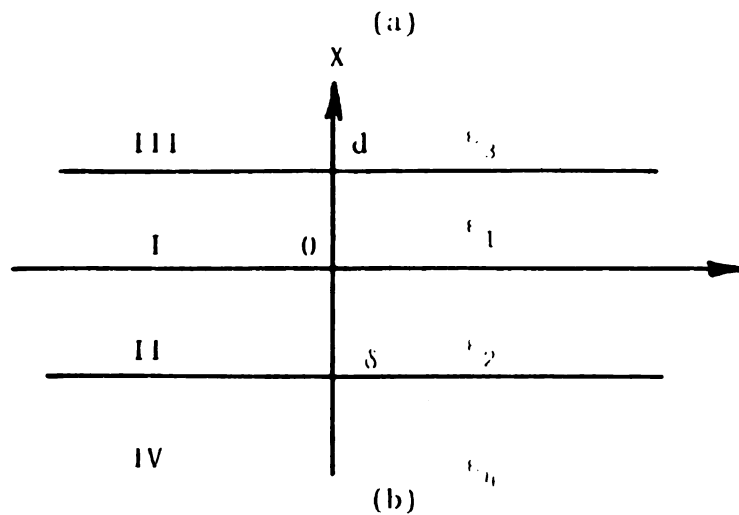
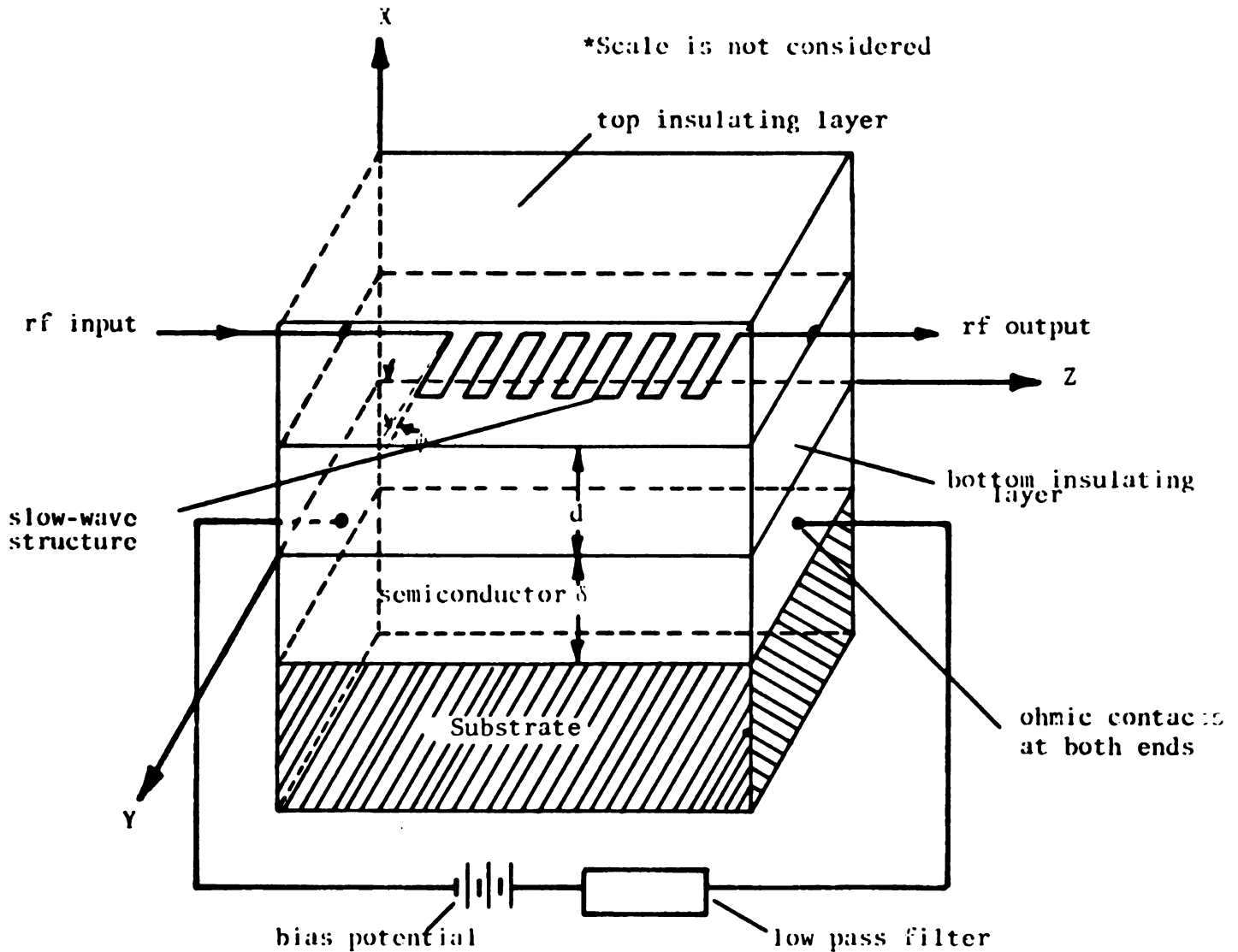


Figure 3.2.1 One possible structure for solid-state traveling-wave amplifier. (a) Sketch showing coupling between space charge waves and external microwave fields (b) Schematic planar layout of (a).



the drift

distance

Su

lapping b

For gener

analysis

distance

wave circ

with the

infinite

with subs

insulator

surface.

Th

layers be

the struc

Th

magnetic

the carr

velocity

a semico

velocity

is rough

and the

slow wav

thousand

A

undernea

the drifting carriers to the slow wave, resulting in wave growth with distance along the device.

Such a circuit structure could be made from metal layers of overlapping bars separated by a capacitive material such as  $\text{SiO}_2$  or mica. For general purposes, the insulating layer will be considered in a field analysis which includes the effect of the dielectric constant and the distance  $d$  between the rf circuit and solid-state material, i.e., a slow wave circuit is located at  $x = d$ . A semi-infinite region  $x < 0$  is occupied with the insulating material of dielectric constant  $\epsilon_1$  and another semi-infinite region  $x < 0$  extends the semiconductor of dielectric constant  $\epsilon_2$  with substrate of  $\epsilon_4$ . The top insulating layer may be either the same insulator as the bottom one, or a different material, or an air dielectric surface.

The three layers can be deposited successively with the metal layers being etched after deposition. The more detailed description of the structure will be explained in Chapter VII.

The necessary condition for active coupling between the electromagnetic wave and carrier wave in solids is that the drift velocity of the carrier should be equal to, or slightly greater than, the phase velocity of the electromagnetic wave. The maximum mean drift velocity in a semiconductor such as InSb is on the order of  $10^7$  cm/sec. Whereas, the velocity of an electromagnetic wave traveling along the slow wave circuit is roughly  $10^{10}$  cm/sec when the dielectric constant of the semiconductor and the insulating layer are taken into account. This means that the slow wave structure should have a transverse-to-longitudinal ratio of one thousand to one.

Assuming that the slow wave electric field in the semiconductor underneath the circuit is mainly in the longitudinal direction, fringe

fields are  
to the fi  
dimension  
be neglect  
and carr  
assumed t

Th  
vacuum.  
of the e  
is the de  
circuit.  
the coup  
solid-sta  
coefficie  
matrix is  
by apply  
all regio  
where  $k =$   
velocity

Th  
substrate

In  
region (i  
(i.e.  $x \geq 0$ )

### 3.3 Wave

In  
conductor

fields are at the edge of the slow wave structure which is negligible due to the fact that the transverse dimension is longer than the longitudinal dimension. The normal component of the circuit field can, however, not be neglected since it is very important to the coupling between circuit and carrier waves. As a result, two dimensional analysis, which  $y$  is assumed to be independent of all variables, will be considered.

This analysis is similar to those for traveling wave tubes in vacuum. The problem is broken into two parts, one is the determination of the electromagnetic fields in the semiconductor region and the other is the determination of the electromagnetic fields about the slow-wave circuit. Field solutions will be used to find a dispersion relation for the coupled system by equating two admittances in the circuit and in the solid-state at the boundary plane, or by equating the determinant of the coefficients matrix to be zero for a nontrivial solution. The coefficients matrix is an expression in a matrix form of linear equations determined by applying boundary conditions to all of field solutions. The fields in all regions of the configuration are assumed to vary with  $e^{j(\omega t - kz)}$  type where  $k = \beta - j\alpha$ . Hence, the solution describes a wave with a phase velocity equal to the drift velocity in the longitudinal direction.

The effects of collision, diffusion, insulator thickness and the substrate material are included in general analyses.

In this chapter the electromagnetic field for the semiconductor region (i.e.  $x \leq 0$ ) will be determined. The solutions in circuit region (i.e.  $x \geq 0$ ) will be considered in the next chapter.

### 3.3 Wave Equation of Charged Carriers in Solids

In this section the wave equation will be derived in semiconductors with permittivity  $\epsilon_2$  as shown in Figure 3.2.1. The semiconductors

used for  
treat one  
A dc elec  
itudinal  
the carri  
as  $\vec{E}_0$ . A  
sample.

For  
varies w  
analyses  
mobility  
equations

In  
because  
permeabi  
type of  
Section

7  
7  
7  
7  
J  
(  
where n  
F  
as

7  
Substitu

used for solid-state devices are usually extrinsic. Therefore we will treat one type of charged particle, say electrons only, as majority carriers. A dc electric field  $\vec{E}_0$  is established in the semiconductor along the longitudinal direction by a bias voltage supply. Because of the applied  $\vec{E}_0$  the carriers are drifting at velocity  $\vec{v}_0$  which is in the same direction as  $\vec{E}_0$ . A dc carrier density  $n_0$  is assumed to be uniform throughout the sample.

For nonuniform mobility, the average carrier effective mass  $m^*$ , varies with ac electric field  $E_1$  as shown in Eq. (2.6.5). In most analyses the negative bulk effect and the nonuniformity of electron mobility are neglected. To take these into account replace  $m^*$  in all equations by Eq. (2.6.5) and  $\mu$  by  $\mu \left( \frac{E_0}{\mu} \right) \left( \frac{\partial \mu}{\partial E_0} \right)$ .

In solid-state plasma the magnetization density  $\vec{M}$  can be neglected because electron spin around the nucleus is ignored, and hence the permeability  $\mu_0$  may be used instead of general  $\mu$ . If the  $\exp [j (\omega t - kz)]$  type of variation for the propagation is recognized, the ac equations in Section 2.4 may be rewritten as follows:

$$\nabla \times \vec{E}_1 = -j\omega\mu_0\vec{H}_1 \quad (3.3.1)$$

$$\nabla \times \vec{H}_1 = \vec{J}_1 + j\omega\epsilon_2\vec{E}_1 \quad (3.3.2)$$

$$\nabla \cdot \vec{E}_1 = -\frac{n_1 e}{\epsilon_2} \quad (3.3.3)$$

$$\nabla \cdot \vec{B}_1 = 0 \quad (3.3.4)$$

$$\vec{J}_1 = -e(n_0\vec{v}_1 + n_1\vec{v}_0) \quad (3.3.5)$$

$$(j\omega + v)\vec{v}_1 + (\vec{v}_1 \cdot \nabla)\vec{v}_1 = \eta^*\vec{E}_1 - \frac{v_t^2}{n_0}\nabla n_1 \quad (3.3.6)$$

where  $\eta^* = \frac{|e|}{m^*}$  = effective charge to mass ratio of electron carrier

From Eq. (3.3.3) the gradient of the rf carrier density is written as

$$\nabla n_1 = -\frac{\epsilon_2}{e}\nabla \nabla \cdot \vec{E}_1 \quad (3.3.7)$$

Substitution of Eq. (3.3.7) into Eq. (3.3.6) yields

$\vec{v}_1$

where  $\omega_v$

and  $u_0$

Un

frequency

materials

effective

ship for

D

where  $\mu$

to be an

constant

dominate

D

The rf v

$\vec{v}$

If colli

(3.3.12)

$\vec{v}$

Even the

picture,

are requ

collisio

T

(3.3.7),

algebra

as:

$$\vec{v}_1 = \frac{j\eta^*}{\omega_v} (\vec{E}_1 - \frac{v_t^2}{\omega_p^2} \nabla \nabla \cdot \vec{E}_1) \quad (3.3.8)$$

$$\text{where } \omega_v = \omega - ku_0 - j\nu \quad (3.3.9)$$

and  $u_0$  is the z component of  $\vec{v}_0$

Under the normal environmental temperature the thermal collision frequency is the dominant scattering process in most semiconductor materials and the thermal collision frequency may be used for the effective collision frequency. In semiconductor the Einstein relationship for the diffusion constant is

$$D = \left(\frac{kT}{e}\right)\mu \quad (3.3.10)$$

where  $\mu$  is the mobility of electron carriers, which is, at the present, to be an independent variable. Since  $v_t^2 = \frac{kT}{m^*}$  and  $u = \frac{\eta^*}{v}$ , the diffusion constant can be defined in an alternate form in the thermal diffusion dominated circumstance

$$D = \frac{v_t^2}{v} \quad (3.3.11)$$

The rf velocity is now rewritten in terms of the diffusion constant as,

$$\vec{v}_1 = \frac{j\eta^*}{\omega_v} (\vec{E}_1 - \frac{Dv}{\omega_p^2} \nabla \nabla \cdot \vec{E}_1) \quad (3.3.12)$$

If collision is considered in solids such that  $|\omega - ku_0| \ll \nu$ , then Eq. (3.3.12) can be reduced to:

$$\vec{v}_1 = -\mu \vec{E}_1 + \frac{\epsilon_2 D}{n_0 e} \nabla \nabla \cdot \vec{E}_1 \quad (3.3.13)$$

Even though the collision dominant solution doesn't give a clear wave picture, it is true for some solids. Therefore, two types of solutions are required to clarify wave phenomena in solids, i.e., general and collision dominated solutions.

Taking the curl of Eq. (3.3.1) and using Eqs. (3.3.2), (3.3.5), (3.3.7), (3.3.11), (3.3.8), and (3.3.13) and performing some subsequent algebraic manipulation, the wave equations of both cases can be obtained as:



$$\nabla \cdot \vec{E}_1 +$$

and

$$\nabla \cdot \vec{E}_1 +$$

where  $c_i = \sqrt{\frac{1}{\mu \epsilon}}$

$$\beta_i = \frac{\omega}{c_i}$$

Eqs. (3.3.14)

collision dom

with dielect

include coll

The m

the ac veloc

device. A l

$$\nabla \cdot \vec{E}_1$$

where

$$\nabla \cdot \vec{E}_1$$

$$= \hat{x}$$

$$\nabla \cdot \vec{E}_1$$

$$\nabla (\nabla \cdot \vec{E}_1)$$

### 3.4 Boundar

The f

dielectric m

configuratio

modes in die

modes but hy

substances c

TM and TE mo

$$\nabla^2 \vec{E}_1 + \beta_2^2 \left(1 - \frac{\omega_p^2}{\omega \omega_v}\right) \vec{E}_1 - j \frac{\beta_2^2 \vec{v}_0}{\omega} \nabla \cdot \vec{E}_1 - \left(1 - \frac{\beta_2^2 v^2}{\omega \omega_v}\right) \nabla \nabla \cdot \vec{E}_1 = 0 \quad (3.3.14)$$

and

$$\nabla^2 \vec{E}_1 + \beta_2^2 \left(1 - j \frac{\omega_p^2}{v \omega}\right) \vec{E}_1 - j \frac{\beta_2^2 \vec{v}_0}{\omega} \nabla \cdot \vec{E}_1 - \left(1 - j \frac{\beta_2^2 D}{\omega}\right) \nabla \nabla \cdot \vec{E}_1 = 0 \quad (3.3.15)$$

where  $c_i = \sqrt{\frac{1}{\mu_0 \epsilon_i}}$  = speed of electromagnetic wave in medium i

$$\beta_i = \frac{\omega}{c_i} = \text{wave number in medium i.}$$

Eqs. (3.3.14) and (3.3.15) are called the general wave equation and the collision dominated wave equation of a majority carrier in solid-state with dielectric constant  $\epsilon_2$ . As seen in the two equations, both equations include collision and diffusion constants.

The more general form of Eq. (3.3.15) can be derived in terms of the ac velocity and dc velocity for the analysis of transverse wave device. A little algebraic manipulation leads to:

$$\nabla^2 \vec{E}_1 + \beta_2^2 \vec{E}_1 + j \frac{\beta_2^2 \omega_p^2}{\omega \eta^*} \vec{v}_1 - j \frac{\beta_2^2}{\omega} \vec{v}_0 (\nabla \cdot \vec{E}_1) = 0 \quad (3.3.16)$$

where

$$\begin{aligned} \nabla^2 \vec{E}_1 &= \hat{x} \left( \frac{\partial^2}{\partial x^2} + \frac{\partial^2}{\partial z^2} \right) \vec{E}_{1x} + \hat{y} \left( \frac{\partial^2}{\partial x^2} + \frac{\partial^2}{\partial z^2} \right) \vec{E}_{1y} + \hat{z} \left( \frac{\partial^2}{\partial x^2} + \frac{\partial^2}{\partial z^2} \right) \vec{E}_{1z} \\ &= \hat{x} \left( \frac{\partial^2}{\partial x^2} - k^2 \right) \vec{E}_{1x} + \hat{y} \left( \frac{\partial^2}{\partial x^2} - k^2 \right) \vec{E}_{1y} + \hat{z} \left( \frac{\partial^2}{\partial x^2} - k^2 \right) \vec{E}_{1z} \end{aligned} \quad (3.3.17)$$

$$\nabla \cdot \vec{E}_1 = \frac{\partial E_{1x}}{\partial x} - j k E_{1z} \quad (3.3.18)$$

$$\nabla (\nabla \cdot \vec{E}_1) = \hat{x} \left( \frac{\partial^2 E_{1x}}{\partial x^2} - j k \frac{\partial E_{1z}}{\partial x} \right) + \hat{z} \left( -j k \frac{\partial E_{1x}}{\partial x} - k^2 E_{1z} \right) \quad (3.3.19)$$

### 3.4 Boundary Conditions in Semiconductors

The finite solid substance (or waveguide) which are bound to a dielectric material are used in various microwave components. A typical configuration is an example which is shown in Figure 3.2.1. The propagating modes in dielectric substances of this type are not, in general, TE or TM modes but hybrid modes. In other words, a finite structure of the substances containing mobile charged carriers cannot support independent TM and TE modes. This inability results from the coupling between two

types of waves brought about by the motion of the charges. Such coupling between TM and TE waves vanishes when  $B_0 = 0$  or  $B_0 = \infty$ , and also for waves with infinite phase velocities (cutoff points in the dispersion diagram), [ST2]. The coupling can be also neglected if the carrier density is very small. For the traveling wave amplifier tube, the analysis falls into the category of pure TM and TE waves since an infinite dc magnetic field is assumed.

In our structural configuration, TM and TE waves can exist independently because dc magnetic field is not applied to the device. Then, the wave solution of the carrier wave equation can be subdivided into two types, namely TE and TM modes.

According to the two dimensional boundary, the TE wave has only the transverse component of the electric field and hence cannot couple with the drifting carriers. Therefore we are not interested in the TE solution where interaction is concerned. We will only consider the TM mode since a longitudinal electric field exists which couples the circuit and the carriers. However, to understand the complete motion of the charged carrier and to determine unknown coefficients of field solutions in a coupled circuit system, the TE solution is also necessary.

From the two dimensional assumption we made earlier,  $\frac{\partial}{\partial y} = 0$ .

Hence the TM wave consists of  $E_{1x}$ ,  $E_{1z}$ , and  $H_{1y}$  and the TE wave  $E_{1y}$ ,  $H_{1z}$ , and  $H_{1x}$  in solids. Field solutions will be derived in the following three sections.

Just as the diffusion constant in wave equations was included, the diffusion effect of the carrier in semiconductor should be taken into account. Further, the conductivity of semiconductor is finite. Therefore, no surface current flows and the tangential component of magnetic field

vect

vani

1.

x

2.

bound

3.

coe

stat

pre

3.5

str

Usi

way

of

may

A.

B.

vector  $\vec{v}$  is continuous at the boundary. In addition, the rf velocity vanishes at two semiconductor boundaries.

The boundary conditions used can be summarized as:

1. The tangential electric field component is continuous at the boundary  $x = -\delta$ .
2. The tangential magnetic field component is also continuous at the boundary  $x = -\delta$ .
3. The normal rf velocity vanishes at the boundaries  $x = 0$  and  $x = -\delta$ .

These three conditions will be used in formulating the field coefficients matrix and in determining the admittance functions in solid-state region. Another five conditions about slow-wave circuit will be presented in Section 4.2.

### 3.5 Field Interpretation in the Solid-State

From Eq. (3.3.14) a general wave equation for a charged carrier stream is:

$$\nabla^2 \vec{E}_1 + \beta_2^2 \left(1 - \frac{\omega_p^2}{\omega \omega_v}\right) \vec{E}_1 - j \frac{\beta_2^2 \vec{v}_0}{\omega} \nabla \cdot \vec{E}_1 - \left(1 - \frac{\beta_2^2 v_t^2}{\omega \omega_v}\right) \nabla \nabla \cdot \vec{E}_1 = 0 \quad (3.5.1)$$

Using algebraic operation of  $\nabla$ , Eq. (3.3.17) through Eq. (3.3.19) the wave equation is split into three component form. Since the direction of a bias potential is easily varied, the direction of carrier velocity may be adjusted such that  $\vec{v}_0 = u_0 \hat{z}$  for convenience.

A. The wave equation for x-component:

$$\frac{\partial^2 E_{1x}}{\partial x^2} + \frac{\omega \omega_v}{\beta_2^2 v_t^2} \left[ \beta_2^2 \left(1 - \frac{\omega_p^2}{\omega \omega_v}\right) - k^2 \right] E_{1x} - jk \left(1 - \frac{\omega \omega_v}{\beta_2^2 v_t^2}\right) \frac{\partial E_{1z}}{\partial x} = 0 \quad (3.5.2)$$

B. The wave equation for the y-component:

$$\frac{\partial^2 E_{1y}}{\partial x^2} - \left[ k^2 - \beta_2^2 \left(1 - \frac{\omega_p^2}{\omega \omega_v}\right) \right] E_{1y} = 0 \quad (3.5.3)$$

C. The wave equation for the z-component:

$$\frac{\partial^2 E_{1z}}{\partial x^2} + \frac{\beta_2^2}{\omega} \left( \omega - \frac{\omega^2}{\omega \omega_v} - k u_o - k^2 \frac{v_t^2}{\omega_v} \right) E_{1z} + jk \left( 1 - \frac{\beta_2^2 u_o}{\omega k} - \frac{\beta_2^2 v_t^2}{\omega \omega_v} \right) \frac{\partial E_{1x}}{\partial x} = 0 \quad (3.5.4)$$

For simplicity, let

$$a^2 = k^2 - \beta_2^2 \left( 1 - \frac{\omega^2}{\omega \omega_v} \right) \quad (3.5.5)$$

$$b^2 = \frac{\omega_v}{v_t^2} \left( -\omega + k u_o + \frac{\omega^2}{\omega_v} + k^2 \frac{v_t^2}{\omega_v} \right) \quad (3.5.6)$$

and

$$g = j \frac{\omega \omega_v}{\beta_2^2 v_t^2} \quad (3.5.7)$$

Then the three wave equations are reduced to simple form as:

$$\left( \frac{\partial^2}{\partial x^2} + jga^2 \right) E_{1x} = jk (1 + jg) \frac{\partial E_{1z}}{\partial x} \quad (3.5.2)'$$

$$\left( \frac{\partial^2}{\partial x^2} - a^2 \right) E_{1y} = 0 \quad (3.5.3)'$$

and

$$\left( \frac{\partial^2}{\partial x^2} - j \frac{b^2}{g} \right) E_{1z} = jk \left( 1 - \frac{\beta_2^2 u_o}{\omega k} + \frac{1}{jg} \right) \frac{\partial E_{1x}}{\partial x} \quad (3.5.4)'$$

Before obtaining the solution one may compare this analysis with a previous simple one-dimensional analysis [VU2]. For one dimensional case  $\frac{\partial}{\partial x} = \frac{\partial}{\partial y} = 0$ . Hence,  $a^2 = b^2 = 0$  since  $E_{1x} \neq 0$ ,  $E_{1y} \neq 0$  and  $E_{1z} \neq 0$  even for the one dimensional analysis. Therefore,

$$k^2 = \frac{\omega^2}{c^2} - \left( 1 - \frac{\omega^2}{\omega \omega_v} \right)$$

and

$$k u_o = \omega - \frac{\omega^2}{\omega \omega_v}$$

The last equation holds under the assumption that  $D = 0$ . If we can further assume  $|\omega - k u_o| \ll D$  and  $\omega^2 / (\omega \omega_v) \ll 1$ , we may obtain the same solutions

$$k = \pm \frac{\omega}{c^2}$$

and

whi

sol

sub

From

Put

Then

Thus

in t

where

and

First

(3.5.

equat.

$$k = \frac{\omega}{u_0} - j \frac{\omega_p^2}{v u_0}$$

which were Vural and Bloom's equations.

The right hand side of Eq. (3.5.4)' is further simplified by solving  $u_0$  in terms of  $a^2$  and  $b^2$  from Eqs. (3.5.5) and (3.5.6) and substituting  $u_0$  into the right hand term as follows:

From Eq. (3.5.6)

$$u_0 = \frac{\omega}{k} - \frac{\omega_p^2 - k^2 v^2 t}{k \omega_v} + \frac{v^2 t}{k \omega_v} b^2$$

Putting  $\omega_p$  of Eq. (3.5.5) in the above equation gives

$$u_0 = \frac{\omega a^2}{k \beta_2^2} + \frac{\omega k}{\beta_2^2} - \frac{k v^2 t}{\omega_v} + \frac{v^2 t}{k \omega_v} b^2 \quad (3.5.8)$$

Then

$$1 - \frac{\beta_2^2 u_0}{\omega k} + \frac{1}{j g} = \frac{a^2}{k^2} + \frac{b^2}{j g}$$

Thus three partial differential equations of second order are rewritten in the form.

$$\left( \frac{\partial^2}{\partial x^2} + j g a^2 \right) U = (j - g) W' \quad (3.5.9)$$

$$\left( \frac{\partial^2}{\partial x^2} - a^2 \right) V = 0 \quad (3.5.10)$$

$$\left( \frac{\partial^2}{\partial x^2} - j \frac{b^2}{g} \right) W = \left( -j a^2 - \frac{b^2}{g} \right) U' \quad (3.5.11)$$

where

$$U = \frac{1}{k} E_{1x}$$

$$V = E_{1y}$$

$$W = E_{1z}$$

and prime variables represent their x-derivatives.

First we are trying to derive the TM solution by using Eqs. (3.5.9) and (3.5.11). In order to solve two simultaneous partial differential equations both coupled equations may be expressed in a matrix form:



$$\frac{a}{ax}$$

The

by 1

Eq.

or

Hence

As w

be c

$E_{12}$

$W =$

where

given

(3.5

equa

field

The e

and (3

$$\frac{a}{ax} \begin{bmatrix} U \\ W \\ U' \\ W' \end{bmatrix} = \begin{bmatrix} 0 & 0 & 1 & 0 \\ 0 & 0 & 0 & 1 \\ -jga^2 & 0 & 0 & (j-g) \\ 0 & j\frac{b^2}{g} & (-ja^2 - \frac{b^2}{g}) & 0 \end{bmatrix} \begin{bmatrix} U \\ W \\ U' \\ W' \end{bmatrix} \quad (3.5.12)$$

The characteristic equation of the 4 x 4 square matrix is easily derived by letting the determinant of  $\lambda I - S$  be zero where  $S$  is the square matrix of Eq. (3.5.12).

$$|\lambda I - S| = \lambda^4 - (a^2 + b^2) \lambda^2 + a^2 b^2 = 0$$

or

$$(\lambda^2 - a^2)(\lambda^2 - b^2) = 0$$

Hence, the characteristic roots are given by

$$\lambda = \pm a, \pm b \quad (3.5.13)$$

As was mentioned earlier, interest is in the longitudinal wave, which can be coupled with drifting carrier. Therefore, first the longitudinal wave  $E_{1z}$  will be obtained, then  $E_{1x}$  from  $E_{1z}$ .

The solution type of  $W$  is of the form

$$W = E_{1z} = A_1 e^{ax} + A_2 e^{-ax} + A_3 e^{bx} + A_4 e^{-bx} \quad (3.5.14)$$

where  $A_1, A_2, A_3$ , and  $A_4$  are all constants to be determined from the given boundary conditions, and  $a$  and  $b$  are defined in Eqs. (3.5.5) and (3.5.6).

Substituting Eq. (3.5.14) into Eq. (3.5.11) and integrating the equation from  $x = -\infty$  to  $x$  give  $E_{1x}$

$$E_{1x} = \frac{jk}{a} (A_1 e^{ax} - A_2 e^{-ax}) + \frac{1}{a^2 - j\frac{b^2}{g}} (A_3 e^{bx} - A_4 e^{-bx}) \quad (3.5.15)$$

For the TM wave the only nonvanishing component of the magnetic field is  $H_{1y}$  while  $H_{1x} = H_{1z} = 0$  due to the two dimensional geometry. The evaluation of  $H_{1y}$  is done by substituting the relations Eqs. (3.5.14) and (3.5.15) into the curl equation of  $\vec{E}_1$ , Eq. (3.3.1).

1

2

3

4

5

6

7

8

9

10

11

TE

$$H_{1y} = \frac{\epsilon_2 c^2}{j\omega} \left[ \frac{a^2 - k^2}{a} (A_1 e^{ax} - A_2 e^{-ax}) + \frac{(a^2 - k^2) - j\frac{1}{g}(b^2 - k^2)}{a^2 - j\frac{b^2}{g}} b (A_3 e^{bx} - A_4 e^{-bx}) \right] \quad (3.5.16)$$

Similarly the solutions of TE mode is obtained from Eqs. (3.5.10)

and (3.3.1) as

$$E_{1y} = B_1 e^{ax} + B_2 e^{-ax} \quad (3.5.17)$$

$$H_{1x} = \frac{-k\epsilon_2 c^2}{\omega} (B_1 e^{ax} + B_2 e^{-ax}) \quad (3.5.18)$$

$$H_{1z} = j\frac{\epsilon_2 c^2 a}{\omega} (B_1 e^{ax} - B_2 e^{-ax}) \quad (3.5.19)$$

where  $B_1$  and  $B_2$  are all constants — noting that the  $e^{j(\omega t - kz)}$  is suppressed in all field equations of Eqs. (3.5.14) through (3.5.19).

All fields in solid-state are obtained in terms of x- and z-coordinates. Next fields in the substrate region should be found to determine unknown coefficients. The conduction current in the insulator region is zero, so the wave equation is reduced to

$$\frac{\partial^2 \vec{E}_1}{\partial x^2} + \gamma_4^2 \vec{E}_1 = 0 \quad (3.5.20)$$

where

$$\gamma_4^2 = k^2 - \omega^2 \mu_0 \epsilon_4 \quad (3.5.21)$$

Keeping in mind that  $\gamma_4$  has a principal real positive value and that fields vanish at  $x = -\infty$ , the electromagnetic fields in the substrate region of dielectric permittivity  $\epsilon_4$  are:

TM wave

$$E_{1z} = F_4 e^{\gamma_4 x} \quad (3.5.22)$$

$$E_{1x} = \frac{jk}{\gamma_4} F_4 e^{\gamma_4 x} \quad (3.5.23)$$

$$H_{1y} = \frac{j\omega\epsilon_4}{\gamma_4} F_4 e^{\gamma_4 x} \quad (3.5.24)$$

TE wave

$$E_{1y} = G_4 e^{\gamma_4 x} \quad (3.5.25)$$

$$H_{1x} = \frac{-k\epsilon_4 c^2}{\omega} G_4 e^{\gamma_4 x} \quad (3.5.26)$$

$$H_{1z} = \frac{j\gamma_4 \epsilon_4 c^2}{\omega} G_4 e^{\gamma_4 x} \quad (3.5.27)$$

V

A

(

t

t

a

W

S

O

t

t

3

a

a

V

Sc

W

et

Of

Sy

gi

where

$$c_4 = \frac{1}{\sqrt{\mu_0 \epsilon_4}}$$

All of unknown coefficients will be interrelated in Section 4.5.

Waves can be interpreted by investigating the wave equation, Eq. (3.5.1). Putting  $\nabla \cdot \vec{E} = 0$  in Eq. (3.5.1) produces the solution of  $e^{ax}$  and  $e^{-ax}$  therefore this wave associated with  $a$  is called the solenoidal wave or transverse wave. Similarly, since  $\nabla \times \vec{E} = 0$  yields the solution of  $e^{bx}$  and  $e^{-bx}$ , the wave with  $b$  is named as the irrotational wave or longitudinal wave. The longitudinal wave is associated with space charges in the semiconductors and this wave is originated from diffusion in the equation of motion of the carriers. According to the device structure both of the fundamental modes must be excited. It is also noted that without the carrier motion, two modes cannot be coupled at all in the solid-state.

### 3.6 Field Analysis in the Influence of Collision Effect

In the previous section general electromagnetic fields in solids are derived without any simplifying assumptions. Practically, a large amount of collisions in solids exists due to the ever-present thermal vibrations of the lattice. Besides photon scattering of the carriers, scattering effects are from ionized impurities and neutral impurities which let the collision frequency increase. The analysis in some collision effective materials may be assumed to be  $|\omega - k u_0| \ll \nu$  since the quantity of  $|\omega - k u_0|$  is small even in asynchronous case while it is zero in synchronous.

Under that situation the wave equation is, from Eq. (3.3.15), given by:

$$\nabla^2 \vec{E}_1 + \beta_2^2 \left(1 - j \frac{\omega_p^2}{\omega \nu}\right) \vec{E}_1 - j \frac{\beta_2^2 u_0}{\omega} \nabla \cdot \vec{E}_1 - \left(1 - j \frac{\beta_2^2 D}{\omega}\right) \nabla \nabla \cdot \vec{E}_1 = 0 \quad (3.6.1)$$

One can get three separate equations in component form by using Eq.

(3.6.1) and operation of  $\nabla$  as follows:

$$\frac{\partial^2 E_{1x}}{\partial x^2} + j \frac{\omega}{\beta_2^2 D} [k^2 - \beta_2^2 (1 - j \frac{\omega p^2}{v \omega})] E_{1x} - j k (1 + j \frac{\omega}{\beta_2^2 D}) \frac{\partial E_{1z}}{\partial x} = 0 \quad (3.6.2)$$

$$\frac{\partial^2 E_{1y}}{\partial x^2} - [k^2 - \beta_2^2 (1 - j \frac{\omega p^2}{v \omega})] E_{1y} = 0 \quad (3.6.3)$$

$$\frac{\partial^2 E_{1z}}{\partial x^2} + \frac{\beta_2^2}{\omega} [(\omega - k u_0) - j (\frac{\omega p^2}{v} + k^2 D)] E_{1z} + j k (1 - \frac{\beta_2^2 u_0}{k \omega} - j \frac{\beta_2^2 D}{\omega}) \frac{\partial E_{1x}}{\partial x} \quad (3.6.4)$$

Similar to the previous analysis, define

$$a_1^2 = k^2 - \beta_2^2 (1 - j \frac{\omega p^2}{v \omega}) \quad (3.6.5)$$

$$b_1^2 = j \frac{1}{D} [(\omega - k u_0) - j (\frac{\omega p^2}{v} + D k^2)] \quad (3.6.6)$$

From the above two equations the drift velocity can be expressed in terms of  $a_1^2$  and  $b_1^2$ .

$$u_0 = g_1 D (k - \frac{a_1^2}{k}) - j (k - \frac{b_1^2}{k}) D \quad (3.6.7)$$

where

$$g_1 = \frac{\omega}{\beta_2^2 D}$$

Combination of Eqs. (3.6.2) through (3.6.8) yields three partial differential equations of second order.

$$(-\frac{\partial^2}{\partial x^2} + j g_1 a_1^2) U = (j - g_1) W' \quad (3.6.9)$$

$$(-\frac{\partial^2}{\partial x^2} - a_1^2) V = 0 \quad (3.6.10)$$

$$(-\frac{\partial^2}{\partial x^2} - j \frac{b_1^2}{g_1}) W = (-j a_1^2 - \frac{b_1^2}{g_1}) U' \quad (3.6.11)$$

Three equations above are the same equations derived in Section 3.5, namely Eqs. (3.5.9), (3.5.10), and (3.5.11) by replacing  $a$  by  $a_1$ ,  $b$  by  $b_1$ , and  $g$  by  $g_1$ . Throughout the similar argument to the Section 3.5, the same solution form is obtained like Eqs. (3.5.14) through (3.5.19). Therefore, all electromagnetic field solutions in the general case are applicable to the solution where collisions are dominant.

a

c

I

E

E

H

T

E

H

H

N

S

3

ec

Eq

E

12

22

22

22

22

22

22



Also, the solution form may be simplified by calculating the terms  $a_1^2 - k^2$  and  $b_1^2 - k^2$  from the definition of  $a_1^2$  and  $b_1^2$  and then fields in collision dominated semiconductor materials are written as:

TM wave

$$E_{1z} = A_1 e^{a_1 x} + A_2 e^{-a_1 x} + A_3 e^{b_1 x} + A_4 e^{-b_1 x} \quad (3.6.12)$$

$$E_{1x} = \frac{jk}{a_1} (A_1 e^{a_1 x} - A_2 e^{-a_1 x}) + j \frac{b_1 k (1 - j \frac{1}{g_1})}{a_1^2 - j \frac{b_1^2}{g_1}} (A_3 e^{b_1 x} - A_4 e^{-b_1 x}) \quad (3.6.13)$$

$$H_{1y} = \left[ \frac{\epsilon_2 c^2}{j \omega} \frac{a_1^2 - k^2}{a_1} (A_1 e^{a_1 x} - A_2 e^{-a_1 x}) + \frac{(a_1^2 - k^2) - j \frac{1}{g} (b_1^2 - k^2)}{a_1^2 - j \frac{b_1^2}{g_1}} b (A_3 e^{b_1 x} - A_4 e^{-b_1 x}) \right] \quad (3.6.14)$$

TE wave

$$E_{1y} = B_1 e^{a_1 x} + B_2 e^{-a_1 x} \quad (3.6.15)$$

$$H_{1x} = \frac{-k \epsilon_2 c^2}{\omega} (B_1 e^{a_1 x} + B_2 e^{-a_1 x}) \quad (3.6.16)$$

$$H_{1z} = j \frac{\epsilon_2 c^2 a_1}{\omega} (B_1 e^{a_1 x} - B_2 e^{-a_1 x}) \quad (3.6.17)$$

Note that all coefficients in this case are not the same as in the previous section, even if same notations are used.

### 3.7 Electromagnetic Field Description for Streaming Carriers in the Absence of Collisions

The collisionless solution can be obtained from the general wave equation, Eq. (3.3.14) letting  $v = 0$ .

$$\nabla^2 \vec{E}_1 + \beta_2^2 \left( 1 - \frac{\omega_p^2}{\omega(\omega - k u_0)} \right) \vec{E}_1 - j \frac{\beta_2^2 u_0}{\omega} \nabla \cdot \vec{E}_1 - \nabla \nabla \cdot \vec{E}_1 = 0 \quad (3.7.1)$$

Eq. (3.7.1) is decomposed in three component form as

$$E_{1x} - j \frac{k}{a^2} \frac{\partial E_{1z}}{\partial x} = 0 \quad (3.7.2)$$

$$\frac{\partial^2 E_{1y}}{\partial x^2} - a_2^2 E_{1y} = 0 \quad (3.7.3)$$

$$\frac{\partial^2 E_{1z}}{\partial x^2} - b_2^2 E_{1z} + jk \left( 1 - \frac{\beta_2^2 u_0}{\omega k} \right) \frac{\partial E_{1x}}{\partial x} = 0 \quad (3.7.4)$$

wh

Ex

Ec

A

be

T

T

I

s

s

th

where

$$a_2^2 = k^2 - \beta_2^2 \left[ 1 - \frac{\omega_p^2}{(\omega - ku_0)} \right] \quad (3.7.5)$$

$$b_2^2 = \frac{\beta_2^2}{\omega} \left[ \frac{\omega_p^2}{\omega - ku_0} - (\omega - ku_0) \right] \quad (3.7.6)$$

Expressing  $u_0$  in terms of  $a_2^2$  and  $b_2^2$ , and substituting of  $\frac{\partial E_{1x}}{\partial x}$  from Eq. (3.7.2) into Eq. (3.7.4) yield

$$\frac{\partial^2 E_{1z}}{\partial x^2} - a_2^2 E_{1z} = 0 \quad (3.7.7)$$

According to arguments similar to Section 3.5, electromagnetic fields can be obtained as:

TM wave

$$E_{1z} = A_1 e^{a_2 x} + A_2 e^{-a_2 x} \quad (3.7.8)$$

$$E_{1x} = \frac{jk}{a_2} (A_1 e^{a_2 x} - A_2 e^{-a_2 x}) \quad (3.7.9)$$

$$H_{1y} = \frac{j\omega\epsilon_2}{a_2} \left( 1 - \frac{\omega_p^2}{\omega(\omega - ku_0)} \right) (A_1 e^{a_2 x} - A_2 e^{-a_2 x}) \quad (3.7.10)$$

TE wave

$$E_{1y} = B_1 e^{a_2 x} + B_2 e^{-a_2 x} \quad (3.7.11)$$

$$H_{1x} = \frac{-k\epsilon_2 c_2}{\omega} (B_1 e^{a_2 x} + B_2 e^{-a_2 x}) \quad (3.7.12)$$

$$H_{1z} = j \frac{\epsilon_2 c_2 a^2}{\omega} (B_1 e^{a_2 x} - B_2 e^{-a_2 x}) \quad (3.7.13)$$

It is noted that for one dimensional analysis by putting  $\frac{\partial}{\partial x} = 0$ , this solution can be reduced to the wellknown Hahn-Ramo space charge wave solution [VU1].

In this chapter the semiconductor slab is assumed to be so thin that reflected waves should be considered. However, if the slab is

thick enough such that the reflected waves ( $e^{-ax}$  and  $e^{-bx}$ ) may be neglected for electromagnetic field solutions, all equations can be reduced to the simple forms, which are tabulated in Appendix B after applying boundary conditions.

## CHAPTER IV

### FIELD ANALYSIS OF SLOW WAVE CIRCUIT AND FORMULATION OF LINEAR EQUATIONS FOR THE COMPLETE SYSTEM

#### 4.1 Introduction

In the preceding chapter the complete field solution was obtained in the region of the solid-state medium. This chapter will be devoted to the field solution of a periodic array of slow-wave tape structures by symmetrically spaced fingers. It is of course impossible to obtain an exact solution to such a complicated geometry; however, by idealizing the circuit it is possible to get a closed form of the solution for the model depicted in Figure 3.2.1. The analysis is restricted to idealized tapes of uniform width and zero thickness. An idealized model of the meander line circuit is then constructed by introducing electrical shorts between tapes at appropriate positions along the tapes although the model may not be easily fabricated practically.

It is desirable at this point to review several typical slow-wave structures before analyzing the main subject. Figure 4.1.1 shows a variety of slow-wave tape structures which can be used for solid-state traveling wave amplifier. Figure 4.1.1 (a) is a helix tape line, which is a popular structure for a travelling wave amplifier tube and Figure 4.1.1 (b) an interdigital tape line. Figure 4.1.1 (c) represents meander tape line which is used for our purpose of the analysis and Figure 4.1.1 (d) tape ladder line. The two structures illustrated in Figure 4.1.1 (b) and (c) are complementary or dual structures. At millimeter wavelengths

a helix has too small a diameter to be a useful slow-wave structure and various forms of interdigital lines, meander lines, and ladder lines are preferred.

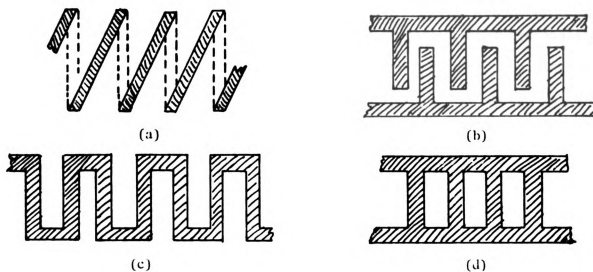


Figure 4.1.1 Several typical tape slow-wave structures.

(a) tape helix line (b) interdigital tape line (c) meander tape line (d) tape ladder line.

In general, a periodic array of uniform tapes can propagate a variety of TM and TE waves corresponding to arbitrary excitation of individual tape elements. The power of various modes is delivered in the direction of group velocity of the system, which was shown in theorem 2.5.2.

In a general slow-wave structure, there are Hartree spatial harmonics associated with wave propagations as indicated in Eq. (2.5.16). For simplicity, only a fundamental harmonic will be treated in the

analysis. One more remark on evaluating the gain and the field distribution of the output is important. The values of the gain and the field at the output terminal can be determined by applying the Floquet theorem that the output signal is different from the input signal in phase by the length of the active region of the slow-wave circuit.

In this chapter, fields about the circuit structure are analyzed and then fourteen linear equations are also formulated by applying all conditions, while unknown coefficients are interrelated in the ratio of the first unknown coefficient, namely  $A_1$ .

#### 4.2 Boundary Conditions about a Slow-wave Circuit Structure

For a tape structure type of slow-wave circuits, two specific boundary conditions are used to obtain unknown coefficients of the field solution. Those conditions were originated by Chu [CH1] and afterwards were used by several authors [CO2], [HU5], [PI2]. Boundary conditions are:

1. Along the direction of the tape-line, the tangential electric field at the edge of the tape must vanish since the tape is considered to be a perfect conductor.
2. The component of magnetic field intensity  $\vec{H}_1$  tangent to the tape-line must be continuous since no current flows perpendicular to the tape.

In addition to these two conditions some typical boundary conditions are also used in this case.

3. The tangential component of electric field intensity  $\vec{E}_1$  at the boundary surfaces  $x = 0$  and  $x = d$  is continuous.
4. The tangential component of magnetic field intensity  $\vec{H}_1$  at the boundary  $x = 0$  is continuous under the assumption that there is no surface

current, which is the same as the second boundary condition in Section 3.4.

One more condition should be added up according to the chosen geometry with the top insulating layer (or free space) in the positive space.

5. In transverse direction, the electric field intensity at positive infinity will vanish since no growing field exists in the passive chosen circuit geometry.

These five boundary conditions about the slow-wave circuit region and another three boundary conditions in the solid-state region will be used together to evaluate unknown coefficients of field solutions and to construct the field coefficients matrix for the coupled system.

#### 4.3 Electromagnetic Field Solutions in the Slow-wave Circuit Region when the Permittivities of Two Insulating Layers are the Same

Here, the problem will be solved in the case of same permittivities of two insulating layers surrounding the slow-wave tape structure. The geometry of the structure is illustrated in Figure 4.3.1. The infinitely thin meander tape line is located in the direction with an angle  $\psi$  to the y-axis between two insulators with the same relative dielectric

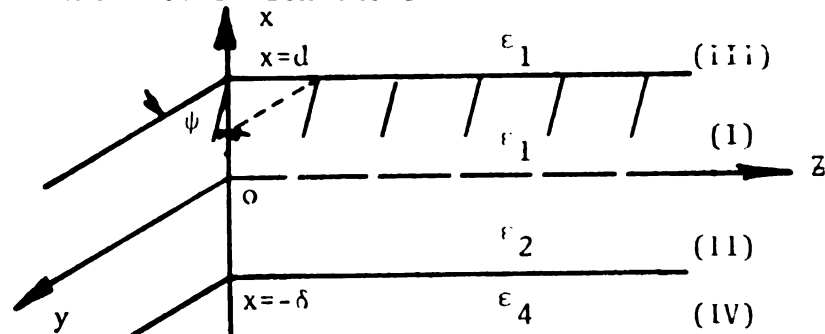


Figure 4.3.1 Geometry of the device structure with the same dielectric constant around the circuit

permittivity  $\epsilon_1$ . Then the circuit phase velocity in the medium I becomes  $c_1 \tan \psi$  where  $c_1$  is the medium wave velocity.



The wave equation of the electric field  $\vec{E}_1$  in the insulating layer with permittivity  $\epsilon_1$  becomes

$$\nabla^2 \vec{E}_1 + \beta_1^2 \vec{E}_1 = 0 \quad (4.3.1)$$

$$\text{or} \quad \frac{\partial^2 \vec{E}_1}{\partial x^2} - \gamma_1^2 \vec{E}_1 = 0 \quad (4.3.2)$$

$$\text{where} \quad \gamma_1^2 = k^2 - \beta_1^2 = k^2 - \omega^2 \epsilon_1 \quad (4.3.3)$$

Eq. (4.3.2) was obtained on the basis that the wave is traveling in the positive  $z$ -direction of the type  $e^{j(\omega t - kz)}$  and that the Laplacian  $\nabla^2$  is separated into  $\frac{\partial^2}{\partial x^2} - k^2$  for a two-dimensional analysis.

In the analysis of the traveling-wave tube amplifier, the helix circuit can be approximated as the helical sheath model and its result is in quite good agreement, but the meander circuit model is a more complicated structure. The complexity of the meander model may be deduced if the meander tape can be reduced by taking an infinite radius in the helical tape. The quasi-helix model will then be chosen for our structure.

The TM and TE modes can be determined by the fact that they are coupled by the boundary conditions of the meander circuit tape. It means that both the TE and TM waves must be excited in the actual device due to the meander circuit structure, but these modes in the semiconductor need not be strongly coupled. This will be discussed later.

The electromagnetic field in various regions can be obtained by solving the second order partial differential equation, Eq. (4.3.2) with the given boundary conditions. In rectangular coordinates, the electromagnetic fields in circuit regions are:

#### A. Region III ( $x \geq d$ )

##### TM wave

$$E_{1z} = F_1 e^{-\gamma_1 x} \quad (4.3.4)$$

$$E_{1x} = \frac{jk}{\gamma_1} F_1 e^{-\gamma_1 x} \quad (4.3.5)$$

$$H_{1y} = \frac{j\omega\epsilon_1}{\gamma_1} F_1 e^{-\gamma_1 x} \quad (4.3.6)$$

TE wave

$$E_{1y} = G_1 e^{-\gamma_1 x} \quad (4.3.7)$$

$$H_{1x} = \frac{-k \epsilon_1 c_1^2}{\omega} G_1 e^{-\gamma_1 x} \quad (4.3.8)$$

$$H_{1z} = \frac{-j \gamma_1 \epsilon_1 c_1^2}{\omega} G_1 e^{-\gamma_1 x} \quad (4.3.9)$$

B. Region I (  $0 \leq x \leq d$  )TM wave

$$E_{1z} = F_2 e^{-\gamma_1 x} - F_3 e^{\gamma_1 x} \quad (4.3.10)$$

$$E_{1x} = \frac{-jk}{\gamma_1} (F_2 e^{-\gamma_1 x} - F_3 e^{\gamma_1 x}) \quad (4.3.11)$$

$$H_{1y} = \frac{-j\omega\epsilon_1}{\gamma_1} (F_2 e^{-\gamma_1 x} - F_3 e^{\gamma_1 x}) \quad (4.3.12)$$

TE wave

$$E_{1y} = G_2 e^{-\gamma_1 x} + G_3 e^{\gamma_1 x} \quad (4.3.13)$$

$$H_{1x} = \frac{-k \epsilon_1 c_1^2}{\omega} (G_2 e^{-\gamma_1 x} + G_3 e^{\gamma_1 x}) \quad (4.3.14)$$

$$H_{1z} = \frac{-j \gamma_1 \epsilon_1 c_1^2}{\omega} (G_2 e^{-\gamma_1 x} - G_3 e^{\gamma_1 x}) \quad (4.3.15)$$

where  $F_1$ ,  $F_2$ ,  $F_3$ ,  $G_1$ ,  $G_2$  and  $G_3$  are all unknown coefficients, and  $e^{j(\omega t - kz)}$  is suppressed in all solutions.

4.4 General Field Analysis in the Circuit Region

In the preceding section, the electromagnetic fields were solved when the same insulating materials are used on both the top and bottom of the slow-wave circuit. In general, different materials with different permittivities are used on different parts of the structure. The other insulator (or free dielectric) with permittivity  $\epsilon_3$  for various generalizations is assumed in Region III as shown in Figure 4.3.1.

Similar to the previous steps, the field solutions in Region III can be written as follows:

TM wave

$$E_{1z} = F_1 e^{-\gamma_3 x} \quad (4.4.1)$$

$$E_{1x} = \frac{-jk}{\gamma_3} F_1 e^{-\gamma_3 x} \quad (4.4.2)$$

$$H_{1y} = \frac{-j\omega\epsilon_3}{\gamma_3} F_1 e^{-\gamma_3 x} \quad (4.4.3)$$

where

$$\gamma_3^2 = k^2 - \beta_3^2 = k^2 - \omega^2 \mu_0 \epsilon_3 \quad (4.4.4)$$

TE wave

$$E_{1y} = G_1 e^{-\gamma_3 x} \quad (4.4.5)$$

$$H_{1x} = \frac{-k\epsilon_3 c^2}{\omega} G_1 e^{-\gamma_3 x} \quad (4.4.6)$$

$$H_{1z} = \frac{-j\gamma_3 \epsilon_3 c^2}{\omega} G_1 e^{-\gamma_3 x} \quad (4.4.7)$$

The solution type of electromagnetic fields in Region I is identical to those in Eq. (4.3.10) through Eq. (4.3.15). Field solutions around the circuit region are listed in Appendix B.

#### 4.5 Formulation of Linear Equations and Determination of Unknown Coefficients for the Coupled System

We have discussed field solutions for the whole system in Chapters III and IV, but we have not dealt with the determination of unknown coefficients in the field solutions. Now we are in a position to apply all boundary conditions in Section 3.4 and 4.2, to formulate linear equations for the coupled system and then to interrelate all coefficients in terms of  $A_1$ .

For convenience, let us consider the boundary conditions for the lower half region of the system, including the semiconductor slab.

The normal rf velocity vanishes at the semiconductor boundaries, accordingly two linear equations are obtained,

$$(A_1 - A_2) - (A_3 - A_4) R = 0 \quad (4.5.1)$$

$$(A_1 e^{-a\delta} - A_2 e^{a\delta}) - (A_3 e^{-b\delta} - A_4 e^{b\delta}) R = 0 \quad (4.5.2)$$

$$\text{where } R = (ab) \left[ -\frac{1-j1/g}{a^2-jb^2/g} + \left(\frac{v_t}{\omega_p}\right)^2 \left( \frac{b^2(1-j1/g)}{a^2-jb^2/g} - 1 \right) \right] \quad (4.5.3)$$

Further, the tangential boundary condition of electric and magnetic fields at  $x = -\delta$  gives four equations. For the TM waves one has

$$A_1 e^{-a\delta} + A_2 e^{a\delta} + A_3 e^{-b\delta} + A_4 e^{b\delta} = F_4 e^{-\gamma_4 \delta} \quad (4.5.4)$$

$$\begin{aligned} & \frac{\epsilon_2 c_2^2}{j\omega} \frac{a^2 - k^2}{a} (A_1 e^{-a\delta} - A_2 e^{a\delta}) + \frac{a^2 - k^2 - j(b - k^2)/g}{a^2 - j b^2/g} b (A_3 e^{-b\delta} - A_4 e^{b\delta}) \\ &= \frac{j\omega\epsilon_4}{\gamma_4} F_4 e^{-\gamma_4 \delta} \end{aligned}$$

or

$$h_1 (A_1 e^{-a\delta} - A_2 e^{a\delta}) + h_2 (A_3 e^{-b\delta} - A_4 e^{b\delta}) = F_4 e^{-\gamma_4 \delta} \quad (4.5.5)$$

where

$$h_1 = \left(\frac{\epsilon_2}{\epsilon_4}\right) \left(\frac{c_2}{\omega}\right)^2 \left(\frac{\gamma_4}{a}\right) (k^2 - a^2) \quad (4.5.6)$$

$$h_2 = \left(\frac{\epsilon_2}{\epsilon_4}\right) \left(\frac{c_2}{\omega}\right)^2 (\gamma_4 b) \frac{(k^2 - a^2) + j \frac{b^2 - k^2}{g}}{a^2 - j \frac{b^2}{g}} \quad (4.5.7)$$

and for the TE waves

$$B_1 e^{-a\delta} + B_2 e^{a\delta} = G_4 e^{-\gamma_4 \delta} \quad (4.5.8)$$

$$\frac{j\epsilon_2 c_2^2 a}{\omega} (B_1 e^{-a\delta} - B_2 e^{a\delta}) = \frac{j\gamma_4 \epsilon_4 c_4^2}{\omega} G_4 e^{-\gamma_4 \delta} \quad (4.5.9)$$

Thus, for the semiconductor region, six equations have been formulated, which determine the characteristics of a carrier stream in solid-state materials.

By manipulating Eqs. (4.5.4) and (4.5.5), the set of six equations can be written in two simple forms

$$\begin{bmatrix} 1 & R & -R \\ 1 & Re^{-(a+b)\delta} & Re^{(-a+b)\delta} \\ (1+h_1)e^{a\delta} & (1-h_2)e^{-b\delta} & (1+h_2)e^{b\delta} \end{bmatrix} \begin{bmatrix} A_2 \\ A_3 \\ A_4 \end{bmatrix} = \begin{bmatrix} 1 \\ e^{-2a\delta} \\ (h_1-1)e^{-a\delta} \end{bmatrix} A_1 \quad (4.5.10)$$

and for the TE waves

$$\begin{bmatrix} e^{-a\delta} & e^{a\delta} \\ e^{-a\delta} & -e^{a\delta} \end{bmatrix} \begin{bmatrix} B_1 \\ B_2 \end{bmatrix} = \begin{bmatrix} 1 \\ \frac{\gamma_4}{a} \end{bmatrix} e^{-\gamma_4\delta} G_4 \quad (4.5.11)$$

After a few algebraic operations Eq. (4.5.10) leads to a coefficient expression in terms of  $A_1$ , namely

$$\begin{bmatrix} A_2 \\ A_3 \\ A_4 \end{bmatrix} = \begin{bmatrix} \Pi_2 \\ \Pi_3 \\ \Pi_4 \end{bmatrix} A_1 \quad (4.5.12)$$

where

$$\Pi_2 = \frac{e^{a\delta} - (h_2 + R(h_1-1)) \sinh b\delta - \cosh b\delta}{e^{-a\delta} - (h_2 + R(h_1+1)) \sinh b\delta - \cosh b\delta} \cdot e^{-2a\delta} \quad (4.5.13)$$

$$\Pi_3 = \frac{e^{(-2a+b)\delta} (1 + h_2 + R(h_1-1)) - e^{b\delta} (1 + h_2 + R(h_1+1)) + 2Re^{-a\delta}}{2R [e^{-a\delta} - (h_2 + R(h_1+1)) \sinh b\delta - \cosh b\delta]} \quad (4.5.14)$$

$$\Pi_4 = \frac{e^{(-2a+b)\delta} (h_1-1 + R(h_1-1)) - e^{-b\delta} [(h_2-1) + R(h_1+1)] + 2Re^{-a\delta}}{2R [e^{-a\delta} - (h_2 + R(h_1+1)) \sinh b\delta - \cosh b\delta]} \quad (4.5.15)$$

Similarly, all relations in case of a collision dominated stream are reduced to little simpler forms, replacing  $a$  by  $a_1$ ,  $b$  by  $b_1$  and  $g$  by  $g_1$  in the above equations. The collisionless case is also obtained even if it is not realistic in most semiconductors.

The expression for  $F_4$  may be obtained directly from Eqs. (4.5.4) and (4.5.12), in the ratio of  $A_1$ ,

$$\frac{F_4}{A_1} = e^{(-a+\gamma_4)\delta} + \Pi_2 e^{(a+\gamma_4)\delta} + \Pi_3 e^{(-b+\gamma_4)\delta} + \Pi_4 e^{(b+\gamma_4)\delta} \quad (4.5.16)$$

Up to this point, four unknown coefficients in the ratio of  $A_1$  have been determined. The remaining coefficients can be obtained by supplementing linear equations about the slow-wave circuit.

Around the slow-wave circuit, the first condition is that the tangential component of the electric field is continuous. Hence

$$F_1 e^{-\gamma_3 d} = F_2 e^{-\gamma_1 d} + F_3 e^{\gamma_1 d} \quad (4.5.17)$$

$$G_1 e^{-\gamma_3 d} = G_2 e^{-\gamma_1 d} + G_3 e^{\gamma_1 d} \quad (4.5.18)$$

The next condition is that the electric field perpendicular to the direction of conduction is continuous; thus

$$G_1 e^{-\gamma_3 d} \cos \psi + F_1 e^{-\gamma_3 d} \sin \psi = 0 \quad (4.5.19)$$

or

$$G_1 = -F_1 \tan \psi$$

and that the tangential component of the magnetic field parallel to the direction of conduction is continuous, which yields

$$\begin{aligned} & \omega^2 \epsilon_1 \gamma_3 (F_2 - F_3 e^{2\gamma_1 d}) + c_1^2 \epsilon_1 \gamma_1^2 \gamma_3 (G_2 - G_3 e^{2\gamma_1 d}) \tan \psi \\ &= \omega^2 \epsilon_1 \gamma_1 F_1 e^{(\gamma_1 - \gamma_3)d} + c_3^2 \epsilon_3 \gamma_1 \gamma_3^2 G_1 e^{(\gamma_1 - \gamma_3)d} \tan \psi \end{aligned} \quad (4.5.20)$$

Finally one applies the condition that the tangential component of fields at the semiconductor slab  $x = 0$  is continuous and hence four more equations are obtained, for the TM waves

$$A_1 + A_2 + A_3 + A_4 = F_2 + F_3 \quad (4.5.21)$$

$$\Delta_0 h_1 (A_1 - A_2) + \Delta_1 h_2 (A_3 - A_4) = F_2 - F_3 \quad (4.5.22)$$

where

$$\Delta_0 = \frac{\epsilon_4 \gamma_1}{\epsilon_1 \gamma_4}$$

and for the TE waves

$$B_1 + B_2 = G_2 + G_3 \quad (4.5.23)$$

$$B_1 - B_2 = -\frac{\gamma}{a} (G_2 - G_3) \quad (4.5.24)$$

Fourteen independent homogeneous equations for fourteen coefficients have been obtained for the configuration sample.

Algebraic manipulation of the above equations determines general forms of the rest of unknown coefficients, with the result

$$\frac{B_1}{A_1} = \frac{2(1 + \Pi_2 + \Pi_3 + \Pi_4)}{-Z_1 + Z_2} \quad (4.5.25)$$

where

$$N_1 = (1 + \frac{a - \gamma_4}{a + \gamma_4} e^{-2a\delta} \cosh \gamma_1 d + \frac{a}{\gamma_4} (1 - \frac{a - \gamma_4}{a + \gamma_4} e^{-2a\delta}) \sinh \gamma_1 d) \quad (4.5.26)$$

$$Z_1 = \frac{N_1 e^{\gamma_1 d}}{\tan \psi} (1 + e^{-2\gamma_1 d}) \quad (4.5.27)$$

$$K_1 = \frac{1}{2} (1 - \frac{a}{\gamma_1}) + \frac{e^{-2a\delta}}{2} \cdot \frac{a - \gamma_4}{a + \gamma_4} (1 + \frac{a}{\gamma_1}) \quad (4.5.28)$$

$$K_2 = \frac{1}{2} (1 + \frac{a}{\gamma_1}) + \frac{e^{-2a\delta}}{2} \cdot \frac{a - \gamma_4}{a + \gamma_4} (1 - \frac{a}{\gamma_1}) \quad (4.5.29)$$

$$Z_2 = \left[ \left\{ \frac{\gamma_1^2 c_1^2}{\omega^2} (K_2 e^{2\gamma_1 d} - K_1) + \frac{c_3^2 \epsilon_3 \gamma_3 \gamma_1 N_1 e^{\gamma_1 d}}{\omega^2 E_1} \right\} \tan \psi - \frac{\epsilon_3 \gamma_1}{\epsilon_1 \gamma_3} \frac{N_1 e^{\gamma_1 d}}{\tan \psi} \right] (1 - e^{-2\gamma_1 d}) \quad (4.5.30)$$

$$\frac{B_2}{A_1} = e^{-2a\delta} \cdot \frac{a - \gamma_4}{a + \gamma_4} \cdot \frac{1 + \Pi_2 + \Pi_3 + \Pi_4}{-Z_1 + Z_2} \quad (4.5.31)$$

$$\frac{F_1}{A_1} = \frac{2N_1 e^{-\gamma_3 d}}{\tan \psi} \cdot \frac{1 + \Pi_2 + \Pi_3 + \Pi_4}{Z_1 - Z_2} \quad (4.5.32)$$

$$\frac{F_2}{A_1} = \frac{1 + \Pi_2 + \Pi_3 + \Pi_4}{-Z_1 + Z_2} \cdot \left( \frac{Z_2}{1 - e^{-2\gamma_1 d}} - \frac{Z_1}{1 + e^{-2\gamma_1 d}} \right) \quad (4.5.33)$$

$$\frac{F_3}{A_1} = \frac{1 + \Pi_2 + \Pi_3 + \Pi_4}{-Z_1 + Z_2} \cdot \left( \frac{Z_2}{e^{2\gamma_1 d} - 1} + \frac{Z_1}{e^{2\gamma_1 d} + 1} \right) \quad (4.5.34)$$

$$\frac{G_1}{A_1} = \frac{2N_1 (1 + \Pi_2 + \Pi_3 + \Pi_4) e^{\gamma_3 d}}{-Z_1 + Z_2} \quad (4.5.35)$$

$$\frac{G_2}{A_1} = \frac{2K_1 (1 + \Pi_2 + \Pi_3 + \Pi_4)}{-Z_1 + Z_2} \quad (4.5.36)$$

$$\frac{G_3}{A_1} = \frac{2K_2 (1 + \Pi_2 + \Pi_3 + \Pi_4)}{-Z_1 + Z_2} \quad (4.5.37)$$

and

$$\frac{G_4}{A_1} = \frac{4a (1+\Pi_2 + \Pi_3 + \Pi_4)}{(-Z_1 + Z_2) (a + \gamma_4)} e^{(\gamma_4 - a)\delta} \quad (4.5.38)$$

Therefore, there are fourteen unknown coefficients in field analysis of the system and they are all interrelated as shown in this section.



## CHAPTER V

### DISPERSION AND GAIN CHARACTERISTICS OF INTERACTION BETWEEN CARRIER WAVES AND SLOW CIRCUIT WAVES

#### 5.1 Introduction

In order to investigate the behavior of the coupling effect of a tape circuit with carrier waves, it is necessary to have a detailed description of their dispersion characteristics. In the characteristic equation most of the important information of the waves is obtained. As was mentioned in Section 2.5, all quantities are assumed to be separated into dc and ac terms of the form  $\vec{A} = \vec{A}_0 + \vec{A}_1 e^{j(\omega t - kz)}$ . The effective mass of carriers  $m^*$  is considered to be a scalar constant. In addition, the carrier collision frequency is assumed independent of carrier velocity.

The dispersion characteristics can be obtained by matching the wave admittance functions of two systems at the circuit-semiconductor boundary. Another alternative of deriving the dispersion relation is to set the determinant of the coefficients matrix equal to zero for a non-trivial solution. This chapter deals with two ways of finding characteristic equations, compares these equations, and afterwards gain relations are derived. Numerical solutions will be plotted using a CDC 6500 computer.

Dispersion characteristic equations for some cases are derived in Section 5.2. Section 5.3 is concerned with some appropriate approximations made for some typical cases, and dispersion and gain relations are accordingly obtained. Section 5.4 introduces normalized constants. The

last two sections investigate the effects of collision frequency, slow-wave circuit velocity, carrier drift velocity and insulating layer thickness.

## 5.2 Dispersion Relations for Carrier Wave Interactions

In this section, we first try to formulate a general dispersion equation relating to solid-state traveling-wave amplifier devices. To achieve that, two methods are used, namely, the field coefficients matrix method and the wave admittance matching method. As has been discussed earlier, in connection with the method of solution, these two methods are based upon the fact that the slow circuit waves are propagating with a phase velocity equal to the carrier drift velocity (i.e., they are synchronized).

Following that we consider the special case of carrier interaction from the point of view of a collision dominated stream.

### 5.2.1 General Dispersion Relation

#### A. Field Coefficients Matrix

As was derived in Section 4.5, application of the boundary conditions to the structure configuration produces fourteen homogeneous linear equations subject to fourteen coefficients. These linear equations may be written in a simple matrix form.

$$[A] [X] = 0 \quad (5.2.1)$$

where  $[X]^T = [A_1, A_2, A_3, A_4, B_1, B_2, F_1, F_2, F_3, F_4, G_1, G_2, G_3, G_4]$  and  $[A]$  is the field coefficients matrix defined in Figure 5.2.1.

A necessary and sufficient condition for a nontrivial solution to Eq. (5.2.1) is that the determinant of the field coefficients matrix  $[A]$  be zero.



Using row operations of the matrix algebra to reduce the size of a 14 x 14 square matrix, we obtain the following 9 x 9 matrix, after long algebraic rearrangement,

$$\left[ \begin{array}{cccccccccc} 1 & -1 & -R & R & & & & & & \\ 1/f^2 & -1 & -R/fg & Rg/f & & & & & & \\ (1-h_1)/f & (1+h_1)/f & (1-h_1^2)/g & (1+h_2)/g & & & & & & \\ \Delta_o h_1 & -\Delta_o h_1 & \Delta_o h_2 & -\Delta_o h_2 & & & -1 & 1 & & \\ 1 & 1 & 1 & 1 & & & -1 & -1 & & \\ & & & & & & -1 & 1 & u^2 & \\ & & & & & K_1 + u^2 K_2 & & & & -1 \\ & & & & & \tan \psi & & & & 1 \\ & & & & \Delta_1 (K_1 - u^2 K_2) & -\Delta_2 & 1 & -u^2 & -\Delta_3 & \end{array} \right] \quad (5.2.2)$$

where  $f = e^{a\delta}$ ,  $g = e^{b\delta}$ , and  $u = e^{\gamma d}$ .

This equation does not seem to be appropriate in taking it as a final form for the characteristic equation and hence further reduction should be carried out. Reducing the sixth column and the ninth column in order and taking the determinant the matrix yield a comparatively simple 7 x 7 matrix of the form,

$$\det \left[ \begin{array}{cccccccc} 1 & -1 & -R & R & & & & \\ 1/f^2 & -1 & -R/fg & Rg/f & & & & \\ (1-h_1)/f & (1+h_1)/f & (1-h_2)/g & (1+h_2)/g & & & & \\ 1 & -1 & h_2/h_1 & -h_2/h_1 & & -1/\Delta_o h_1 & 1/\Delta_o h_1 & \\ 1 & 1 & 1 & 1 & & -1 & -1 & \\ & & & & Z_1/(1+\frac{1}{u^2}) & 1 & u^2 & \\ & & & & Z_2/(1-\frac{1}{u^2}) & 1 & -u^2 & \end{array} \right] = 0 \quad (5.2.3)$$

Applying the Laplace expansion theorem to Eq. (5.2.3), this determinant can be expanded as follows:

$$D_1 \cdot D_2 - D_3 \cdot D_4 = 0 \quad (5.2.4)$$

where

$$D_1 = \begin{vmatrix} 1 & -1 & -R & R \\ 1/f^2 & -1 & -R/fg & Rg/f \\ (1-h_1)/f & (1+h_1)f & (1-h_2)/g & (1+h_2)g \\ 1 & -1 & h_2/h_1 & -h_2/h_1 \end{vmatrix} = \det B \left[ 1 - \Pi_2 + \frac{h_2}{h_1}(\Pi_3 - \Pi_4) \right]$$

$$\det B = \begin{vmatrix} -1 & -R & R \\ -1 & -R/fg & Rg/f \\ (1+h_1)f & (1-h_2)/g & (1+h_2)g \end{vmatrix}$$

$$D_2 = \begin{vmatrix} 0 & -1 & -1/4 \\ Z_1 u^2 / (1+u^2) & 1 & 1 \\ Z_2 u^2 / (1-u^2) & 1 & -1 \end{vmatrix} = -u^2 \left( \frac{Z_1}{1+u^2} + \frac{Z_2}{1-u^2} \right) - \left( \frac{Z_1}{1+u^2} - \frac{Z_2}{1-u^2} \right)$$

$$D_3 = \begin{vmatrix} 1 & -1 & -R & R \\ 1/f^2 & -1 & -R/fg & Rg/f \\ (1-h_1)/f & (1+h_1)f & (1-h_2)/g & (1+h_2)g \\ 1 & 1 & 1 & 1 \end{vmatrix} = \det B (1 + \Pi_2 + \Pi_3 + \Pi_4)$$

and

$$D_4 = \begin{vmatrix} 0 & -1/\Delta_o h_1 & 1/\Delta_o h_1 u^2 \\ Z_1 u^2 / (1+u^2) & 1 & 1 \\ Z_2 u^2 / (1+u^2) & 1 & -1 \end{vmatrix} = \frac{1}{\Delta_o h_1} \left[ -u^2 \left( \frac{Z_1}{1+u^2} + \frac{Z_2}{1-u^2} \right) + \left( \frac{Z_1}{1+u^2} - \frac{Z_2}{1-u^2} \right) \right]$$

Since Eq. (5.2.4) is a result of  $\det [A] = 0$ , it is clear that this equation represents the dispersion relation of the system. We now

substitute four determinants,  $D_1, D_2, D_3, D_4$  into the dispersion equation then the corresponding expression is

$$\frac{\Delta_0 h_1 (1 - \Pi_2) + \Delta_0 h_2 (\Pi_3 - \Pi_4)}{1 + \Pi_2 + \Pi_3 + \Pi_4} = \frac{K_3 (\Gamma_1 + \tanh \gamma_1 d) - K_4 (\Gamma_2 - \tanh \gamma_1 d)}{-K_3 (\Gamma_1 \tanh \gamma_1 d + 1) + K_4 (\Gamma_2 \tanh \gamma_1 d - 1)} \quad (5.2.5)$$

where

$$K_3 = (1 + e^{-2\gamma_1 d}) \left( \frac{\gamma_1 - a}{\gamma_1 + a} - \frac{\gamma_4 - a}{\gamma_4 + a} e^{-2a\delta} \right)$$

$$K_4 = (1 + e^{2\gamma_1 d}) \left( 1 - \frac{(\gamma_4 - a)(\gamma_1 - a)}{(\gamma_4 + a)(\gamma_1 + a)} e^{-2a\delta} \right)$$

$$\Gamma_1 = \gamma_1 \left( \frac{\gamma_1}{\beta_{s1}^2} + \frac{\epsilon_3 \gamma_3}{\beta_{s3}^2} \pm \frac{\epsilon_3}{\epsilon_1 \gamma_3} \right)$$

$$\beta_{s1} = \frac{\omega}{v_{s1}} = \frac{\omega}{c_1 \tan \psi} = \text{circuit propagation constant in medium I}$$

$$\beta_{s3} = \frac{\omega}{v_{s3}} = \frac{\omega}{c_3 \tan \psi} = \text{circuit propagation constant in medium III}$$

and  $v_{s1}, v_{s3}$  represent circuit phase velocities in each medium. Eq.

(5.2.5) is an exact final form which has been derived without making any approximations.

The dispersion equation can be simplified by arranging the left hand side of Eq. (5.2.5). Hence, one has

$$\begin{aligned} & \frac{K_3 (\Gamma_1 + \tanh \gamma_1 d) - K_4 (\Gamma_2 - \tanh \gamma_1 d)}{-K_3 (\Gamma_1 \tanh \gamma_1 d + 1) + K_4 (\Gamma_2 \tanh \gamma_1 d - 1)} \cdot \frac{\gamma_4 \epsilon_1}{\gamma_1 \epsilon_4} \\ &= \frac{(h_1 + h_2/R) \cosh b\delta + R(h_1 + h_2/R)(h_1 + h_2/R + 1) \sinh b\delta}{-8e^{-a\delta} + (h_1 + h_2/R + 2) \cosh b\delta + [R + 1/R + R(h_1 + h_2/R)] \sinh b\delta} \end{aligned}$$

provided that  $a\delta \ll 1$ .

Eq. (5.2.6) is almost an exact expression giving the nature and propagation characteristics of waves in the coupled system.

#### B. Admittance Matching Method

Equating the carrier wave admittance to the circuit wave admittance leads to the dispersion relation whose details are shown in

Appendix C. The relation obtained from  $Y^S = Y^C$  yields Eq. (5.2.5).

Therefore, the dispersion characteristic equation resulting from the admittance matching method is identical to that expressed by the field coefficients matrix method.

We conclude that two methods lead to the same dispersion equation in any cases and must be rigorous at the same time if one way or another is right.

### 5.5.2 Dispersion Relation in a Collision Dominated Stream

The dispersion relation, Eq. (5.2.5), as it shows now, is quite complicated and some reasonable approximations, which are discussed in Appendix C, are required in permitting an investigation as to the possibilities and the general trend of growing waves. Taking these approximations such as  $\gamma_1 \approx \gamma_3 \approx \gamma_4 = k$ ,  $a \approx k$  and  $b \approx \omega_p / v_t$ , we may arrive at the simple form of the dispersion equation.

If  $v \gg |\omega - ku_0|$ , the dispersion relation is obtained by letting  $w_v = -jv$ . With the same type of insulating layers on the top and bottom of the slow-wave circuit, the dispersion equation becomes

$$\frac{(1 + e^{2kd})k^2 - \beta_{s1}^2 e^{2kd}}{(1 - e^{kd})k^2 + \beta_{s1}^2 e^{2kd}} = \kappa \cdot \frac{E \cosh(\omega_p / v_t) + j S \sinh(\omega_p^\delta / v_t)}{T \cosh(\omega_p^\delta / v_t) + j W \sinh(\omega_p^\delta / v_t)} \quad (5.2.7)$$

where

$$\kappa = \frac{\epsilon_2}{\epsilon_1} \quad (5.2.8)$$

$$E = E_0 + E_1 k + E_2 k^2 \quad (5.2.9)$$

$$S = S_0 + S_1 k + S_2 k^2 \quad (5.2.10)$$

$$T = T_0 + T_1 k + T_2 k^2 \quad (5.2.11)$$

$$W = W_0 + W_1 k + W_2 k^2 \quad (5.2.12)$$

$$E_0 = u_0 \left( \frac{\omega}{c_2} \right)^2 \left[ \left( \frac{\omega p}{v} \right)^2 \left( \frac{v t}{c_2} \right)^2 - 1 + j \frac{\omega u_0}{c_2^2 v} \omega p^2 + \omega^2 \left( \frac{v t}{c} \right)^2 \right]$$

$$E_1 = \omega \left[ \left( \frac{u_0}{c_2} \right)^2 + \left( 1 - \left( \frac{\omega}{v} \right)^2 \left( \frac{v t}{c_2} \right)^2 \right)^4 - 2 \left( \frac{\omega p v t}{v c_2} \right)^2 \right] - j \left[ \frac{\omega p}{v} \left( 1 - \left( \frac{\omega}{v} \right)^2 \left( \frac{v t}{c_2} \right)^2 \right)^4 + 2 \frac{1}{v} \left( \frac{v t}{c_2} \right)^2 \right]$$

$$E_2 = -u_0 + j u_0 \left( \frac{\omega}{v} \right) \left( \frac{v t}{c_2} \right)^2$$

$$S_0 = \frac{1}{v t} \left[ \frac{\omega^2}{\omega p} v \left( 1 + \frac{\epsilon_2}{\epsilon_4} \right) - \frac{\epsilon_2}{\epsilon_4} \frac{\omega p^3}{v} \right] \left[ 1 - \left( \frac{\omega}{v} \right)^2 \left( \frac{v t}{c_2} \right)^4 \right] - 2 \frac{\omega^2 v t \omega p}{v c_2^2} \left( 1 + 2 \frac{\epsilon_2}{\epsilon_4} + j \omega \right)$$

$$\left[ 2 \left( \frac{\epsilon_2}{\epsilon_4} \right) \left( \frac{v t}{c_2} \right) \left( \frac{\omega p^3}{v^2} - \frac{\omega^2}{\omega p} \left( 1 + \frac{\epsilon_4}{\epsilon_2} \right) \right) - \left( \frac{\omega p}{v t} \right) \left( 1 + \frac{\epsilon_2}{\epsilon_4} \right) \left\{ 1 - \left( \frac{\omega}{v} \right)^2 \left( \frac{v t}{c_2} \right)^4 \right\} \right]$$

$$S_1 = \omega u_0 \left[ \left( 1 + 2 \frac{\epsilon_2}{\epsilon_4} \right) \left( \frac{\omega p}{v} \right) \left( \frac{v t}{c_2} \right) - 2 \left( 1 + \frac{\epsilon_2}{\epsilon_4} \right) \left( \frac{v}{\omega p v t} \right) \right] + j u_0 \left[ \left( 1 + 2 \frac{\epsilon_2}{\epsilon_4} \right) \left( \frac{\omega p}{v t} + \frac{\omega^2 v}{\omega p c_2^2} \right) + \left( \frac{v t}{\omega p} \right) \left( \frac{\omega}{c_2} \right)^2 \right]$$

$$S_2 = \frac{v u_0^2}{\omega p v t} \left( 1 + \frac{\epsilon_2}{\epsilon_4} \right)$$

$$T_0 = u_0 \left( \frac{\omega}{c_2} \right)^2 \left[ \frac{\epsilon_2}{\epsilon_4} \left( \frac{\omega p v t}{v} \right)^2 - \left( 2 + \frac{\epsilon_2}{\epsilon_4} \right) \right] + j \frac{\omega u_0}{v c_2^2} \left[ \frac{\epsilon_2}{\epsilon_4} + \left( 2 + \frac{\epsilon_2}{\epsilon_4} \right) \left( \frac{\omega v t}{c_2} \right)^2 \right]$$

$$T_1 = \omega \left( 2 + \frac{\epsilon_2}{\epsilon_4} \right) \left[ 1 + \left( \frac{u_0}{c_2} \right)^2 - \left( \frac{\omega}{v} \right)^2 \left( \frac{v t}{c_2} \right)^4 \right] - 2 \left( \frac{\epsilon_2}{\epsilon_4} \right) \omega \left( \frac{\omega p v t}{v c_2} \right)^2 + j \left( \frac{\omega}{v} \right) \left( \frac{v t}{c_2} \right)^2 \left[ \frac{\epsilon_2}{\epsilon_4} \left( \frac{v t \omega p}{c_2 v} \right)^2 \omega - 2 \omega - \frac{\omega p^2}{v} \right] - 4 \omega$$

$$T_2 = u_0 \left( 2 + \frac{\epsilon_2}{\epsilon_4} \right) \left[ -1 + j \frac{\omega}{v} \left( \frac{v t}{c_2} \right)^2 \right]$$

$$W_0 = \left( \frac{v}{\omega p} \right) \left( \frac{\omega^2}{v t} \right) \left( 1 + \frac{\epsilon_2}{\epsilon_4} \right) \left( 1 - \left( \frac{\omega}{v} \right)^2 \left( \frac{v t}{c_2} \right)^4 \right) - \frac{\omega p v t}{v} \left( \frac{\omega}{c_2} \right)^2 \left[ 2 \left( \frac{\epsilon_2}{\epsilon_4} \right) + \left( \frac{u_0}{c_2} \right)^2 \right] - j \omega$$

$$\left[ 2 \left( 1 + \frac{\epsilon_2}{\epsilon_4} \right) \left( \frac{v t}{\omega p} \right) \left( \frac{\omega}{c_2} \right)^2 + \frac{\epsilon_2}{\epsilon_4} \left( \frac{\omega p}{v} \right) \left( 1 - \left( \frac{\omega}{v} \right)^2 \left( \frac{v t}{c_2} \right)^4 \right) \right]$$

$$W_1 = 2 \omega u_0 \left( 1 + \frac{\epsilon_2}{\epsilon_4} \right) \left[ \frac{\omega p v t}{v c_2^2} - \frac{v}{\omega p v t} \right] - \left( \frac{\epsilon_2}{\epsilon_4} \right) \frac{\omega p v t \omega u_0}{v c_2^2} + j u_0 \left[ \frac{2 \omega^2 v t}{\omega p c_2^2} \left( 1 + \frac{\epsilon_2}{\epsilon_4} \right) - 2 \left( \frac{\omega}{v} \right)^2 \right]$$

$$\left( \frac{v t}{c_2} \right)^3 \left( \frac{\omega p}{c_2} \right) + \frac{\epsilon_2}{\epsilon_4} \left( \frac{\omega p}{v t} \right) \right]$$



1

and

$$W_2 = (1 + \frac{\epsilon_2}{\epsilon_4}) \frac{v u_0^2}{\omega_p v_t} - \frac{\omega_p v_t}{v} (1 - (\frac{\omega}{v}) (\frac{v_t}{c_2})^4) + j2 \frac{\omega_p v_t^3 \omega}{v^2 c_2^2}$$

It is, however, a wellknown fact that the wave can best be amplified when the drift velocity is nearly equal to the velocity of the rf slow circuit wave. When this occurs, it is usually referred to as synchronous coupling. Therefore, if a device is used under this situation, the value of  $|\omega - ku_0|$  may not be a significant quantity. Actually the collision frequency in most cases could always be considered as much higher than  $|\omega - ku_0|$  and thus a general case might be reduced to the case of collision dominated stream.

### 5.3 Relations of Dispersion Characteristic and Gain

In practice, when the device is fabricated it is much easier to choose a single material for the insulating layers. Therefore, this case will be taken for our analysis hereafter.

The bottom insulating layer of the circuit is not also required when the ideal capacitively coupled circuit is to be used. Hence, with  $d = 0$ , the dispersion relation becomes

$$2(\frac{k}{\beta_{s1}})^2 - 1 = \kappa \cdot \frac{E + jS \tanh(\frac{\omega_p \delta}{v_t})}{T + jW \tanh(\frac{\omega_p \delta}{v_t})} \quad (5.3.1)$$

In actual device fabrication, the insulating layer,  $d$ , is a few microns thick and then one may use the approximation of  $e^x \doteq 1+x$  for small  $x$  ( $x \ll 1$ ). Therefore, the characteristic equation for dispersion is

$$\frac{\beta_{s1}^2 - 2k^2(1-kd)}{2k^3d - \beta_{s1}^2} = \kappa \cdot \frac{E + jS \tanh(\frac{\omega_p \delta}{v_t})}{T + jW \tanh(\frac{\omega_p \delta}{v_t})} \quad (5.3.2)$$

and in polynomial form it can be rewritten as

$$A_5 k^5 + A_4 k^4 + A_3 k^3 + A_2 k^2 + A_1 k^1 + A_0 = 0 \quad (5.3.3)$$

where

$$A_5 = 2d(T_2 - \kappa E_2) + j2d(W_2 - \kappa S_2) \tanh(\omega_p \delta / v_t) \quad (5.3.4)$$

$$A_4 = 2[d(T_1 - \kappa E_1) - T_2] + j 2[d(W_1 - \kappa S_1) - W_2] \tanh(\omega_p^\delta / V t) \quad (5.3.5)$$

$$A_3 = 2[d(T_0 - \kappa E_0) - T_1] + j 2[d(W_0 - \kappa S_0) - W_1] \tanh(\omega_p^\delta / V t) \quad (5.3.6)$$

$$A_2 = \beta_{s1}^2 (T_2 + \kappa E_2) - 2T_0 + j[\beta_{s1}^2 (W_2 + \kappa S_2) - 2W_0] \tanh(\omega_p^\delta / V t) \quad (5.3.7)$$

$$A_1 = \beta_{s1}^2 (T_1 + \kappa E_1) + j \beta_{s1}^2 (W_1 + \kappa S_1) \tanh(\omega_p^\delta / V t) \quad (5.3.8)$$

and

$$A_0 = \beta_{s1}^2 (T_0 + \kappa E_0) + j \beta_{s1}^2 (W_0 + \kappa S_0) \tanh(\omega_p^\delta / V t) \quad (5.3.9)$$

For better approximation one expresses the exponentials in their continued fraction approximation

$$e^x = 1 + \frac{12x}{12-6x+x^2} \quad \text{provided that } x \leq 1.$$

and then the sixth order polynomial is obtained as:

$$\frac{2d^2 k^4 + (6-d^2 \beta_{s1}^2) k^2 - 3d \beta_{s1}^2 k - 3 \beta_{s1}^2}{-6dk^3 + d^2 \beta_{s1}^2 k^2 + 3d \beta_{s1}^2 k + 3 \beta_{s1}^2} = K \cdot \frac{E + j S \tanh(\omega_p^\delta / V t)}{T + j W \tanh(\omega_p^\delta / V t)} \quad (5.3.10)$$

It can be easily seen that Eq. (5.3.10), of three dispersion relations, gives the best result in the frequency range of x-band, for our chosen semiconductor materials, InSb, Ge, Si, GaAs.

In general, an explicit analytical solution for fifth or sixth order polynomial may not always be feasible. Even if it is possible, it is too complicated to derive the final form. One way of solving higher order equation is to approximate with the aid of a computer, using numerical methods.

Once complex roots of  $k$  are obtained, in any way, the gain is also computed from the imaginary roots of  $k$  and is expressible as:

$$\text{Gain (db)} = 20 \log e^{(\text{Im } k) \cdot z}$$

Since  $\log_{10} e = 0.434$  and  $\text{Im } k = -\alpha$ , it becomes

$$\text{Gain (db)} = 8.68 \cdot (-\alpha) \cdot z \quad (5.3.11)$$

The gain in db per mm becomes

$$\text{Gain (db/mm)} = 8.68 \times 10^{-3} \cdot (-\alpha) \quad (5.3.12)$$

where  $\alpha$  is the metric unit.

This gain expression can also be expressed in db per wavelength.

$$\text{Gain (db/}\lambda_c) = \frac{2\pi}{\beta} \cdot \text{Gain (db/mm)} \times 10^3 \quad (5.3.13)$$

Instead of using db unit, the gain per micrometer is also used for the microwave devices in an exponential form such as

$$\text{Gain (}\mu\text{m)} = \text{Exp } (-\alpha \times 10^{-6}) \quad (5.3.14)$$

In each expression, the gain is proportional to the imaginary part of the propagation constant  $k$ .

#### 5.4 Wave Interaction Analysis with Numerical Method

The dispersion relation of Eq. (5.3.10) will be solved by a CDC 6500 computer. It is useful to introduce normalized quantities for computer programming. The propagation constant is chosen as a dependent variable and the other constants as independent variables. The dispersion equation can be put in terms of normalized constants.

The normalized operating frequency and collision frequency are defined as

$$q = \frac{\omega}{\omega_p} \quad (5.4.1)$$

$$s = \frac{\nu}{\omega_p} \quad (5.4.2)$$

Also the normalized drift velocity and slow circuit wave velocity are defined as

$$p = \frac{u_0}{v_t} \quad (5.4.3)$$

$$r = \frac{v_s}{v_t} \quad (5.4.4)$$

With the use of these normalized constants, the independent variables for device parameters will be manipulated as required in calculation.

The purpose of solving the equation is to find the complex roots of the propagation constant  $k$  with arbitrary complex coefficients. Each root is located approximately by the Lehmer method and then improved upon by Newton-Raphson method. Then a reduced polynomial is obtained by removing the first root. This process is repeated until all of the roots are removed. The detailed explanation of this method is given in Appendix D. Some typical values pertinent to the description of solid-state materials that will be used for the numerical analysis are illustrated in Table 5.4.1.

Redefining coefficients of  $k$  in Eq. (5.2.9) through Eq. (5.2.12) in terms of real and imaginary coefficients as

$$E_o = E_{or} + jE_{oi}$$

$$E_1 = E_{1r} + jE_{1i}$$

$$E_2 = E_{2r} + jE_{2i}$$

$$S_o = S_{or} + jS_{oi}$$

$$S_1 = S_{1r} + jS_{1i}$$

$$S_2 = S_{2r} + jS_{2i}$$

$$T_o = T_{or} + jT_{oi}$$

$$T_1 = T_{1r} + jT_{1i}$$

$$T_2 = T_{2r} + jT_{2i}$$

$$W_o = W_{or} + jW_{oi}$$

$$W_1 = W_{1r} + jW_{1i}$$

and

$$W_2 = W_{2r} + jW_{2i}$$

we arrived at the best approximate form of the dispersion characteristic equation with complex coefficients, which are rearranged by

TABLE 5.4.1  
TYPICAL NUMERICAL VALUES FOR SEVERAL SOLID-STATE MATERIALS

Material	Energy gap $E_g(\text{eV})$	Rel. perm. $\epsilon_r$	$m^*/m_e$	Mobility ( $\text{cm}^2/\text{v.s}$ )	Resistivity ( $\Omega\text{-cm}$ )	Drift velocity $u_0(\text{cm/sec})$	Density ( $\text{g/cm}^3$ )
Si	1.11	11.8	0.33	$1.2 \times 10^3$	45	$1 \times 10^6 - 2 \times 10^7$	$10^{14}$
				$3.8 \times 10^3$	60		$10^{14}$
Ge	0.67	16.0	0.04	$3.6 \times 10^3$	5	$6 \times 10^6 - 1 \times 10^7$	$10^{15}$
				$7.4 \times 10^3$	44.2		$10^{13}$
GaAs	1.53	12.5	0.072	$5.8 \times 10^3$	9.68	$6 \times 10^6 - 1 \times 10^7$	$10^{14}$
				$5.5 \times 10^3$	2.50		$10^{15}$
				$3.15 \times 10^5$	0.50		$10^{13}$
InSb	0.18	15.7	0.016	$5.45 \times 10^5$	0.031	$6 \times 10^7 - 9 \times 10^7$	$10^{14}$
				$4.0 \times 10^5$	0.013		$10^{15}$

$$B_6 k^6 + B_5 k^5 + B_4 k^4 + B_3 k^3 + B_2 k^2 + B_1 k + B_0 = 0 \quad (5.4.5)$$

where

$$X_0 = 3\beta_{s1}^2, \quad X_1 = dX_0, \quad X_2 = 6 - (d\beta_{s1})^2, \quad X_4 = 2d^2, \quad X_5 = 6d, \quad X_6 = (d\beta_{s1})^2$$

$$Q = \tanh(\omega_p \delta / v_t)$$

$$E_{01} = E_{or} - S_{oi} \cdot Q, \quad E_{02} = E_{oi} + S_{or} \cdot Q$$

$$E_{11} = E_{1r} - S_{1j} \cdot Q, \quad E_{12} = E_{li} + S_{ir} \cdot Q$$

$$E_{21} = E_{2r} - S_{2i} \cdot Q, \quad E_{22} = E_{2r} + S_{2r} \cdot Q$$

$$T_{01} = T_{or} - W_{oi} \cdot Q, \quad T_{02} = T_{oi} + W_{or} \cdot Q$$

$$T_{11} = T_{1r} - W_{li} \cdot Q, \quad T_{12} = T_{li} + W_{2r} \cdot Q$$

$$T_{21} = T_{2r} - W_{2i} \cdot Q, \quad T_{22} = T_{2i} + W_{2r} \cdot Q$$

$$B_6 = X_4(T_{21} + j T_{11})$$

$$B_5 = X_4(T_{11} + j T_{12}) + \kappa X_5(E_{21} + j E_{22})$$

$$B_4 = X_2(T_{21} + j T_{22}) + X_4(T_{01} + j T_{02}) + \kappa[X_5(E_{11} + j E_{12}) - X_6(E_{21} + j E_{22})]$$

$$B_3 = -X_1[(T_{21} + j T_{22}) + \kappa(E_{21} + j E_{22})] + X_2(T_{11} + j T_{12}) + \kappa(X_5(E_{01} + j E_{02}) - X_6(E_{11} + j E_{12}))$$

$$B_2 = -X_0[(T_{21} + j T_{22}) + \kappa(E_{21} + j E_{22})] - X_1[(T_{11} + j T_{12}) + \kappa(E_{11} + j E_{12})] + X_2(T_{01} + j T_{02}) - \kappa X_6(E_{01} + j E_{02})$$

$$B_1 = -X_0[(T_{11} + j T_{12}) + \kappa(E_{11} + j E_{12})] - X_1[(T_{01} + j T_{02}) + \kappa(E_{01} + j E_{02})]$$

$$B_0 = -X_0[(T_{01} + j T_{02}) + \kappa(E_{01} + j E_{02})]$$

Eq. (5.4.5) is the approximate dispersion relation which satisfies the boundary conditions of the device structure chosen.

## 5.5 Solution of Dispersion Equations for Different Materials

Numerical results of the dispersion equation in the previous section are presented and discussed in this section. Solid-state materials chosen for that analysis are InSb, GaAs, Ge and Si. The wave propagation and attenuation characteristics corresponding to the structure configuration should be investigated numerically for several materials. The  $f$ - $\beta$  diagram is useful in interpreting the behavior of a wave propagation and the attenuation curve is helpful in determining whether growing modes exist.

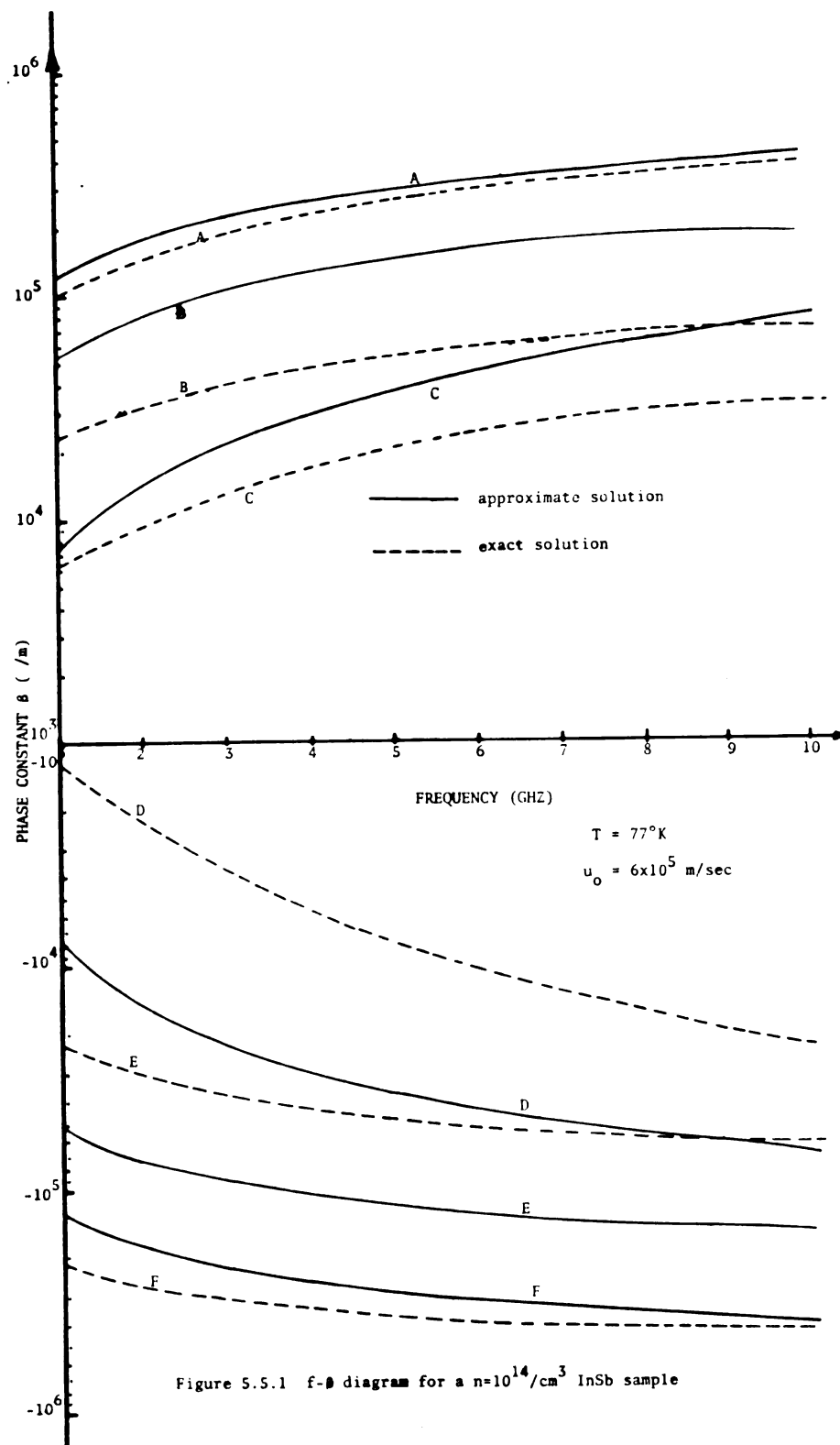
Both wave propagation and attenuation characteristics are determined by finding complex roots of the dispersion equation in  $k$  where  $k = \beta - j\alpha$ . The thickness of the semiconductor slab will be assumed  $\delta = 1 \times 10^{-4}$  m throughout the numerical analysis.

### 5.5.1 Continuous Type of Tape-circuit Model

In connection with the sample configuration, if a continuous tape-line is used instead of a capacitively coupled tape-line, an insulating layer between the semiconductor and the circuit line should be deposited to prevent the dc field from being bypassed. This implies that the characteristic equation remains an infinite order polynomial in  $k$  since the thickness of the insulating layer  $d$  can not be neglected in the range of high frequencies. For the thickness of the insulator between the slow wave circuit and the semiconductor slab,  $d = 1$  micron is used in the continuous tape model.

Figure 5.5.1 shows the functional dependence of  $\beta$  vs.  $f$ , determined by Eq. (5.2.5) and Eq. (5.4.5) for a device of InSb wafer. The drift velocity was taken as  $u_0 = 6 \times 10^5$  m/sec, the relative permittivity as  $\epsilon_{2r} = 15.7$ , the carrier density as  $n = 10^{14}$ /cm<sup>3</sup>, the normalized collision



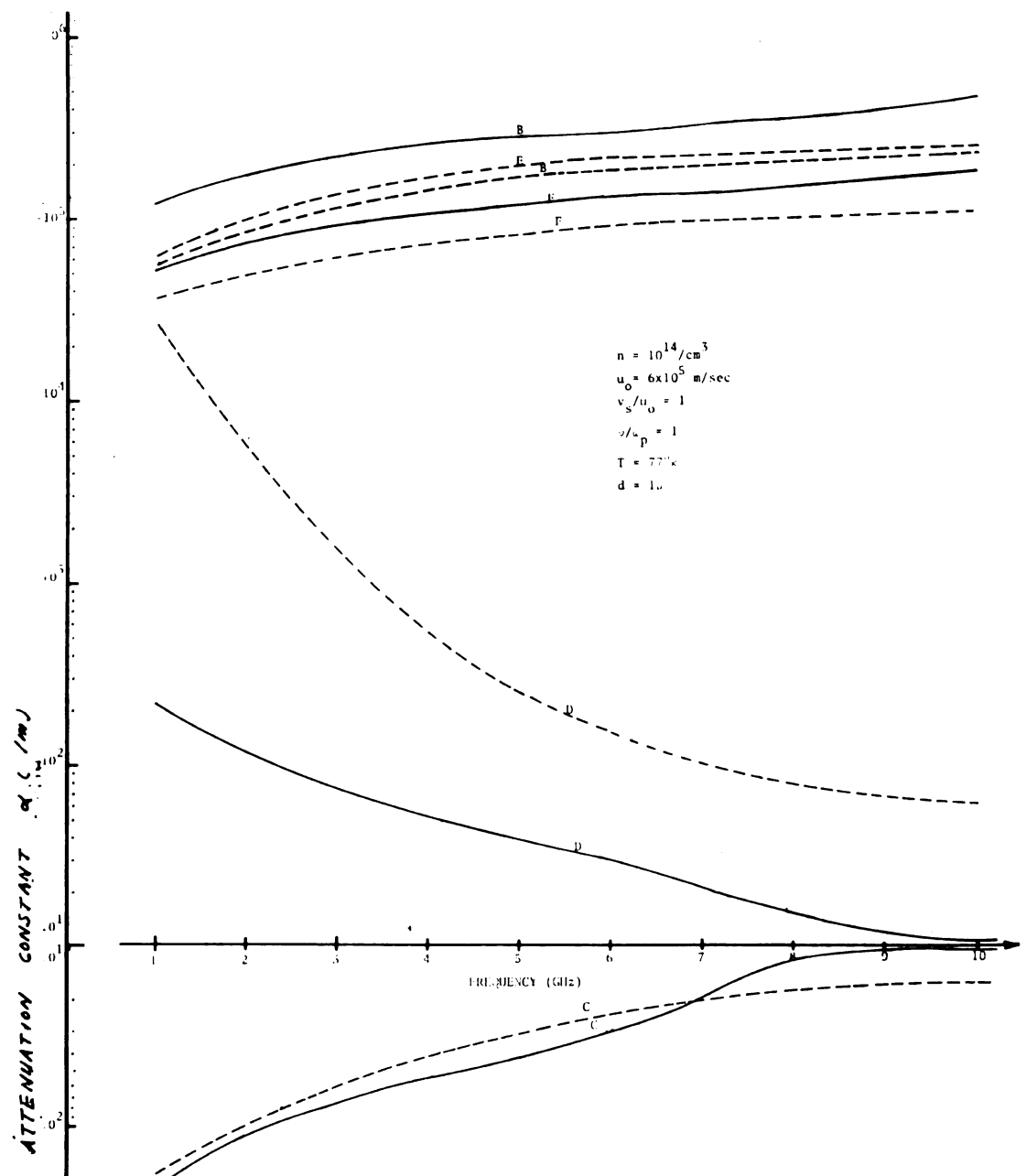


frequency as  $\omega/\omega_p = 1.0$ , the normalized circuit velocity as  $v_s/u_o = 1.0$  and the carrier temperature as  $T = 77^\circ\text{K}$ .

Real roots of the exact equation are obtained by taking six roots of the approximate equation as starting solution of the numerical iteration method. Then both the exact and approximate solutions of the possible six modes are plotted for comparison. As can be seen from the graph, both solutions have the same general shape of variation, except that the exact solution indicates a slight faster phase velocity. The exact dispersion equation requires tremendous computing time and preparative effort to obtain the solution for each operating frequency. However, as far as two dispersion equations for an amplifying mode exhibit similar general trends in the nature of wave propagation and considering only the amplifying wave, the approximate equation may be used in order to investigate effects of material parameters for convenience.

Figure 5.5.2 illustrates the variation of attenuation constant corresponding to the phase constant of Figure 5.5.1. Here, both the approximate and exact solutions of the attenuation constant are plotted. Since the attenuation constant is attained from the imaginary part of the wave propagation constant  $k$ , for forward propagating waves a negative value implies growing wave. It is noted that the exact dispersion equation gives a smaller growing factor than that of the approximate dispersion equation and only one mode indicates amplification. The results showed that the rest of the five modes are highly attenuated.

In order to understand the wave propagation phenomena and to identify the growing wave, it is necessary to investigate the nature of the propagating modes from the  $f-\beta$  diagram. By comparing the phase velocities of the waves with the carrier drift velocity, one can identify



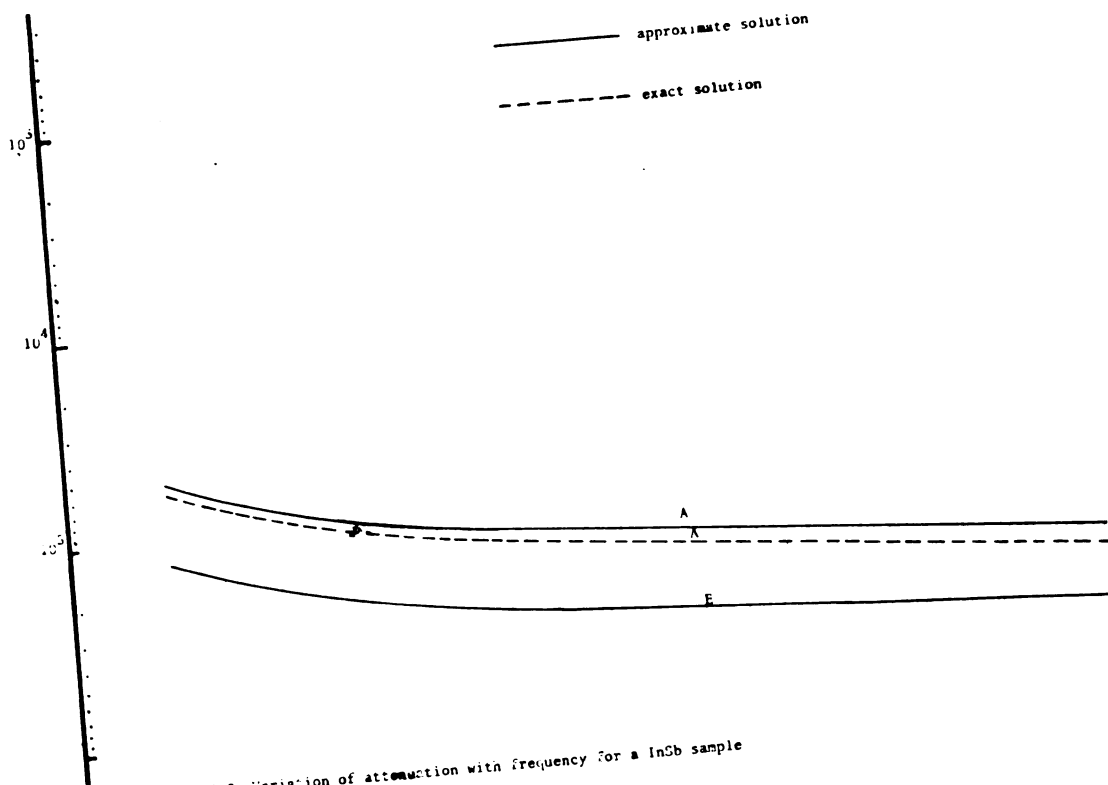


Figure 5.5.2 Variation of attenuation with frequency for a InSb sample

which mode is actively coupled to the carrier stream. The growing mode should be approximately synchronized (the same phase velocities) with the dc drift velocity of the carriers. As can be seen in Figure 5.5.1, the phase velocity of the forward propagating mode is approximately equal to the stream velocity of carriers. Therefore, the forward propagating mode which produces amplification is traveling along the device in the same direction and with approximately the same velocity as the carrier stream.

Using Eq. (5.4.5), also shown in Figure 5.5.3 is the variation of attenuation constant for four different semiconductor wafers, those are, InSb, Si, Ge, and GaAs. Parameters are chosen to have  $T = 77^\circ\text{K}$ ,  $n = 10^{14}/\text{cm}^3$ ,  $q = 1$ ,  $s = 1$  and  $p/r = 1$ . Typical values for the silicon are  $u_0 = 1 \times 10^4$  m/sec,  $\epsilon_{2r} = 11.8$  and  $m^* = 0.33m_e$  and for the germanium  $u_0 = 6 \times 10^4$  m/sec,  $\epsilon_{2r} = 16$  and  $m^* = 0.04m_e$  while for the gallium arsenide,  $u_0 = 6 \times 10^4$  m/sec,  $\epsilon_{2r} = 12.5$  and  $m^* = 0.072m_e$  are used.

### 5.5.2 Capacitively Coupled Tape-circuit Model

As was presented in Figure 3.2.1, if capacitively coupled tape lines are used ideally for a slow-wave circuit, the insulating-layer thickness between the circuit and the solid-state in the device can be reduced to zero because a bottom insulating layer may be removed. Under such a structure the dispersion equation is then reduced to a fourth order polynomial from Eq. (5.4.5). The fourth order equation predicts four possible waves to be traveled along the device. Two additional modes due to the effect of the insulating layer, and turned out a pair of forward and backward traveling modes.

Figure 5.5.4 contains the results for the forward growing mode when the layer does and not exist. The upper curve indicates the gain

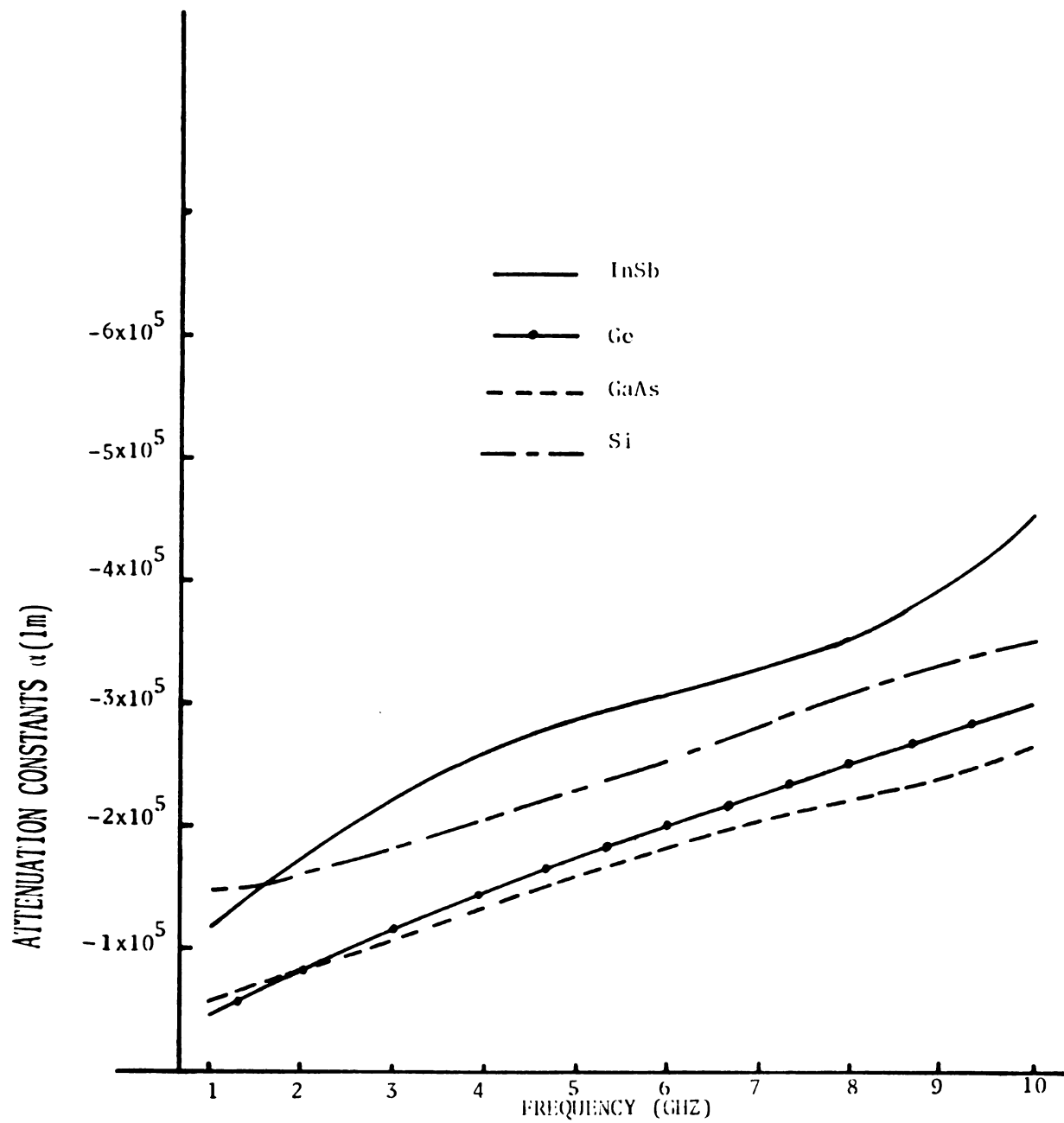


Figure 5.5.3  $f$ - $\alpha$  diagram of the growing mode for four different materials

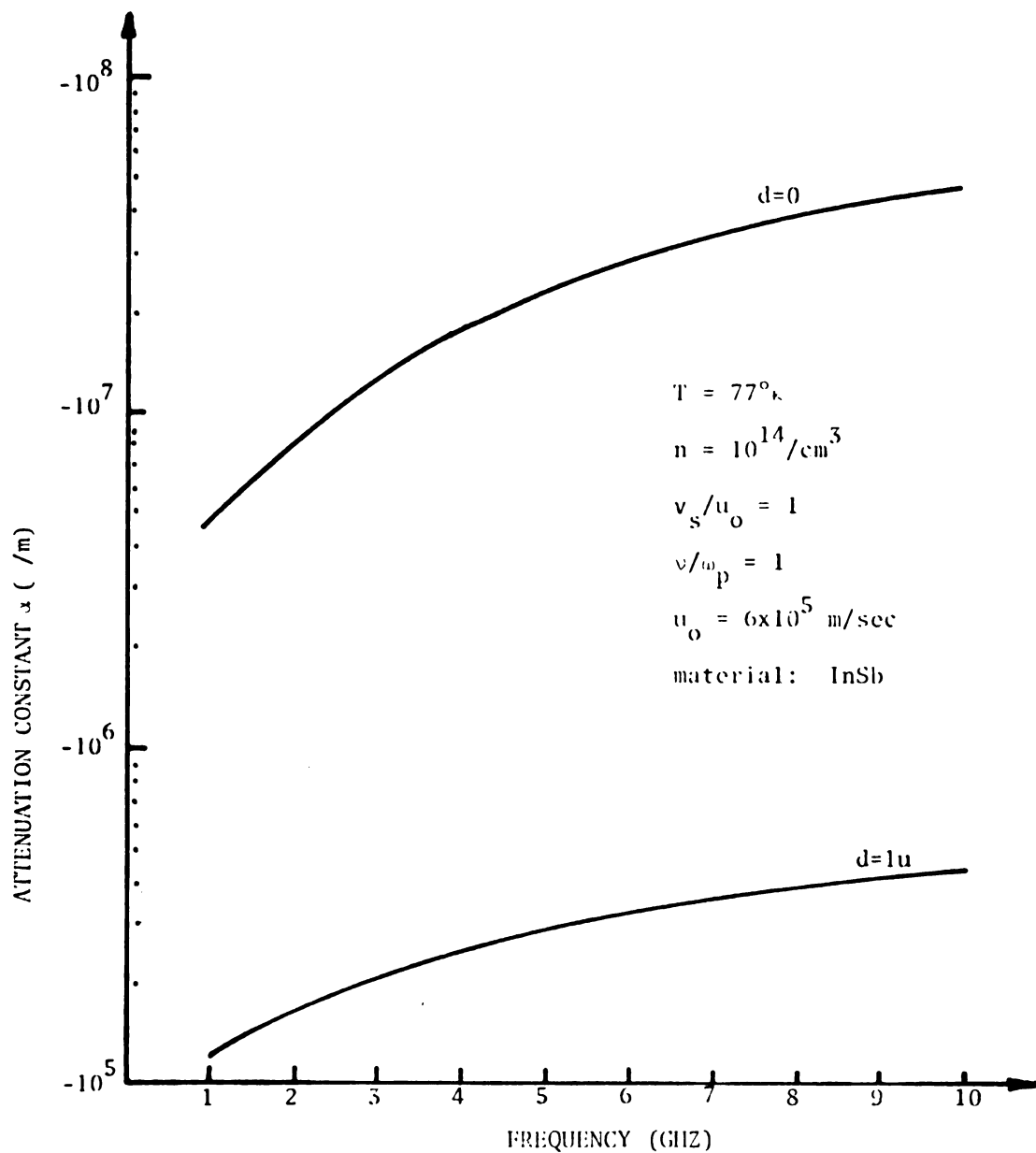


Figure 5.5.4 Comparison of attenuation constants when the insulating layer between the circuit and the semiconductor exists and not exists.

of the InSb model without the insulating layer while the lower curve indicates the layer effect of one micron thick. For high frequencies the insulating layer makes a big difference in the growing rate but for lower frequencies it approaches a small loss. As a result of increasing the frequency of operation, the decrease of the net gain corresponds to the increase of the dielectric loss. A comparison of the continuous tape model and the capacitively coupled ideal tape model shows that although the insulating layer significantly affects the coupling of carrier waves with the rf waves, the behavior of the growing mode is nearly identical.

#### 5.6 Gain Characteristics as a Function of Collision Frequency, Circuit Velocity and Carrier Drift Velocity

In this section the effects on gain due to various collision frequencies, circuit velocities, and carrier drift velocities will be examined. For the purpose of this analysis a heavily doped N-type material is used with a majority carrier  $n = 10^{13}/\text{cm}^3$  and the lattice temperature  $T = 77^\circ\text{K}$ . Gain will be plotted for various parameters of four semiconductor materials, InSb, Ge, GaAs and Si.

The plot of gain as a function of the normalized collision frequency  $\nu/\omega_p$  is presented in Figure 5.6.1, where the normalized circuit velocity for the continuous circuit model is unity.

In gaseous plasmas the higher collision frequency causes gain to decrease. There are, however, two hypotheses for the effect of collision frequency in solid-state plasmas: Birdsall, Brew, Whinney, Haeff and Misawa argued that collisions would induce instability in solids and that collisions are another mechanism of a solid-state amplification [MI2], [BI1], [BI2]. On the other hand, Vural and Bloom proposed that



collisions tend to decrease the amplification while collisions may lead to amplification in the presence of a magnetic field [VU1].

The first hypothesis does not physically interpret amplification phenomena. Even in the case of no collisions, the instability is due to interaction between the positive-energy-carrying circuit wave and the negative-energy-carrying slow space-charge wave supported by a stream of carriers. It is seen that the plot of gain has analogous shapes for materials, Si, GaAs, Ge and InSb, and that with collision effects alone the gain tends to decrease, which supports second hypothesis.

The effects of the normalized circuit velocity  $v_s/u_o$  is displayed in Figure 5.6.2, where the capacitively coupled model is used and  $f = 1 \times 10^9$  Hz. A larger value of the normalized circuit velocity indicates lower gain. Therefore, the circuit velocity, for the optimum operation, should always be smaller than the carrier drift velocity.

The relative gain for InSb, Ge, GaAs and Si as a function of the normalized drift velocity is shown in Figure 5.6.3. The highest gain was obtained as the normalized drift velocity varied between 2.9 and 3.2. This statement disagrees with Sumi's simplified approximate analysis [SU1] in which the maximum gain occurs at  $u_o/v_t = 7.3$ . In reality, the highest possible value of the normalized drift velocity  $u_o/v_t$  is limited due to the hot-carrier effect [GL1]. The attainable highest normalized drift velocity in the liquid nitrogen temperature is around 2.0 for the indium antimonide and 0.5 for the gallium arsenide. Therefore, it can be concluded that for a good solid-state traveling-wave amplifier device, the lower collision frequency and higher carrier drift velocity material, and the lower temperature operation are all desirable.

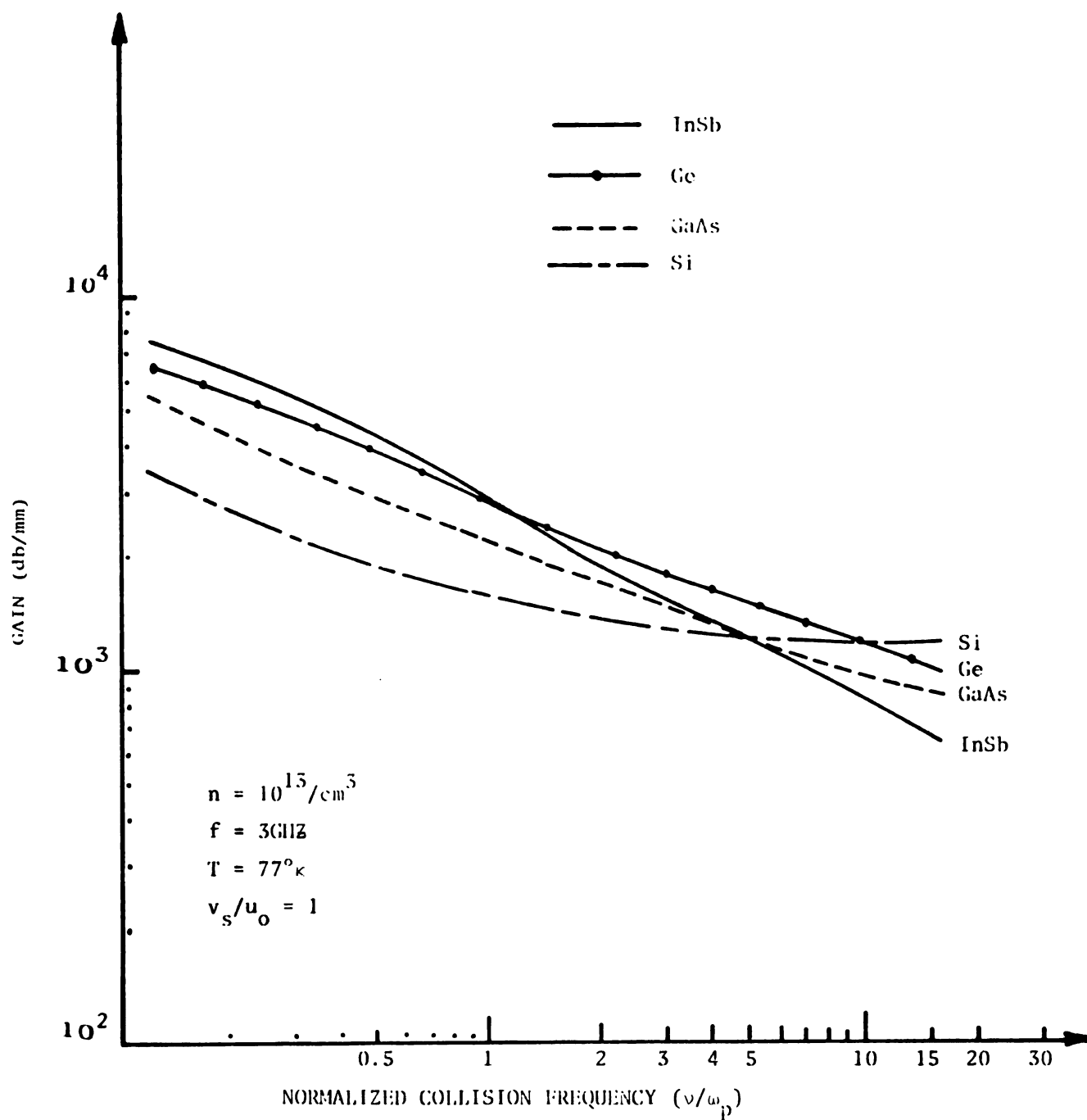


Figure 5.6.1 Gain characteristics with respect to the normalized collision frequency for several solid-state materials.

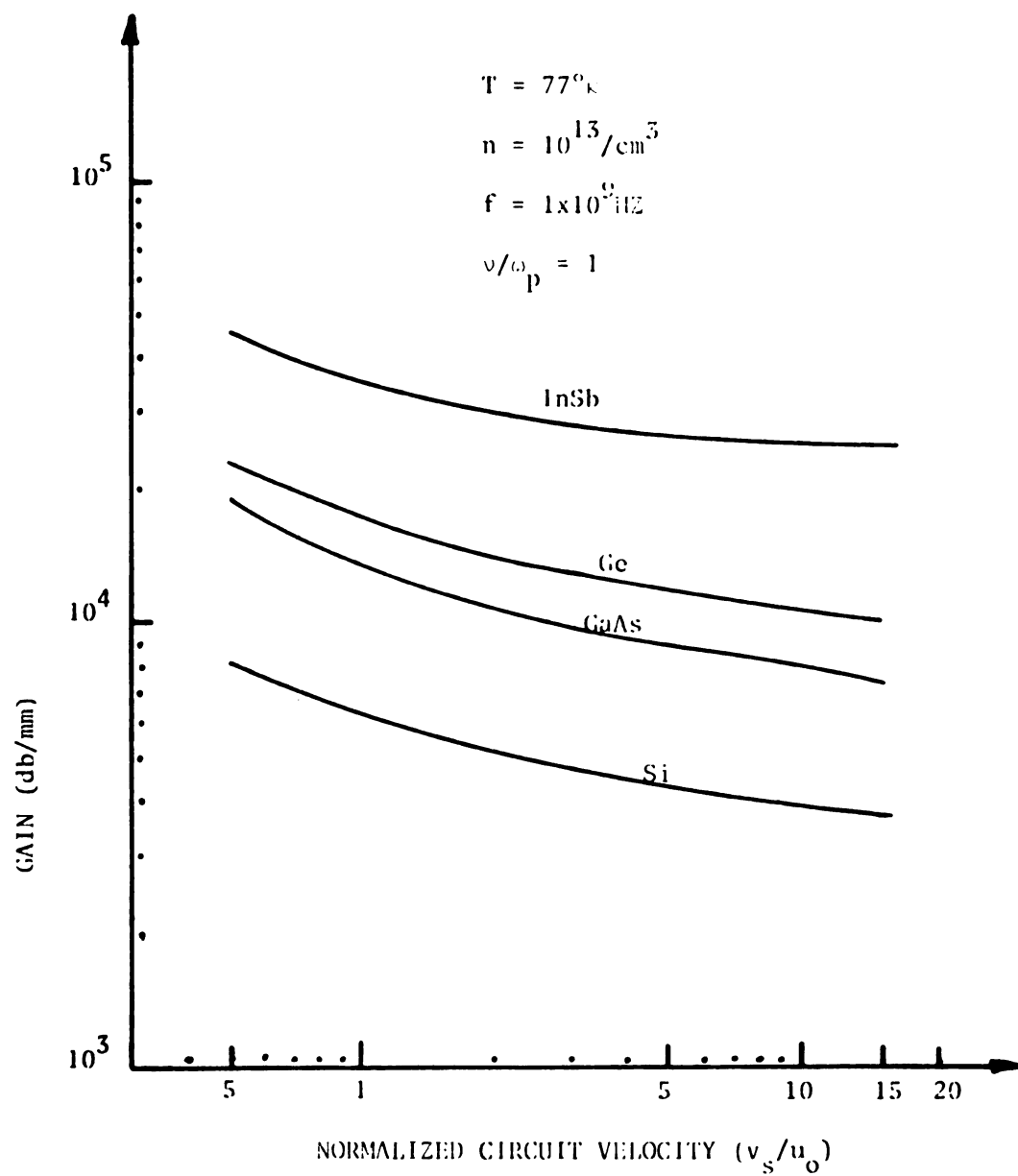


Figure 5.6.2 Gain characteristics with respect to the normalized circuit velocity for several solid-state materials.

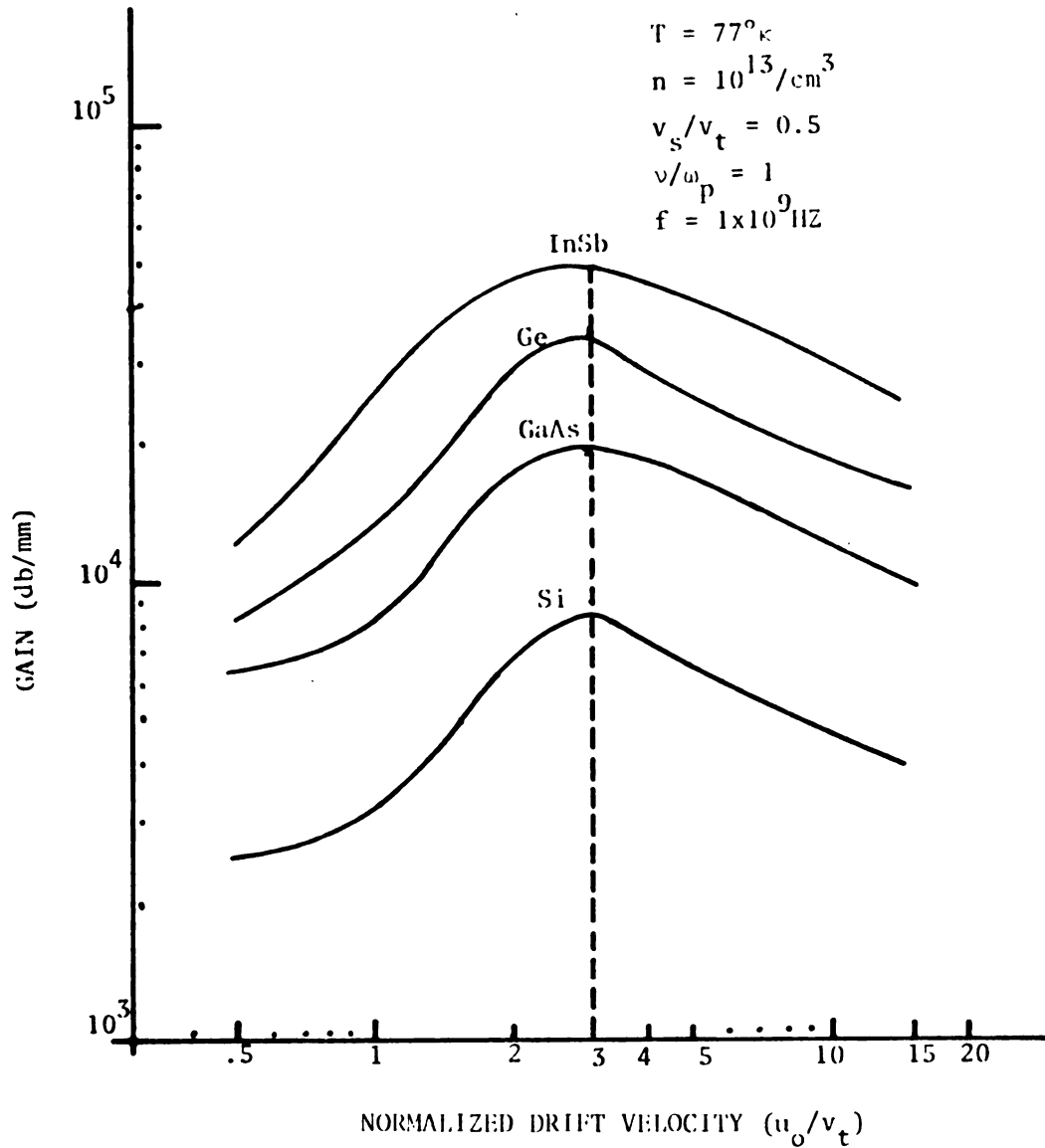


Figure 5.6.3 Gain vs. normalized drift velocity for various solid-state materials.

### 5.7 The Functional Dependence of Device Gain Upon the Variation of Insulating-layer Thickness

The carrier wave is supported by the applied dc field. As was mentioned in the continuous type model, the degree of coupling is a strong function of the insulating layer thickness which separates the tape-line and the solid-state material. In the tape-line circuit structure the field configuration of the slow-wave circuit decreases transversally to zero in a finite depth. Consequently the excited field intensity in the tape-line becomes very weak, which results in weak coupling. Numerically, extensive calculations were performed for four materials at several values of the thickness  $d$ .

The functional dependence of gain is plotted in Figure 5.7.1 for the variation of the thickness of an insulating layer. From the result it can be seen that a rather high gain is obtainable at a thickness of  $d = 10^{-7}$  m. With today's integrated circuit technology, depositing such a thin layer on the semiconductor surface is difficult. Besides that, the other problem is in practically achieving a reasonable uniformity of a thin layer.

The gain decreases drastically as the layer thickness increases as illustrated in Figure 5.7.1. The possible fabricated thickness ranges  $10^{-6} \sim 10^{-4}$  m.

Judging from the theoretical and practical point of view, the best result of the device does not heavily depend upon materials themselves but how to fabricate the device and to maximize their drift velocities. As far as the drift velocity is concerned, indium antimonide seems to be the favorable material for this type of device. It is also interesting to note that the solid-state type of device is a potential device for high frequency applications, which may be an attraction feature, as seen in

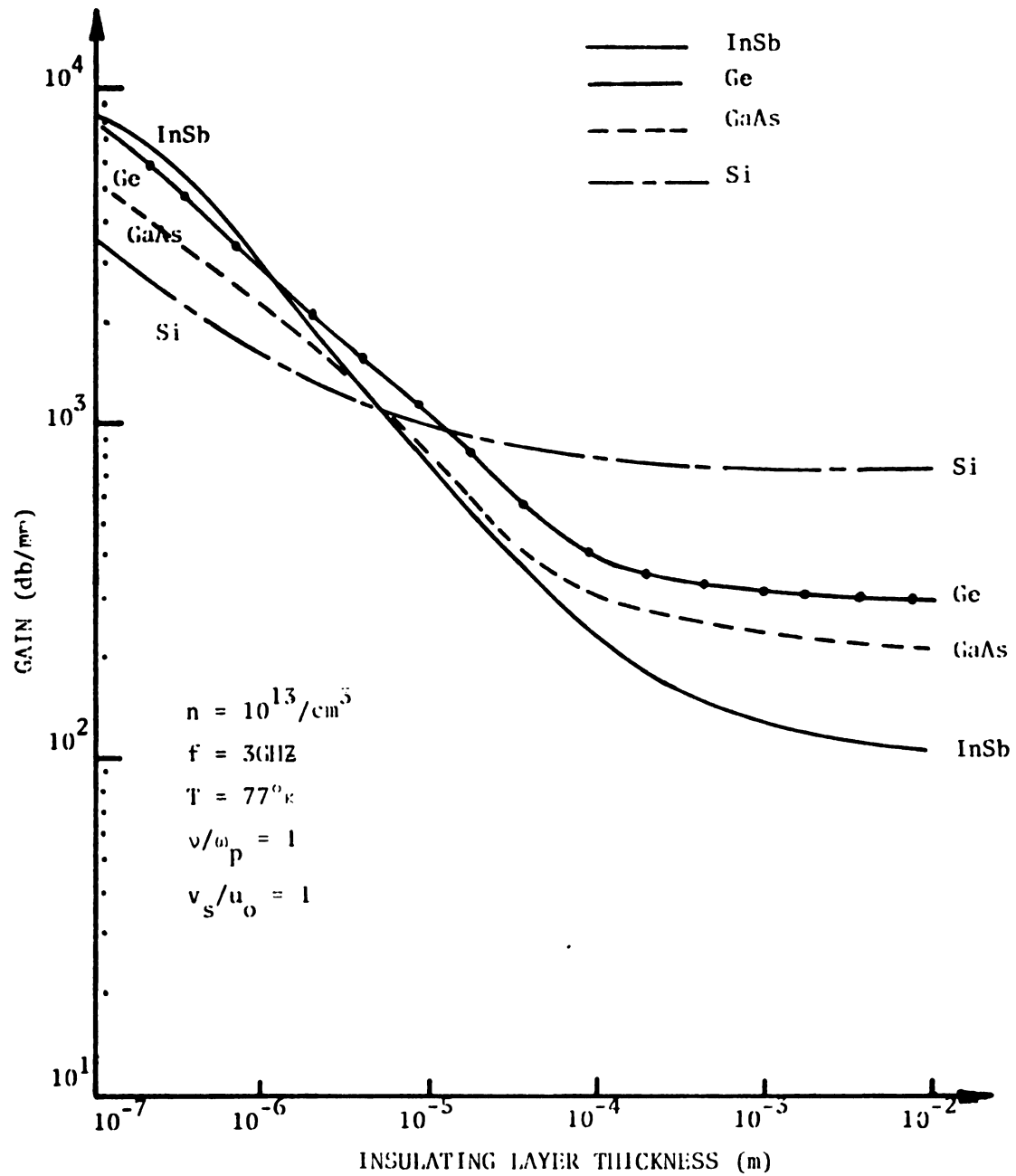


Figure 5.7.1 Gain characteristics for various values of an insulating layer thickness ( $d$ )

the analysis of this chapter. However, the circuit and semiconductor losses are a serious problem, and as a result a high gain as anticipated in the curve should not be expected.

## CHAPTER VI

### TWO STREAM INSTABILITY IN SOLIDS

#### 6.1 Introduction

The theory of traveling-wave amplification in a thin semiconductor layer and a slow electromagnetic tape line deposited on the layer was treated in Chapter III through Chapter V. As was mentioned in Section 2.6, instability can also be obtained between the upper and lower valley electrons without using a rf circuit.

The instability mechanism in solid-state materials is explained by the concept of wave interaction which has been successfully used in electron beam devices. Kino [KI1] described the charged carrier motion in semiconductor by a space charge wave concept, referring to them as "carrier waves." The kinetic power carried by these carrier waves were given by Vural and Bloom [VU2].

Assume that a Gunn sample of length  $\ell$  has been biased with a constant voltage so that the net internal electric field reaches a negative-slope region which starts from a little over threshold voltage. Ridley [RI1] [RI2] proposed that this condition is unstable and leads to a theory of lower and higher valley model. This type of transferred-electron device is completely different from the established devices such as transistors, tunnel diode, or varactor. The mechanism comes from the bulk property of GaAs and is not based upon the ordinary p-n junction theory. The device structure consists of an electrically uniform doping and geometrically regular semiconductor with two ohmic contacts for the application of a bias voltage. The instability occurs during a transit time between two



contacts; thus, the higher operating frequency is, the thinner the sample length becomes. Consequently, the power output for a given device decreases as the operating frequency is raised.

Several parameters such as material resistivity, temperature, and the low conversion efficiency induce a high power loss throughout the device which requires efficient heat sinking. Although, for continuous wave operation, heat sinking is possible for small size devices, the limitation restricts practically the lowest operating frequency to around 4 GHz and the total active length limitation restricts the output power to several hundred milliwatts. However, the pulsed operation lets the power loss be reduced with the reduction of the duty cycle. Hence, the low frequency restriction is removed and pulsed output power can be increased by enlarging the sample length and thickness. Unfortunately, there is a limit to the pulse width to protect the danger of overheating during the pulse period. The existing pulse widths and duty cycles are within these limits for systems such as mobile radars, aircraft direction- and height-finding equipment and aircraft identification. This type of solid-state device can be designed to operate in any part of the microwave equipments and it is small in size and simple. For these reasons the solid-state device coupled with the newly developed integrated circuit technology in electronics is compatible with the high voltage microwave devices.

A simple configuration for transferred electron devices is illustrated in Figure 6.1.1. Since the reactance of the device is usually capacitive, an inductive reactance must be provided to obtain resonance at the operating frequency. This mechanism is obtained by using waveguide, coaxial or microstrip cavities which are wellknown in conventional methods.

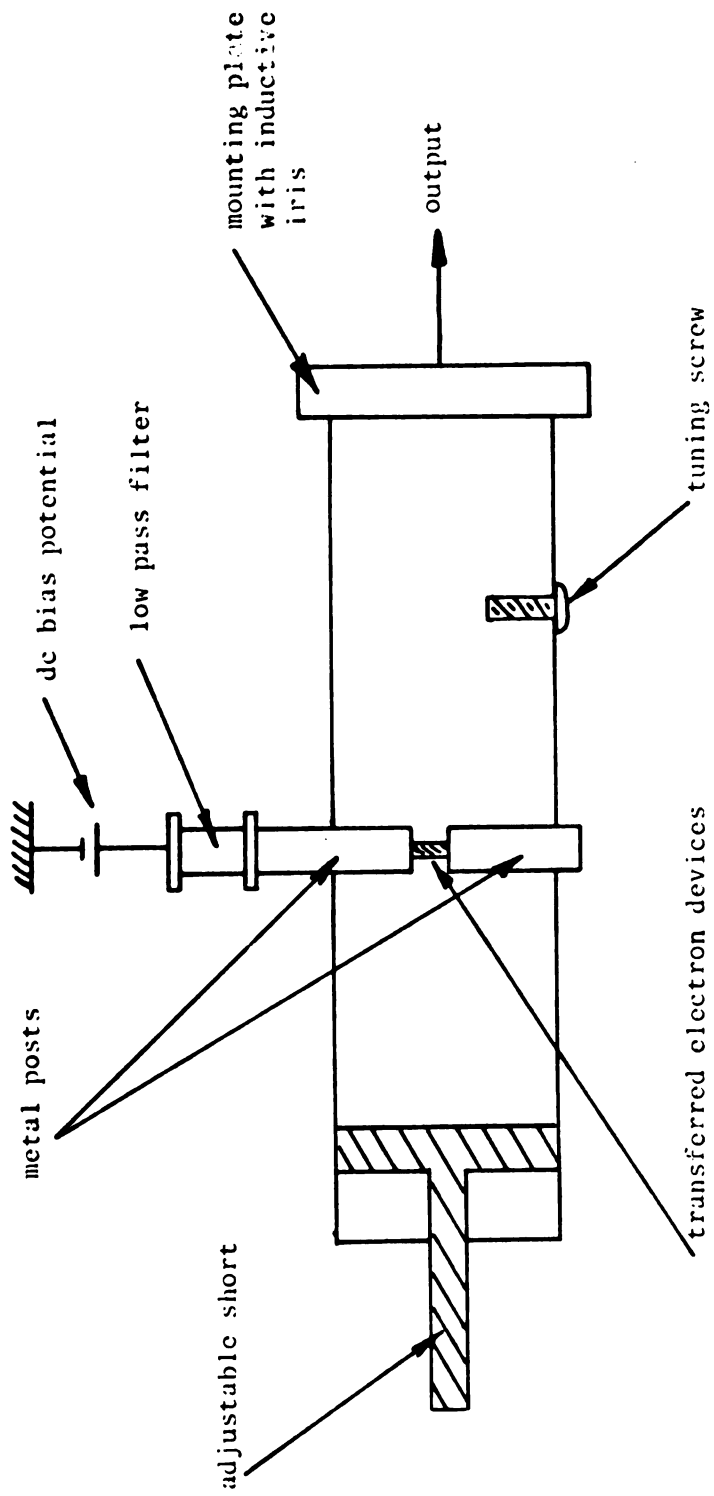


Figure 6.1.1 A possible configuration for two-stream instability devices.

The reactance may be supplemented by constructing the inductive iris in the waveguide. In addition, tuning can be accomplished either electronically or mechanically using varactors or YIGs. Typical varactor-tuned and YIG-tuned devices covers a  $10 \sim 20\%$  range for the frequency of  $1 \sim 10$  GHz.

This chapter is devoted to describing the formation of two-valley model and to developing the two-stream instability analysis. Finally, a computer solution will be carried out, based on the theoretical analysis.

## 6.2 Formation of Two-Valley Model

The transferred electron mechanism of some semiconductors such as GaAs, InP, CdTe and InSb was predicted theoretically by several workers. The Gunn effect is a typical example found in GaAs by Gunn in 1963. This effect has not been observed at room temperature and normal pressure in Si and Ge, mainly due to not being able to get a sufficient number of carriers to populate the negative effective mass states.

When a large enough potential is applied across the sample, negative differential conductance is obtained. When this occurs, a phenological transfer mechanism of carriers from one energy band to the other is followed up in the physical sense. Once they are separated in two energy states, these carriers in two different states have completely different physical characteristics. Thus, two distinct groups of carriers moving across the sample can be considered, namely the upper and lower valley carrier. Then it is possible to explain the instability by two stream formation.

The two valley structure in GaAs is illustrated in Figure 6.2.1. The energy gap separation between the conductance band minimum and valence band is 1.53 eV. Carriers are distributed between light-mass lower valley and heavy-mass upper valley whose minima are separated by an energy displacement of 0.36 eV. As shown in Figure 6.2.1, the mass of a carrier

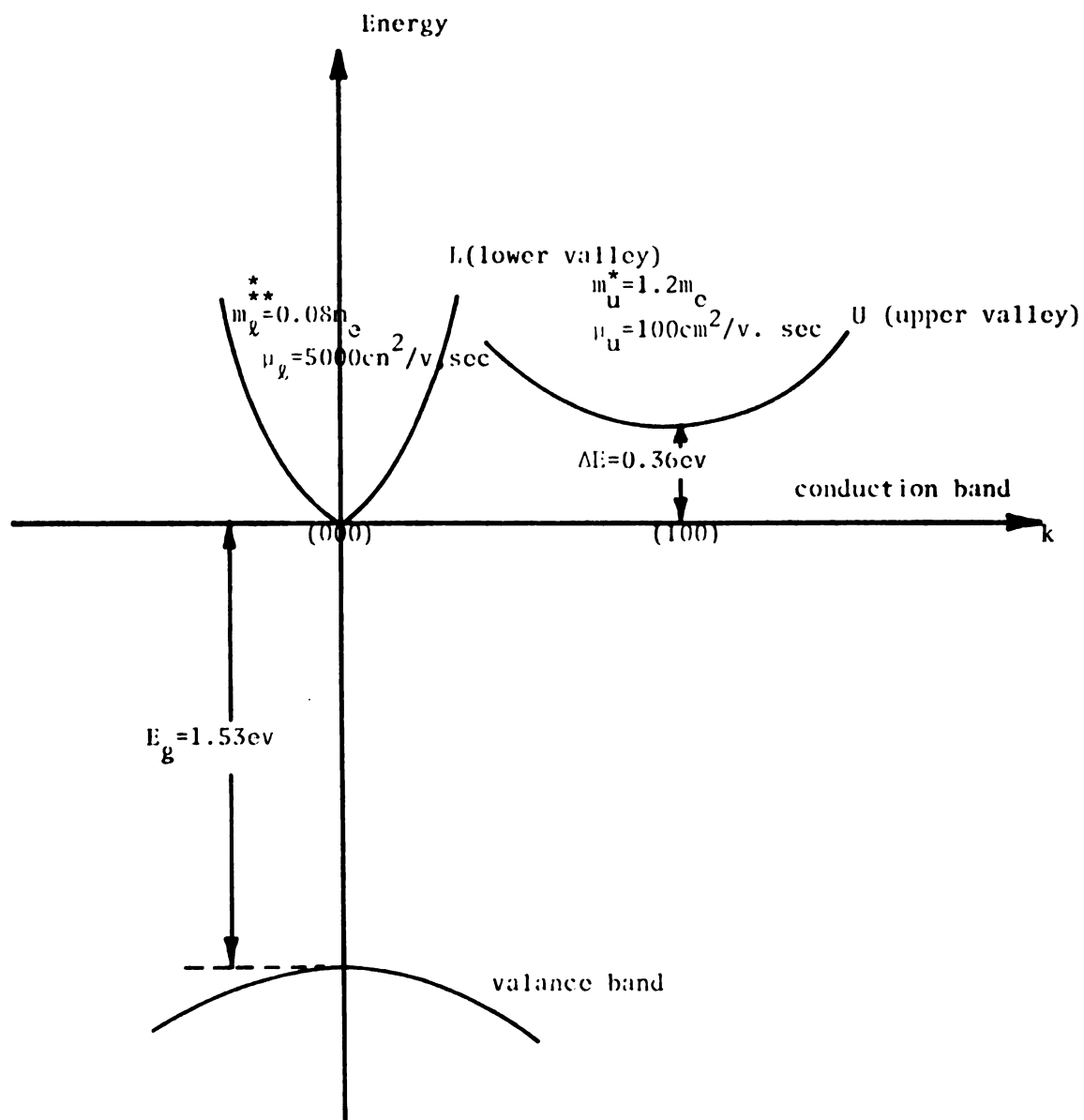


Figure 6.2.1 Simplified energy band structure of two-valley model. The numerical values are taken from a GaAs sample.

in the lower valley is  $m_l^* = 0.08 m_e$  at the minimum of conduction band and the mass of an upper-valley carrier  $m_u^* = 1.2 m_e$  at the bottom of the upper valley. Subscripts  $l$  and  $u$  refer to the lower valley and upper valley, respectively. Carrier mobility in lower valley ( $\mu_l = 5000 \text{ cm}^2/\text{volt-sec}$ ) is much greater than that in the upper valley ( $\mu_u = 100 \text{ cm}^2/\text{volt-sec}$ ). The numerical values used here pertain to GaAs. GaP has a similar band structure to GaAs material but its upper-valley mass is lighter than the lower-valley mass ( $\Delta E < 0$ ).

Inside a semiconductor there always exists a slight nonuniform field distribution, which can cause a transition of carrier to a slightly higher energy state. It was proposed by Ridley that the space charge distribution would have a narrow region of high field intensity, which is called a domain. Such distribution arises from material inhomogeneity in doping and polishing or from a noise fluctuation. At the front- and back-edges of this higher field region there are temporarily charge accumulation and depletion layers, respectively. This is because the lower-field upper stream leads to an increased rate of feeding electrons into the region around high field and the higher-field lower stream to a decreased rate of removal from there.

The domain travels from the negative contact to the positive contact with a uniform drift velocity in the order of  $10^7 \text{ cm/sec}$ . The formation of domain starts when the applied potential is above the threshold voltage. Field induced transfer of carriers between two valleys in the conduction band is directly related to the differential conductance.

Alternatively, a two valley model may be formed by raising the lattice temperature in semiconductor materials at low field and then a negative differential conductance can be produced. Law<sup>[1A]</sup> proposed the

possibility of achieving the negative conductance by joule heating in the semiconductor. As the electric field is increased, the temperature of semiconductor is raised above the temperature at zero by joule heating. Then the carrier density and mobility will change with changing joule heating rate. Hence, a two valley model forms. However, this mechanism doesn't seem to be possible for Gunn devices because the joule heating produces tremendous collision and thermal effect.

Whenever transfer of carriers occurs, carrier interactions exist between two types of carriers in the lower and upper valley. The carrier interaction mechanism will be discussed later.

Figure 6.2.2 shows the theoretical and experimental  $v$  vs.  $E$  characteristic [BU2], [RU1] for a typical GaAs material. A negative differential conductivity exists for electric fields exceeding the threshold field  $E_T = 3.4$  KV/cm. Above the threshold field, the drift velocity of the carrier decreases as the electric field increases.

### 6.3 Population Densities of Carriers in Two-valley Model

In a two valley semiconductor there are  $n_l$  carriers per unit volume in the lower valley of the conduction band and  $n_u$  carriers per unit volume in the upper valley, and  $n_l + n_u$  is a constant. The population density in two energy bands strongly varies with the applied bias field and environmental temperature. The number of carriers in the lower energy level of the conduction band will decrease as the bias electric field is increased. The decrease comes from a transfer of some carriers from a lower to a upper valley within the conduction band at the microwave frequency or to ionized traps in the forbidden band at the lower frequency. When the transfer rate of carriers between the two valleys exceeds a certain value, a material exhibits differential negative conductance.

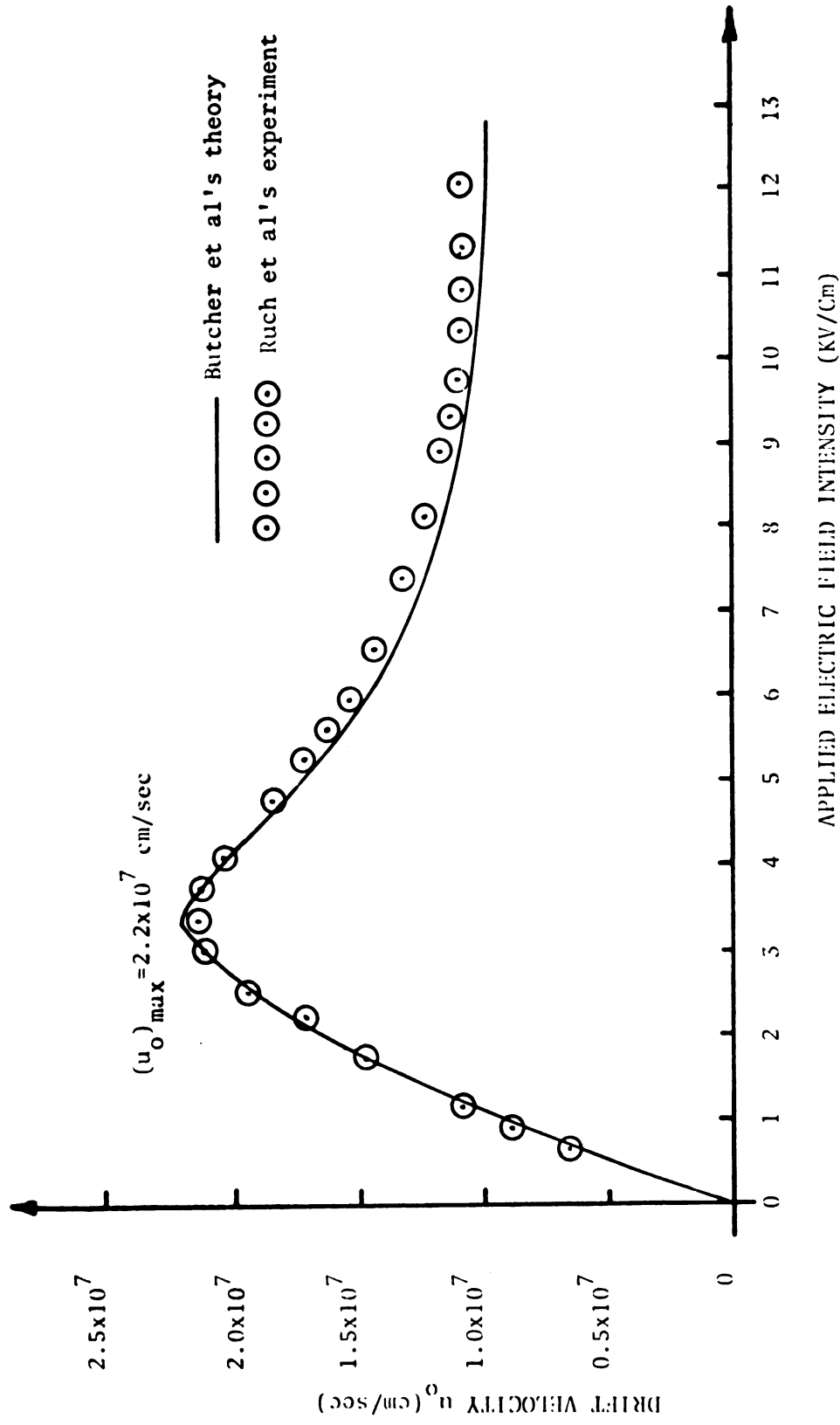


Figure 6.2.2 Theoretical and experimental drift velocity with electric field of GaAs sample.

Under the assumption of Maxwell-Boltzmann distribution of carrier densities, McCumber and Chynoweth [MC1] calculated the carrier densities of lower valley and upper valley as

$$n_l = \frac{n}{1 + \alpha \exp(-\frac{\Delta E}{T})} \{1 - (1 + \frac{\Delta E}{T}) \exp(-\frac{\Delta E}{T})\} \quad (6.3.1)$$

$$n_u = \frac{n \exp(-\frac{\Delta E}{T})}{L + \alpha \exp(-\frac{\Delta E}{T})} (1 + \alpha + \frac{\Delta E}{T}) \quad (6.3.2)$$

where  $T$  = average carrier temperature (ev)

$\Delta E$  = energy separation between the upper and lower valley (for GaAs,  $\Delta E = 0.35$  ev)

$\alpha = \frac{N_u}{N_l}$  = the dimensionaless ratio of the upper-valley to lower-valley density of states (for GaAs,  $\alpha = 60$ )

$n = n_l + n_u$  = carrier doping concentration rate (carriers/cm<sup>3</sup>)

This calculation of the simple temperature model was compensated by expressing the average carrier temperature as a function of the bias fields relevant to the Gunn effect.

#### 6.4 Carrier Interaction in a Two-valley Semiconductor

Whenever carriers of the lower valley are transferred to the upper valley, interaction between valley carriers is anticipated. As indicated in previous sections, the carrier mass in the upper valley is much heavier than that in the lower valley, while velocity in the upper valley is slower than that in the lower valley. Consequently, the lower-valley carriers can be considered relatively mobile while the upper-valley ones can be considered at a standstill. Then the upper valley can be treated as a stationary plasma or a circuit and the lower valley as an electron stream. This is primarily based on the fact that carrier waves resemble to the space charge wave in an electron beam.



This type of approach has been used by Pierce [PI2] for the traveling-wave tube. The approach which seems likely to yield the best results is that of writing the appropriate partial differential equations for the interactions between two valleys. This analysis enables evaluation of certain quantities which can be estimated, and the numerical results do not differ qualitatively and are in a fair quantitative agreement with Perlman's experimental result [PE1].

The modulation produced in the upper-valley carriers can be represented by an equivalent lumped transmission line, having series impedance and shunt admittance. The circuit is uniformly distributed with series resistance, inductance and capacitance, and shunt inductance and capacitance. Recently Ho [HO2] calculated equivalent series impedance  $Z_s$  and shunt admittance  $Y_{sh}$  of an upper valley carrier stream in solids which are given by

$$Z_s = j \frac{\omega}{\epsilon \omega_{pu}^2} \left\{ \frac{\omega_{pu}^2}{\omega^2} + \frac{v_{tu}^2}{u_{ou}^2 - v_{tu}^2} \left( 1 + \frac{v_u}{j\omega} \right) - \frac{u_{ou}^2}{u_{ou}^2 - v_{tu}^2} \cdot \frac{v_u}{4\omega^2} \right\} \quad (6.4.1)$$

$$Y_{sh} = j \frac{\omega \epsilon \omega_{pu}^2}{u_{ou}^2 - v_{tu}^2} \quad (6.4.2)$$

where

$\omega_{pu}$  = plasma frequency of upper valley carriers

$v_{tu}$  = thermal velocity of upper-valley carriers

$u_{ou}$  = drift velocity of upper-valley carriers

$v_u$  = collision frequency of upper-valley carriers

It is noted that the transferred electron devices indicate capacitance property since the drift velocity is usually greater than the thermal velocity, as seen in Eq. (6.4.2). Thus, inductive tuning must be constructed to resonate it with the capacitance of the device in Figure 6.1.1.

Physically, the coupling of the stream and the circuit is due to the displacement current originated from the carrier stream. When carriers transfer to the upper valley, a displacement current from the lower valley will be flown to the circuit. Summarizing the mutual movement of two valley carrier, the equivalent over-all lumped representation can be approximated as illustrated in Figure 6.4.1.

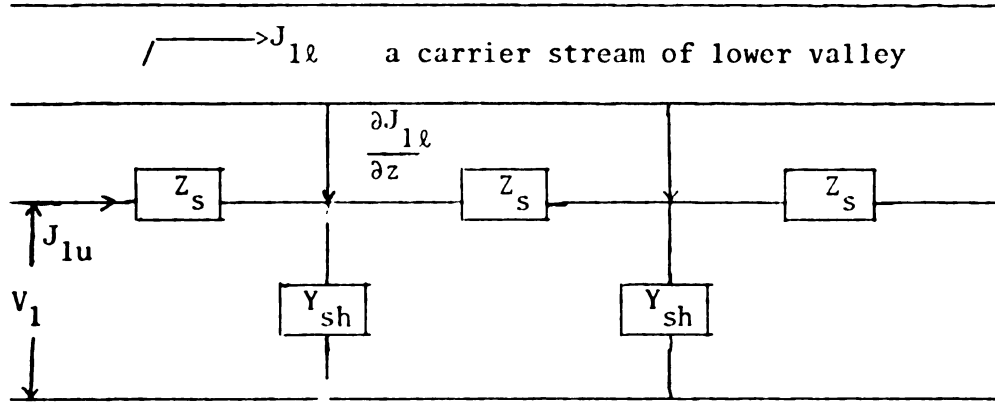


Figure 6.4.1 An over-all equivalent representation of two valley model. A displacement current is flown to the circuit.

The sum of the lower valley convection current  $J_{1l}$  and the displacement current  $J_{1d}$  in a volume of a carrier stream should vanish, because the total current flowing out of the volume of a carrier stream is zero.

In a stream

$$\vec{J}_{1l} + \vec{J}_{1d} = 0 \quad (6.4.3)$$

Over the surfaces of a stream,

$$\begin{aligned} \int_{sd} \vec{J}_{1d} \cdot d\vec{A} &= - \int_{sc} [-\vec{J}_{1l} + (\vec{J}_{1l} + \frac{\partial J_{1l}}{\partial z} dz)] \cdot d\vec{A} \\ &= - \int_{sc} (\frac{\partial J_{1l}}{\partial z} dz) \cdot d\vec{A} \end{aligned} \quad (6.4.4)$$

Eq. (6.4.4) may be rewritten as

$$\frac{\partial J_{1d}}{\partial z} = - \frac{\partial J_{1l}}{\partial z} \quad (6.5.5)$$

### 6.5 Circuit Equation of Carriers in the Upper Valley

A one dimensional analysis will be assumed for simplicity throughout this chapter. In Figure 6.4.2 a set of circuit equation can be written as

$$\frac{\partial V_1}{\partial z} = -Z_s J_{1u} \quad (6.5.1)$$

$$\frac{\partial J_{1u}}{\partial z} = -Y_{sh} V_1 - \frac{\partial J_{1\ell}}{\partial z} \quad (6.5.2)$$

where

$V_1$  = rf induced voltage

$J_{1u}$  = rf upper circuit current

$J_{1\ell}$  = rf lower-valley convection current.

Since  $e^{j(\omega t - kz)}$  type of variation for all quantities is assumed, the above equations become

$$-jkV_1 = Z_s J_{1u} \quad (6.5.3)$$

$$-jkJ_{1u} = Y_{sh} V_1 + jkJ_{1\ell} \quad (6.5.4)$$

Eliminating  $J_{1u}$ , the following circuit equation is obtained,

$$\frac{J_{1\ell}}{V_1} = \frac{k^2 + Y_{sh}Z_s}{jkZ_s} \quad (6.5.5)$$

In Eq. (6.5.5) series impedance  $Z_s$  and shunt admittance  $Y_{sh}$  were defined in Eqs. (6.4.1) and (6.4.2). Note that the convection lower valley current produces the circuit voltage in the equivalent transmission line.

### 6.6 The Electronic Equation of the Lower Valley Carriers

From force equation, rf velocity of lower valley carriers is:

$$\vec{v}_{1\ell} = \frac{\eta_{\ell}^*}{j\omega} \left( -\vec{E}_1 + \frac{v_{t\ell}^2}{\omega_{p\ell}^2} \nabla \nabla \cdot \vec{E}_1 \right) \quad (6.6.1)$$

where

$$\omega_{v\ell} = \omega - ku_{o\ell} - jv_{\ell}$$

$v_{\ell}$  = collision frequency of lower-valley carriers

$u_{o\ell}$  = drift velocity of lower-valley carriers

$\eta_{\ell}^*$  = effective charge to mass ratio of lower-valley carriers

$v_{t\ell}$  = thermal velocity of lower-valley carriers

$\omega_{p\ell}$  = plasma frequency of lower-valley carriers

$\vec{E}_1$  = rf E field due to rf potential  $V_1$

The continuity equation is written as

$$-jkJ_{1\ell} + j\omega\rho_{1\ell} = 0 \quad (6.6.2)$$

where  $\rho_{1\ell}$  refers to lower valley rf charge density. The lower valley convection current is written in terms of charge density and velocity of carriers.

$$\vec{J}_{1\ell} = \rho_{o\ell} \vec{v}_{1\ell} + \rho_{1\ell} \vec{u}_{o\ell} \quad (6.6.3)$$

where  $\rho_{o\ell}$  stands for lower valley dc charge density.

From Eqs. (6.6.2) and (6.6.3), rf charge density and current density are given by

$$\rho_{1\ell} = \frac{-k\rho_{o\ell} \vec{v}_{1\ell}}{\omega - ku_{o\ell}} \quad (6.6.4)$$

$$\vec{J}_{1\ell} = \frac{-\omega\rho_{o\ell}}{\omega - ku_{o\ell}} \vec{v}_{1\ell} \quad (6.6.5)$$

Substituting Eq. (6.6.1) into Eq. (6.6.5) yields

$$\vec{J}_{1\ell} = \frac{-\omega\rho_{o\ell}\eta_{\ell}^*}{j(\omega - ku_{o\ell})\omega_{v\ell}} (-\vec{E}_1 + \frac{v_{t\ell}^2}{\omega_{p\ell}^2} \nabla \nabla \cdot \vec{E}_1) \quad (6.6.6)$$

For one dimensional analysis  $\nabla \nabla \cdot \vec{E}_1 = -k^2 E_1 \hat{z}$  and

$\vec{E}_1 = \frac{\partial V_1}{\partial z} \hat{z} = jkV_1 \hat{z}$  where  $e^{j(\omega t - kz)}$  is recognized:

Hence, Eq. (6.6.6) is reduced to a simple scalar equation as

$$J_{1\ell} = \frac{-k\omega\rho_{o\ell}\eta_{\ell}^* (1 + \frac{v_{t\ell}^2}{\omega_{p\ell}^2} k^2) V_1}{(\omega - ku_{o\ell}) (\omega - ku_{o\ell} - jv_{\ell})} \quad (6.6.7)$$

Therefore, the electronic equation can be obtained as

$$\frac{J_{1l}}{V_1} = \frac{\beta_{el} \rho_{ol} \eta_l^* k (1 + \frac{v_{tl}^2}{\omega_{pl}^2} k^2)}{u_{ol} (k - \beta_{el}) (k - \beta_{el} + j\beta_{vl})} \quad (6.6.8)$$

where

$$\beta_{el} = \frac{\omega}{u_{ol}}$$

$$\beta_{vl} = \frac{v_l}{u_{ol}}$$

### 6.7 The Dispersion Characteristic Equation in Carrier Wave Interaction

Equating the circuit, and electronic equation, Eqs. (6.5.5) and (6.6.8) gives the following characteristic equation.

$$\frac{k^2 + Y_{sh} Z_s}{jk Z_s} = \frac{\beta_{el} \rho_{ol} \eta_l^* k (1 + \frac{v_{tl}^2}{\omega_{pl}^2} k^2)}{u_{ol} (k - \beta_{el}) (k - \beta_{el} + j\beta_{vl})} \quad (6.7.1)$$

The characteristic equation is a fourth order polynomial in  $k$  with complex coefficients.

The normalized velocity and operating frequency are defined as

$$p_u = \frac{u_{ou}}{v_{tu}} \quad (6.7.2)$$

$$Q_u = \frac{\omega}{\omega_{pu}} \quad (6.7.3)$$

Collision frequency is also normalized in the following way,

$$S_u = \frac{v_u}{\omega_{pu}}$$

The thermal propagation constants are,

$$\beta_{tu} = \frac{\omega_{pu}}{v_{tu}} \quad (6.7.4)$$

and

$$\beta_{tl} = \frac{\omega_{pl}}{v_{tl}} \quad (6.7.5)$$

With these definitions, the equivalent series impedance  $Z_s$  and shunt admittance  $Y_{sh}$  of the upper valley carrier stream may be rewritten as

$$Z_s = \frac{1}{\omega \epsilon} \frac{Q_u S_u}{P_u^2 - 1} - j \frac{1}{\omega \epsilon} \cdot \frac{4(1 - Q_u^2) + P_u^2 (S_u^2 - 4)}{4(P_u^2 - 1)} \quad (6.7.6)$$

$$Y_{sh} = j \omega \epsilon \frac{\beta_{tu}^2}{P_u^2 - 1} \quad (6.7.7)$$

and

$$Y_{sh} Z_s = \frac{4(1 - Q_u^2) + P_u^2 (S_u^2 - 4)}{4(P_u^2 - 1)^2} \beta_{tu}^2 + j \frac{Q_u S_u \beta_{tu}^2}{(P_u^2 - 1)^2} \quad (6.7.8)$$

The characteristic equation is obtained after combining Eq. (6.7.1) with Eqs. (6.7.6) through (6.7.8).

$$\begin{aligned} (1 - \frac{a}{\beta_{tl}^2}) k^4 - (b + \beta_{el}) k^3 + (b\beta_{el} + c - a) k^2 - (b + \beta_{el}) c k \\ + \beta_{el} b c = 0 \end{aligned} \quad (6.7.9)$$

where

$$a = \frac{\rho_{ol} \eta_l^*}{\omega^2 \epsilon} \beta_{el}^2 \frac{4(1 - Q_u^2) + P_u^2 (S_u^2 - 4)}{4(P_u^2 - 1)} + j \frac{Q_u S_u}{P_u^2 - 1} \quad (6.7.10)$$

$$b = \beta_{el} - j \beta_{vl} \quad (6.7.11)$$

$$c = \frac{4(1 - Q_u^2) + P_u^2 (S_u^2 - 4)}{4(P_u^2 - 1)} \beta_{tu}^2 + j \frac{Q_u S_u \beta_{tu}^2}{(P_u^2 - 1)^2} \quad (6.7.12)$$

As mentioned in Chapter V, an analytical solution for a fourth order equation cannot easily be, in general, obtained. Computer solution of such an equation is more practical. Complex roots of  $k$  with complex coefficients will be solved by both Lehmer method and Newton-Raphson method.

With these roots, the gain of a device is obtained.

$$\text{Gain (db/mm)} = 8.68 \times 10^{-3} (-\alpha) \quad (6.7.13)$$

and

$$\text{Gain (db}/\lambda\text{e)} = \frac{2\pi}{\beta} \cdot \text{Gain (db/mm)} \times 10^3 \quad (6.7.14)$$

where  $k = \beta - j\alpha$  and  $\alpha$  is the metric unit.

Note that the device length of a typical Gunn device is on the order of ten microns for x - band frequencies. The operating frequency of a Gunn diode can be extended to the range of millimeter wavelength.

## 6.8 Solution of the Dispersion Characteristic Equation for Gunn Devices

The device material chosen for this analysis is GaAs. The applied electric field  $E$  is taken as  $E = 7\text{KV/cm}$ , the mobilities of the upper stream and the lower stream as  $\mu_u = 100 \text{ cm}^2/\text{v.sec}$  and  $\mu_l = 5000 \text{ cm}^2/\text{v.sec}$ , respectively and the relative dielectric constant is  $\epsilon_r = 12.5$ .

Various doping concentrations are considered in investigating the effect of various levels. The frequency dependence of the propagation constant  $\beta$  and the attenuation constant  $\alpha$  will be plotted. The drift velocities of the lower and upper stream are assumed to be  $u_{ol} = 2.2 \times 10^5 \text{ m/sec}$  and  $u_{ou} = 9 \times 10^4 \text{ m/sec}$  respectively.

### 6.8.1 Collisionless Analysis

The collision frequency of the upper valley is neglected here, considering the fact that the upper-stream density is much smaller than that of the lower stream.

The functional dependence of  $f - \beta$  are displayed in Figure 6.8.1, Figure 6.8.2 and Figure 6.8.3 for three different carrier densities  $n = 10^{13}$ ,  $10^{14}$  and  $10^{15}/\text{cm}^3$  as determined by Eq. (6.7.9) when  $v_u = 0$ . From these figures, it can be seen that four possible waves are propagating along the device. It is also noticed that the  $f - \beta$  curves are slightly shifted by carrier densities, although the wave forms remain almost the same.

100



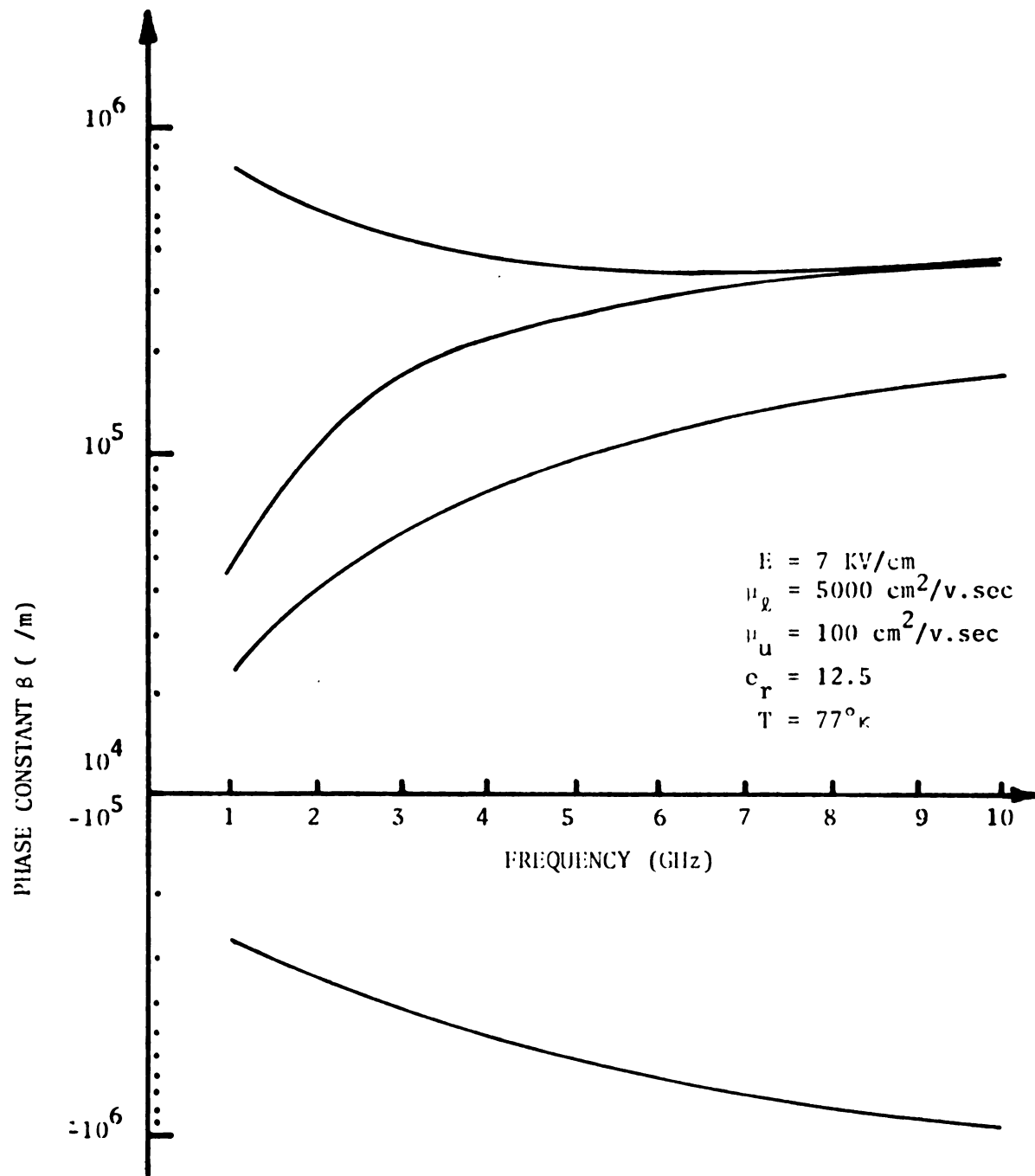


Figure 6.8.1 F- $\beta$  diagram of four waves for a  $n=10^{13}/\text{cm}^3$  GaAs sample when the collision frequency of an upper stream is neglected.

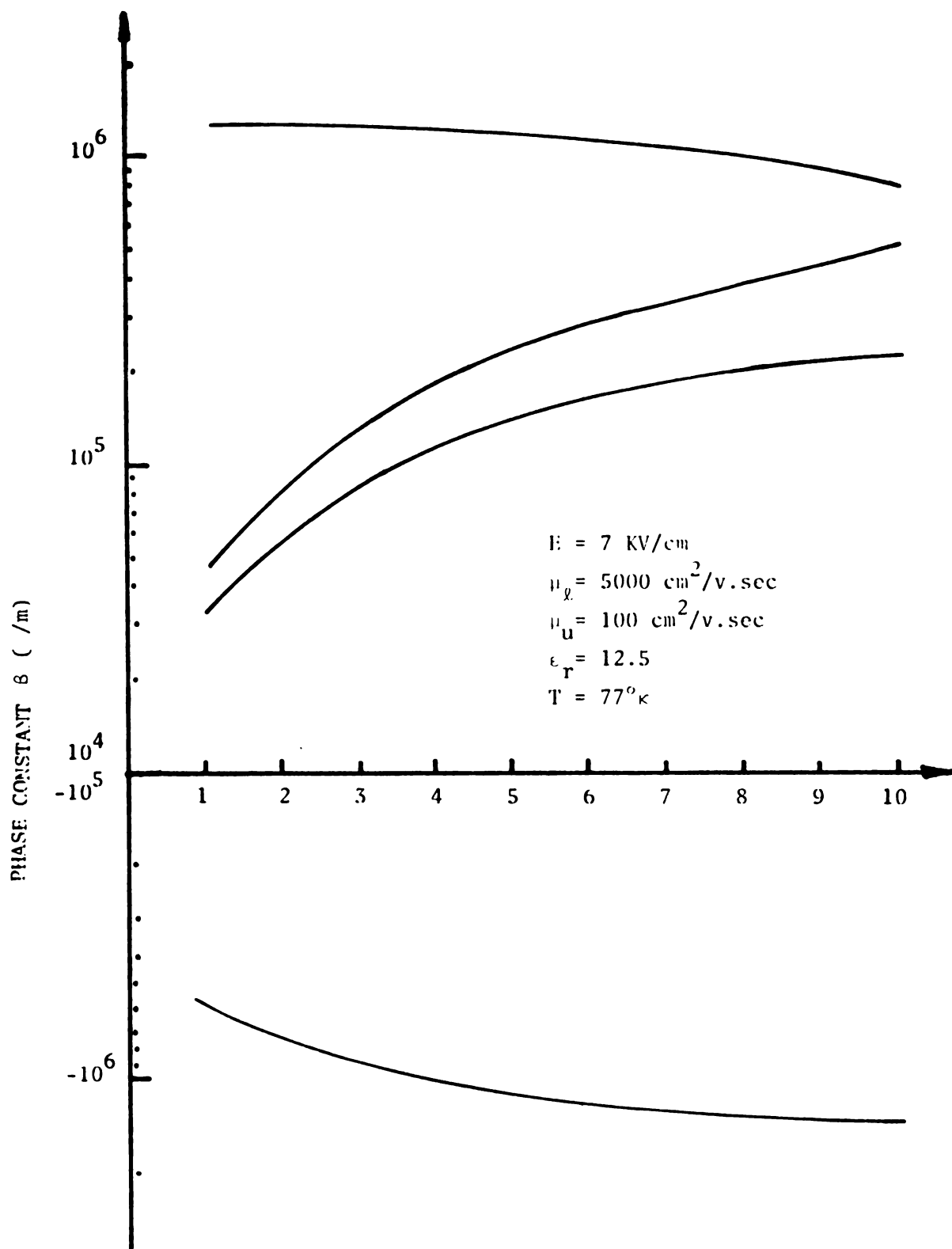


Figure 6.8.2  $f$ - $\beta$  diagram of four waves for a  $n=10^{14}/\text{cm}^3$  GaAs sample when the collision frequency of an upper stream is neglected.



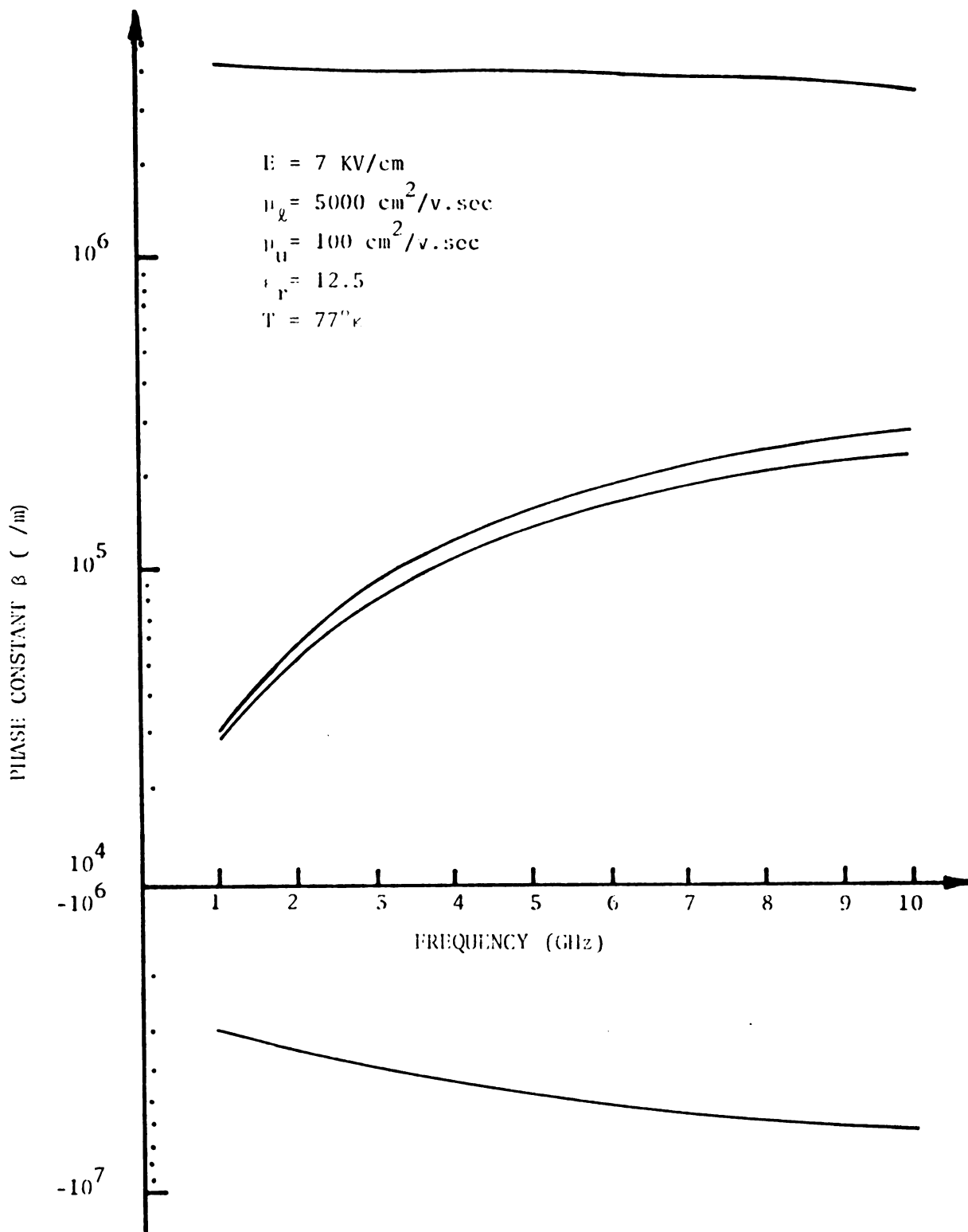


Figure 6.8.3  $\Gamma$ - $\beta$  diagram of four waves for a  $n=10^{15}/\text{cm}^3$  GaAs sample when the collision frequency of an upper stream is neglected.

In addition to the  $f - \beta$  curves the variations of attenuation constant are illustrated in Figures (6.8.4), (6.8.5), and (6.8.6). By comparing the  $f - \beta$  diagrams with the  $f - \alpha$  curves, one forward wave can be used for amplifier devices and one backward wave for oscillator devices while the other two waves drastically attenuate. The lattice temperature of semiconductor materials restrict the amplification rate of devices due to the diffusion and the collision effects, as shown in figures. The dotted line for room temperature of  $300^\circ \text{K}$  is shifted down from the liquid-nitrogen temperature line of  $77^\circ \text{K}$ .

As pointed out in connection with the solid-state traveling-wave devices, the transferred electron device also has better response of the gain at the higher frequencies.

#### 6.8.2 General Analysis

The general solution will be obtained by including the effect of collision frequencies in both the upper-and lower-valley from Eq. (6.7.9). The normalized collision frequencies at both valleys are assumed to be unity. In Figures (6.8.7), (6.8.8) and (6.8.9) the numerically computed phase constant is plotted as a function of operating frequency in the range of  $1 \sim 10 \text{ GHz}$  for three different carrier densities. Four waves correspond to the solution of fourth order equation.

As discussed earlier, the wave shapes for several doping levels are nearly identical while the phase curves are slightly shifted. Three figures are similar to the curves shown in Figures (6.8.1), (6.8.2) and (6.8.3) which were calculated by neglecting the upper-valley collision frequency.

Numerical solutions of the attenuation constant are plotted in Figures (6.8.10), (6.8.11) and (6.8.12). Seeing the possibility of

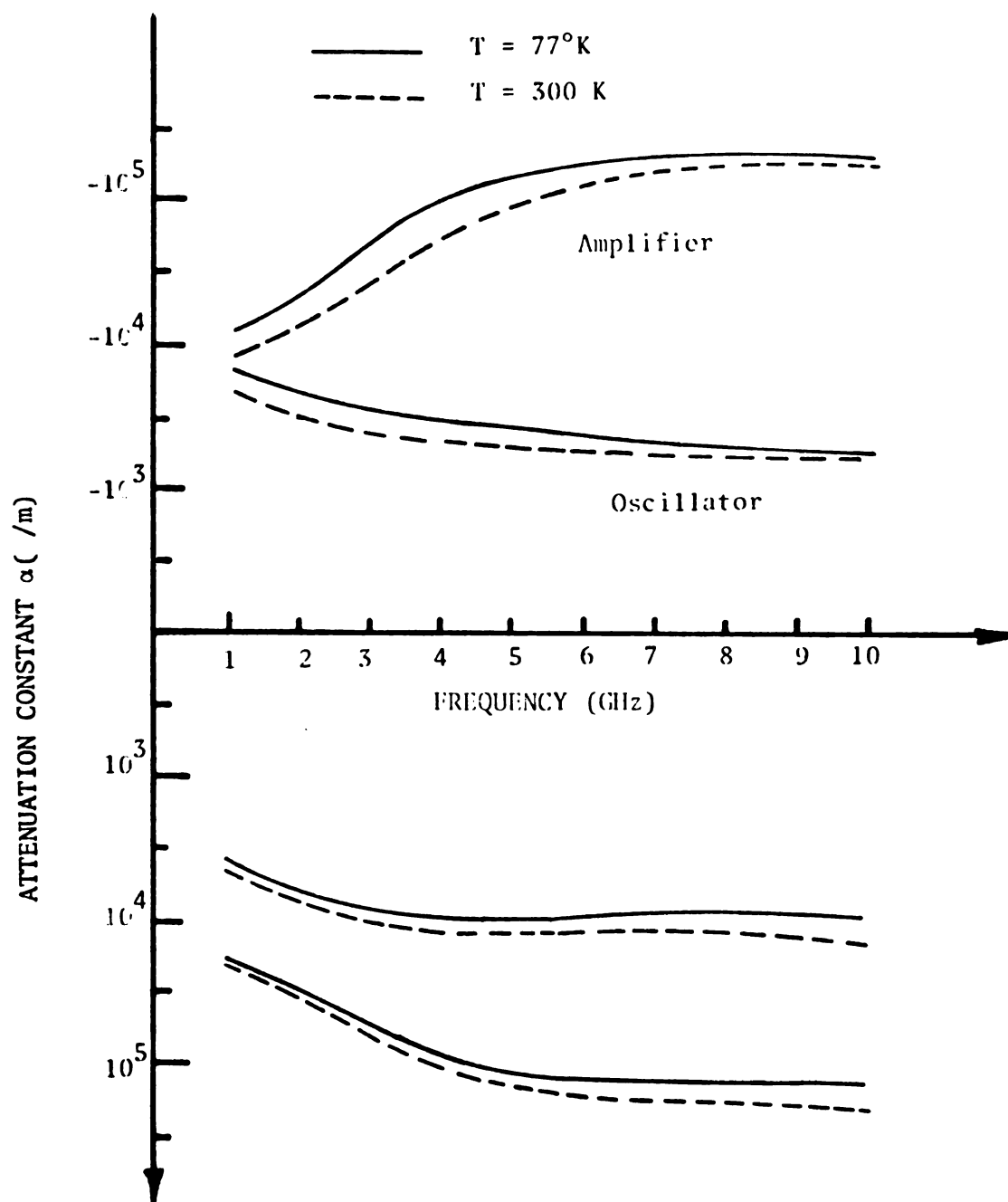


Figure 6.8.4 Variation of attenuation with frequency for four waves where  $v_c = 0$ ,  $E = 7$  KV/cm,  $\mu_d = 5000$  cm<sup>2</sup>/v.sec,  $\mu_u = 100$  cm<sup>2</sup>/v.sec,  $\epsilon_r = 12.5$ , and  $n = 10^{13}$ /cm<sup>3</sup>.

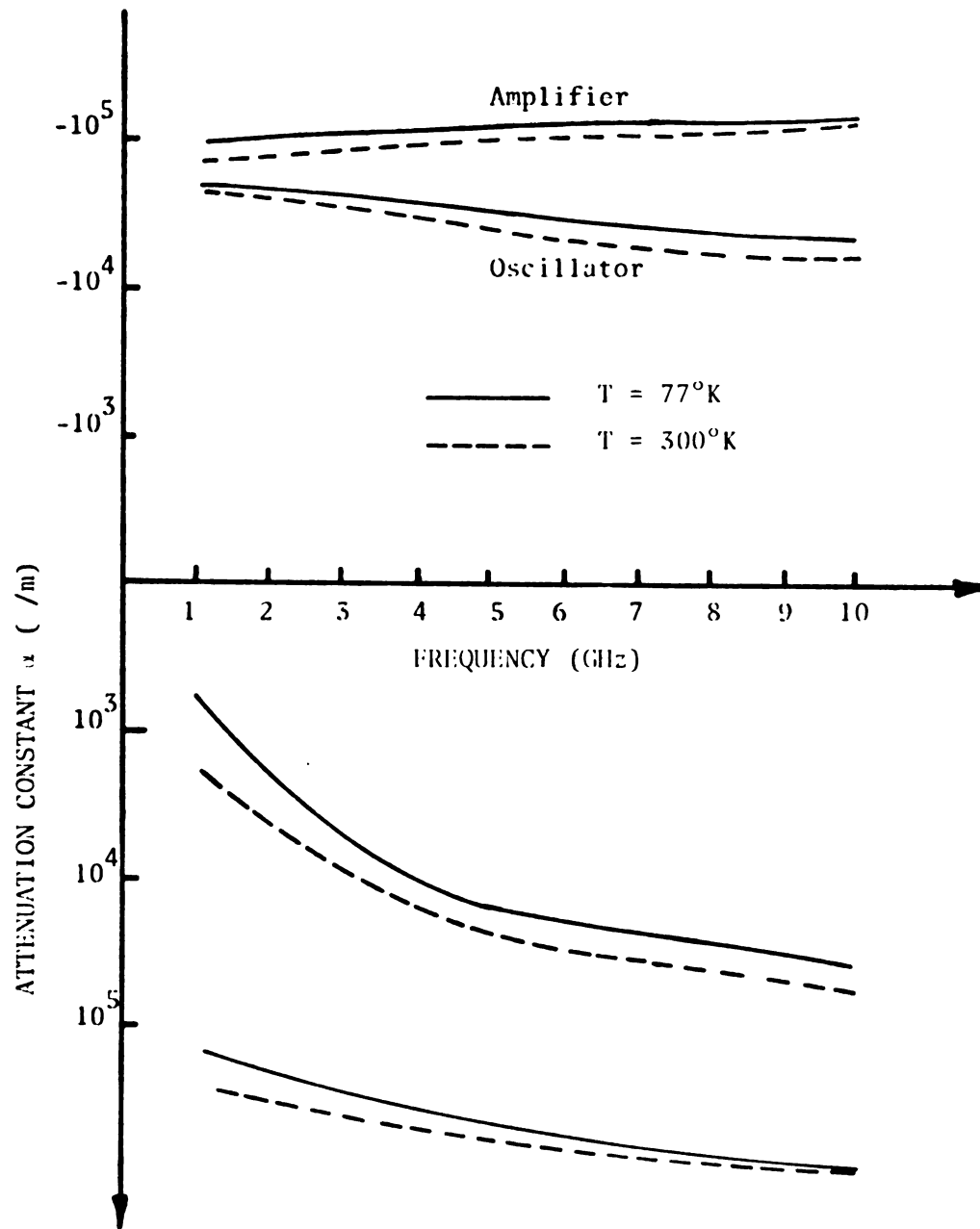


Figure 6.8.5 Attenuation vs. frequency curves of four waves where  $\epsilon_r = 12.5$ ,  $v_u = 0$ , and  $n = 10^{14}/\text{cm}^3$ .

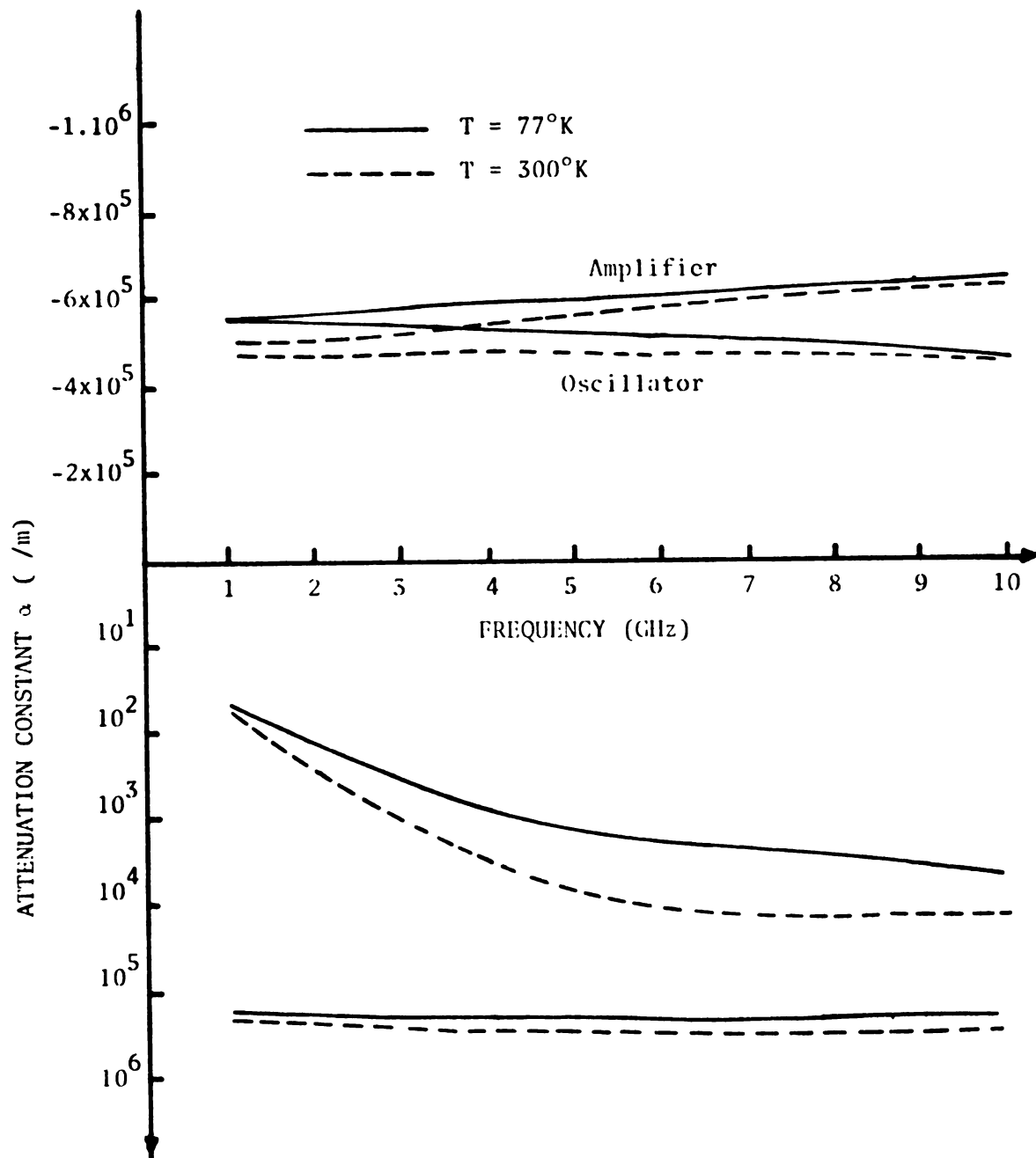


Figure 6.8.6 Attenuation vs. frequency curves of four waves where  $\epsilon_r = 12.5$ ,  $v_{ii} = 0$  and  $n = 10^{15}/\text{cm}^3$



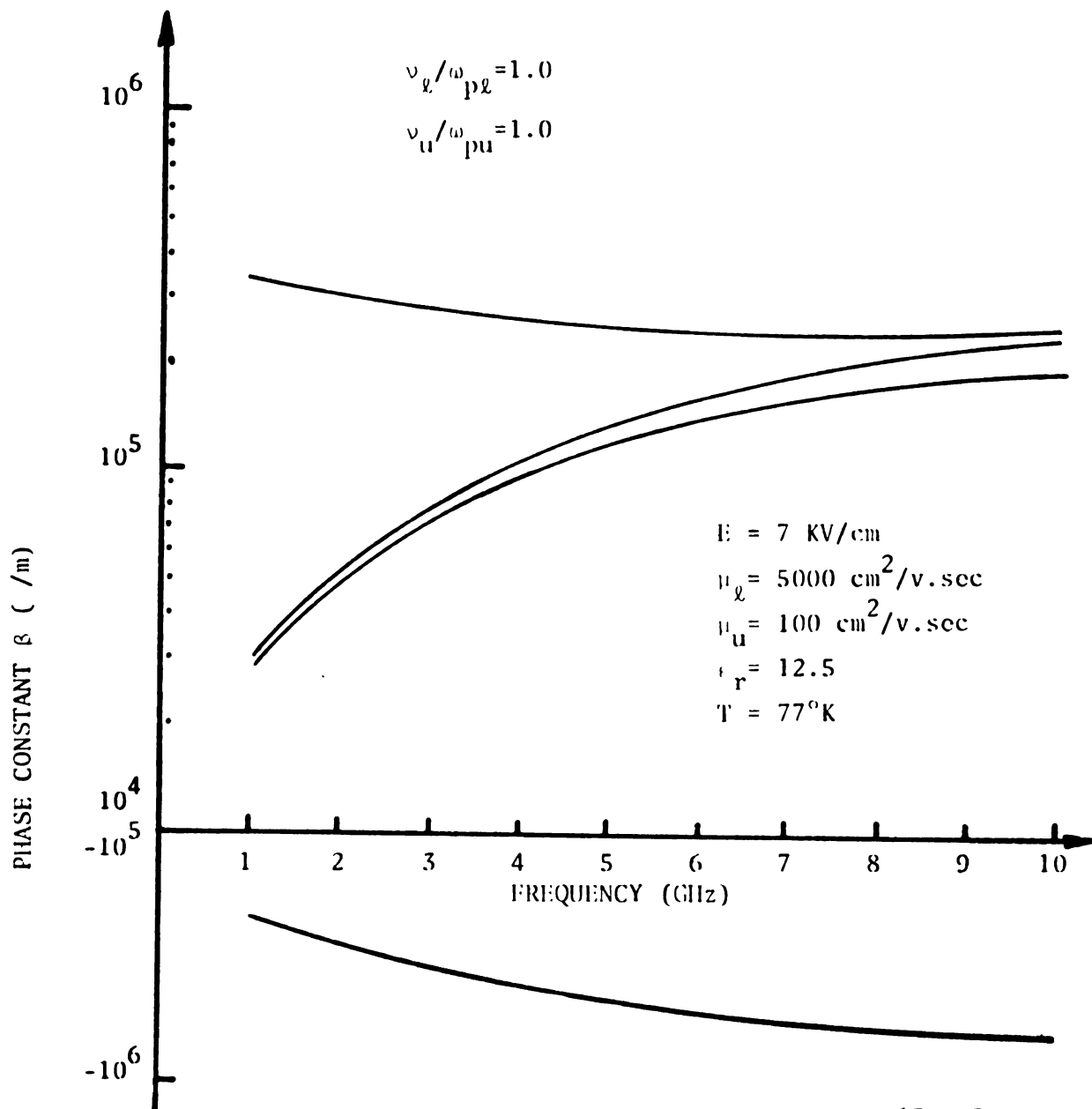


Figure 6.8.7  $f$ - $\beta$  curves of four waves for a  $n=10^{13}/\text{cm}^3$  GaAs sample when all collision frequencies are considered.

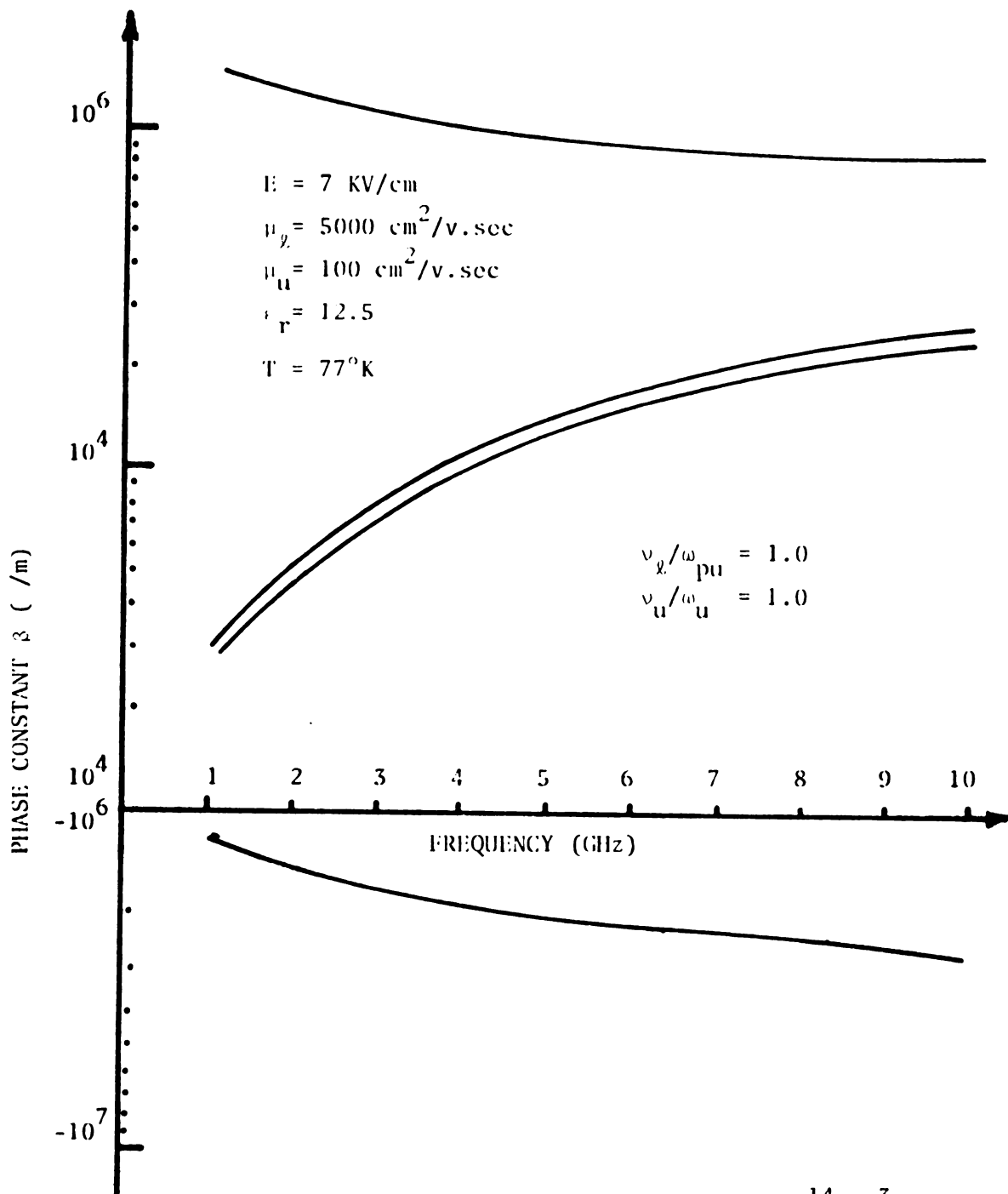


Figure 6.8.8  $f$ - $\beta$  curves of four waves for a  $n=10^{14}/\text{cm}^3$  GaAs sample when collision frequencies are considered.

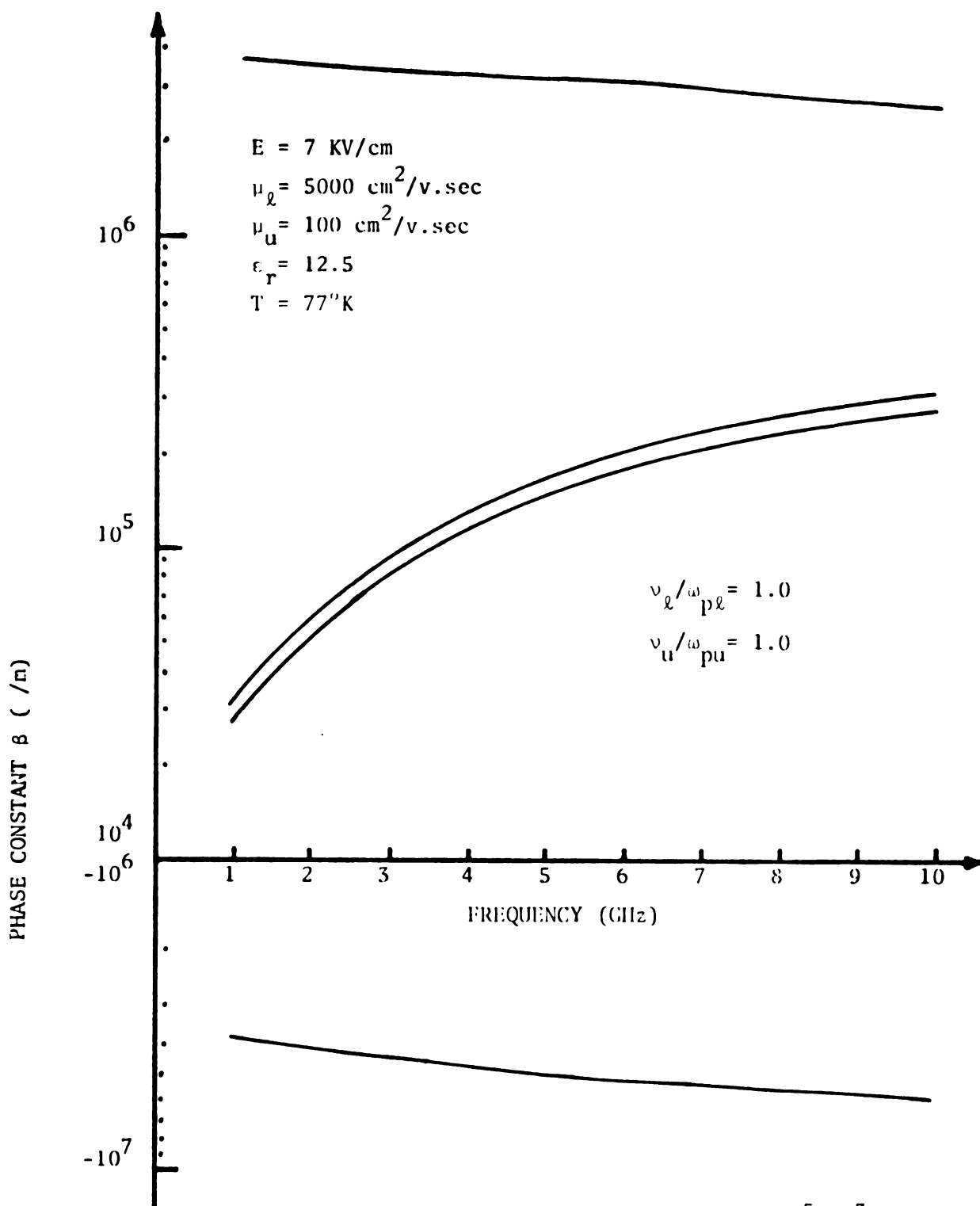


Figure 6.8.9  $f$ - $\beta$  curves of four waves for a  $n=10^{15}/\text{cm}^3$  GaAs sample when collision frequencies are considered.

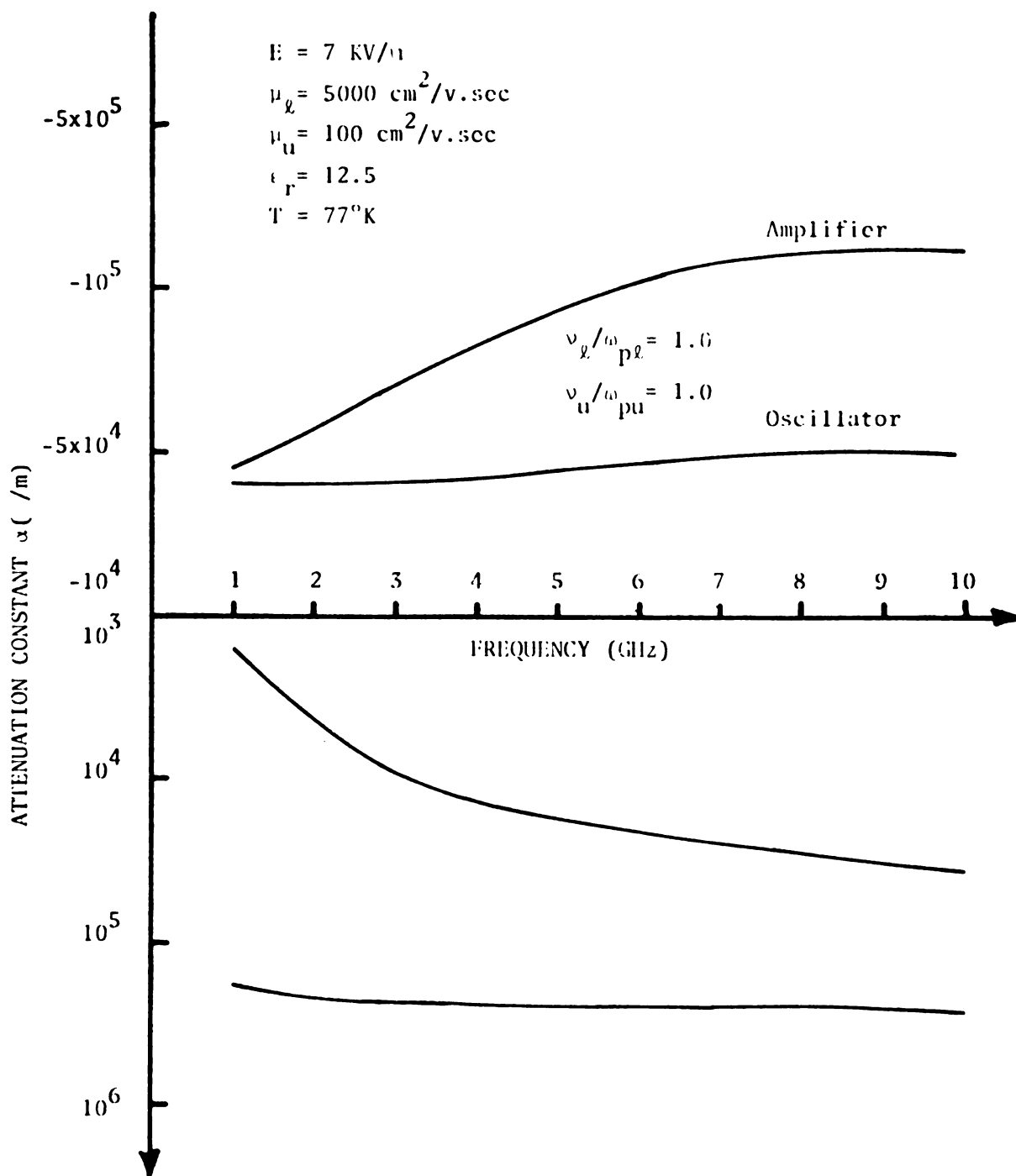


Figure 6/8/10 Variation of attenuation with frequency for a  $n=10^{13}/\text{cm}^3$  GaAs device when collisions are considered.

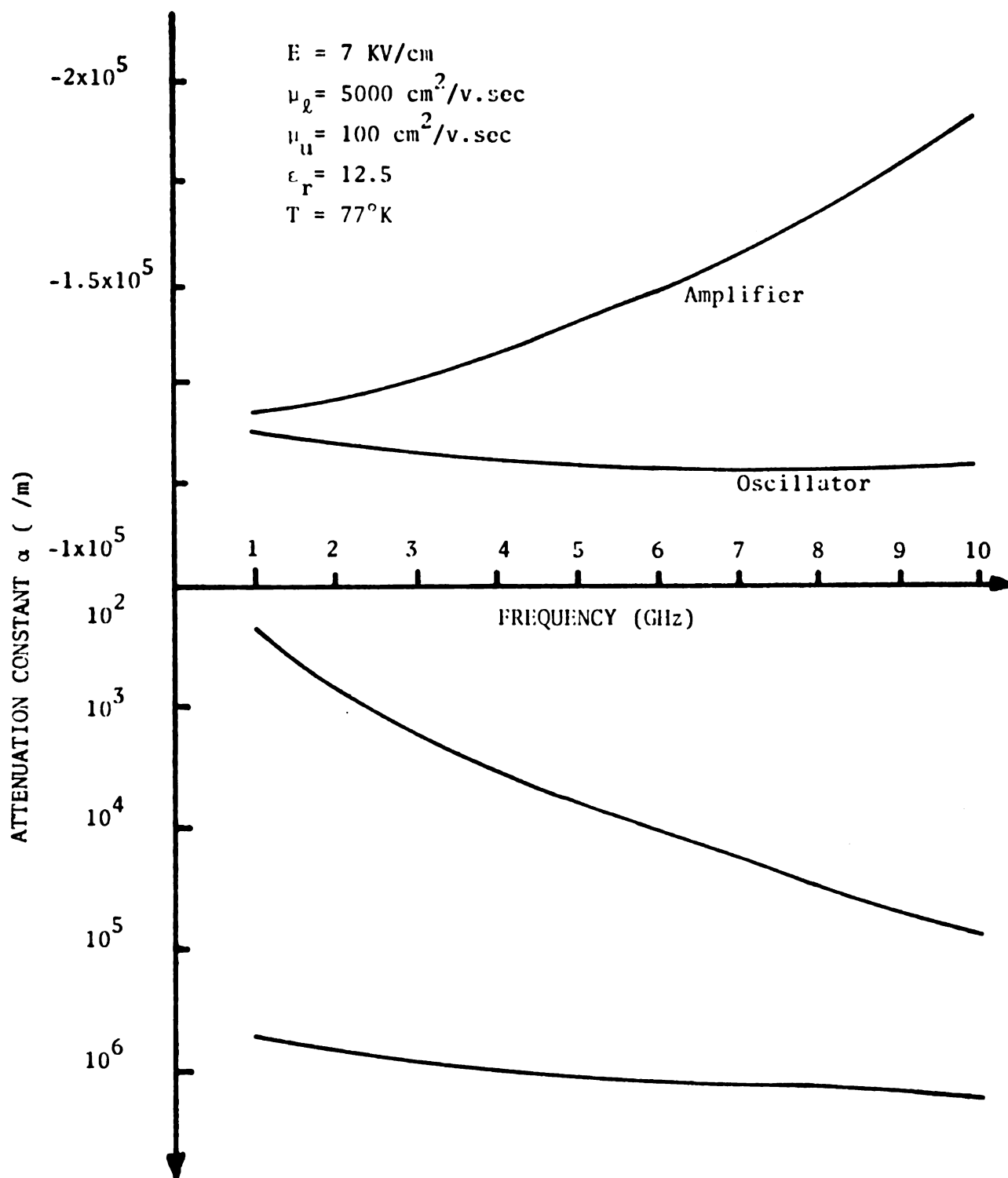


Figure 6.8.11 Variation of attenuation with frequency for a  $n=10^{14}/\text{cm}^3$  GaAs sample when the lower and upper valley collision are considered.

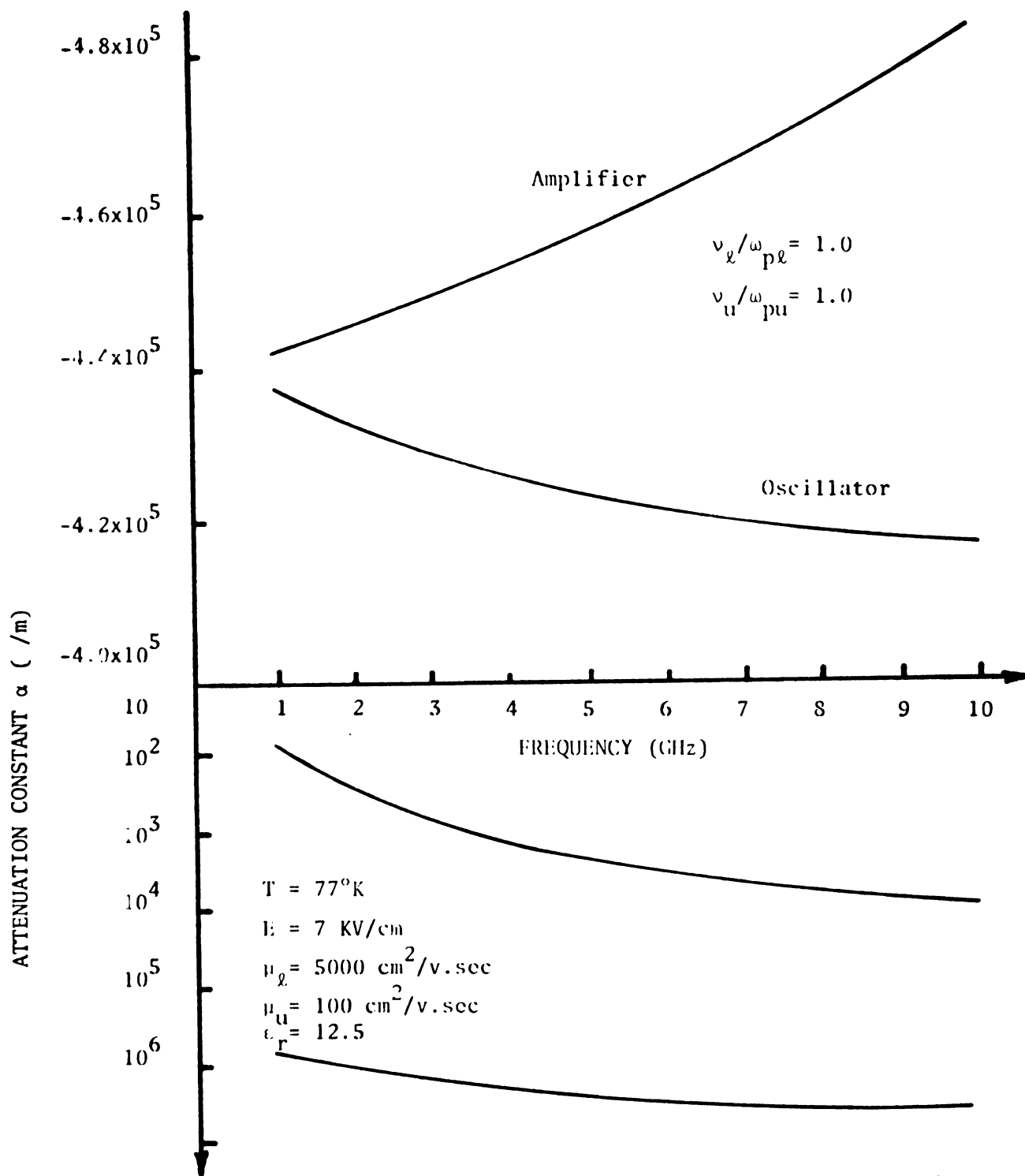


Figure 6.8.12 Variation of attenuation with frequency for  $n=10^{15}/\text{cm}^2$  GaAs device when all collisions are considered.



operating the device as either an amplifier or an oscillator, one has to investigate two curves shown in the upper quadrant. In order to find out which curve is fit for an oscillator or an amplifier - device, the dispersion curve is required to search the direction of wave propagation. In other words, the distinction between the amplifier and the oscillator can be determined from the  $\beta$  vs.  $f$  curves. Again higher carrier density sample shows higher amplification as anticipated. For oscillator devices the  $10^{13}$  and  $10^{14}/\text{cm}^3$  sample is more stable than the  $10^{15}/\text{cm}^3$  sample, while for amplifier devices the  $10^{15}/\text{cm}^3$  sample is suggested. This statement supports the basic criterion of  $n\lambda$  product described in Eq. (2.6.10).

The results of the analysis may be checked with the calculation of gain by using Eq. (6.7.13).

For a frequency of 10 GHz and an active length of approximately 15 microns, gain is calculated directly from the curve as follows:

(i)  $10^{13}/\text{cm}^3$  sample

$$\text{Gain (db/mm)} = 8.68 \times 10^{-3} \text{ } (-\infty)$$

$$\text{Gain} = \text{Gain (db/mm)} \times 15 \times 10^{-3}$$

$$\text{For amplifier: Gain} = 1.74 \times 10^3 \times 15 \times 10^{-3} = 26 \text{ db}$$

$$\text{For oscillator: Gain} = 4.68 \times 10^2 \times 15 \times 10^{-3} = 7 \text{ db}$$

(ii)  $10^{14}/\text{cm}^3$  sample

$$\text{For amplifier: Gain} = 1.86 \times 10^3 \times 15 \times 10^{-3} = 28 \text{ db}$$

$$\text{For oscillator: Gain} = 1.13 \times 10^3 \times 15 \times 10^{-3} = 17 \text{ db}$$

(iii)  $10^{15}/\text{cm}^3$  sample

$$\text{For amplifier: Gain} = 4.21 \times 10^3 \times 15 \times 10^{-3} = 63 \text{ db}$$

$$\text{For oscillator: Gain} = 3.61 \times 10^3 \times 15 \times 10^{-3} = 54 \text{ db}$$



Perlman showed [PE1] the evidence of microwave amplification experimentally with GaAs device and measured gain of the device. If a typical noise figure of 15 db for the amplifier devices, which was suggested by Perlman, is taken into consideration, the above gain calculations is in good agreement with his experimental results, which confirms the validity of this approach of analyzing transferred electron devices.

## CHAPTER VII

### DESIGN AND FABRICATION CONSIDERATIONS OF PRACTICAL DEVICES

#### 7.1 Introduction

The theoretical analysis based on the computer simulation has revealed a possibility of a high-gain solid-state amplifier in the micro-wave frequency range. Several important factors must be taken into account when the experimental device is fabricated. Of these the most important are the tape lengths, tape pitches, semiconductor materials and the slowing factor. In addition, other factors may be essential in designing and fabricating the device.

The criterion stated in Eq. (2.6.10) for wave amplification will be followed in the subsequent design procedure. Here solid-state traveling-wave amplifiers will mainly be treated.

Finally, some guidelines will be established after the design factors are qualitatively discussed.

The design of transferred electron devices is rather simpler than the solid-state traveling-wave devices. The Gunn devices are comprised of an active gallium arsenide layer, with or without a GaAs substrate, and two ohmic contacts. The thickness of the solid-state material is the major factor which determines the optimum operating frequency. The output power is a function of the cross sectional area of the wafer and the conversion efficiency. Usually the ohmic contact on the active layer is an evaporated film of silver tin alloyed in at several hundred degrees of celsius.

In designing the traveling-wave solid-state devices, extra care must be taken in selecting the slow-wave circuit and insulating layer since they are critical to the device operation. The operating frequency in Gunn devices is tuned by using waveguide techniques mechanically such as iris tuning or an adjustable short. The tuning can also be obtained electronically with the use of YIGs or varactors. However, the range of operating frequencies is limited. In solid-state traveling-wave devices the operating frequency is quite broad and generally such a tuning is not required.

## 7.2 Effect of the Insulating Layer Between Circuit and Semiconductor

The purpose of using an insulating layer between the slow-wave circuit and the semiconductor slab is to prevent a short circuit for the applied drift field.

In the capacitively coupled circuit, such a layer is not required but a similar layer must be deposited between the fingers of the slow-wave structure. As was mentioned in Section 5.7, the total gain of the device is greatly influenced by the insulating layer whose thickness, limited by integrated circuit technology, should be minimized. A thickness of 1 micron can be achieved by putting the wafer on the high-speed rotating disk but it is questionable how precise a degree of uniformity can be obtained in an average laboratory setup.

Besides the effect of the layer thickness, the dielectric constant of the insulating layer influences the circuit velocity which becomes a factor in determining the device size. The permittivity of several insulating materials are given in Table 7.2.1. As can be seen from the table, the permittivity of most materials for this type of device ranges

between 3 and 10. Fortunately, the effect of permittivities does not significantly affect the net gain.

TABLE 7.2.1  
DIELECTRIC PERMITTIVITY

Material	Dielectric permittivity	
SiO <sub>2</sub>	3	5
Alumina silitate	4.8	
Muscovite mica	7	7.3
Synthetic mica	6.3	
Alumina	8.1	10.2
Methylethacrylate	3.6	
Kodak KMER	3.8	4.5

It can be concluded that the use of high permittivity material reduces the transverse dimension of the circuit structure and hence eliminates some difficulties in the circuit fabrication. In the photo-etching process, if the tape length is too long, compared with its width dimension, the tape width lengthens into a concave form due to lense effect and results in the disconnection of the tape line.

### 7.3 Selection of Solid-state Materials

Many factors are involves in choosing an appropriate semiconductor material, which affects the performance of the solid-state traveling-wave devices. Selection of the solid-state material is basically concerned with the semiconductor losses, the carrier drift velocity and the carrier concentration density. In addition, the conversion efficiency losses, circuit losses, contact losses and transmission losses should not be overlooked. Most of these losses can be minimized if an appropriate material together with an excellent technique of fabrication is selected.

Further, cryogenic operation such as at liquid helium (4°K) or liquid nitrogen (77°K) temperature plays an important role in reducing some losses.

Solymer expressed the semiconductor loss [S01] as:

$$L_s = 4.35 \frac{\sqrt{\mu_o} \sigma_t}{\epsilon_o \sqrt{\epsilon_t}} \quad [\text{db/m}] \quad (7.3.1)$$

where  $L_s$  is the loss of semiconductor materials with relative permittivity  $\epsilon_r$ , in db per meter and  $\sigma_t$  the transverse conductivity in the presence of the applied drift electric field intensity, i.e. a material which has the characteristic of a sharp saturation, as far as the transverse conductivity is concerned. However, when  $\sigma_t$  is reduced the longitudinal conductivity is possibly reduced simultaneously in the metallurgical process and therefore extreme care must be taken in such a treatment.

Secondly, a material with high relative permittivity would give low loss, as indicated in Eq. (7.3.1). Referring to Table 5.4.1, Ge is the best, considering this aspect. For optimum operation the carrier drift velocity to the thermal ratio is 3.1 as discussed in Section 5.6. This range does not fall into that of most solid-state materials even under cryogenic operation. Therefore, the problem is in choosing a reasonable material which has a nearly close ratio and in deriving a maximum carrier drift velocity.

The carrier density or the carrier resistivity should be considered since they are related to each other. Theoretically Eq. (5.2.3) indicates that the gain is saturated at a high doping level. Due to the debunching effects of carriers in physical sense, too high doping concentration will not increase the net gain. The appropriate resistivities of semiconductor materials range from 1  $\Omega$ -cm to 20  $\Omega$ -cm.

Finally, the physical dimensions of the semiconductor wafer must be minimized to reduce the losses.

#### 7.4 Design of Slow-wave Circuit Structure

The main function of the periodic structure is to provide an adequate slowing factor of the propagating waves to match the carrier velocity in a reasonable length of structure. The slowing factor (s.f) in the construction of the slow-wave circuit is expressed by the ratio of the light velocity in the medium to the carrier drift velocity:

$$\text{s.f} = \frac{c}{\sqrt{\epsilon_r} v_g} \quad (7.4.1)$$

where  $c$  is the velocity of the light and  $v_g$  the group velocity of the circuit. The slowing factor for the traveling-wave amplifier ranges from  $10^3$  to  $10^4$ .

In selecting a slow-wave circuit, qualitative estimates of the slowing factor can be made by checking the permittivity of the medium and the drift velocity of the material. In order to overcome the difficulty in constructing such a large slowing-factor, the permittivity of the material and the carrier drift velocity should be increased. However, the drift velocity is limited and therefore increasing the medium permittivity to a maximum is desirable. Under any circumstances the slowing factor must always be large enough to make the circuit traveling-wave synchronize with the drifting carrier stream and be fairly constant over the circuit length.

Also, the complete system of the slow-wave structure should be matched to a usual transmission line over the broadest possible frequency range. A  $50 \Omega$  transmission line is commonly used for the micro-strip line structure. Here, a meander-line or a helix-tape line will be convenient to match the microstrip-line. The effect of a ground plane is negligible if the ground plane spacing is much greater than the tape spacing. If the circuit is very close to the ground, some field lines will terminate on the ground plane, and such effects must be taken into account.

The meander-tape line is shown in Figure 7.4.1. The longitudinal velocity down the tape-line is written in terms of the circuit dimensions as:

$$v_g = \frac{d+s}{h} \cdot \frac{c}{\sqrt{\epsilon_r}} \quad (7.4.2)$$

Since the dispersion curve is not generally a straight line the dispersion factor  $f_s$  also should be accounted for in an actual design. Then the slowing factor can be rewritten as:

$$s.f = \frac{h}{d+s} \cdot f_s \quad (7.4.3)$$

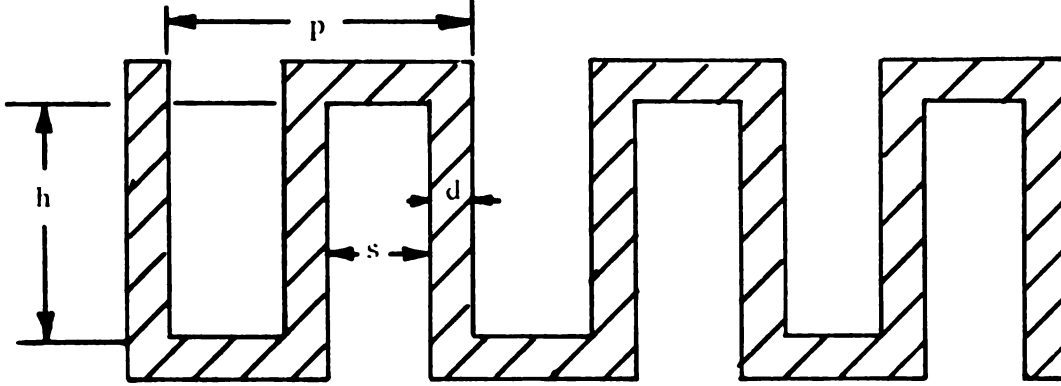


Figure 7.4.1 A meander-tape line

In practice,  $f_s$  ranges from  $1 \sim 3$  since it varies with the circuit condition. When  $s = d$ , the value of  $f_s$  is approximately 2. Furthermore, Butcher suggested that the field distribution down the tape-line is maximum when  $s = d$  and  $h = 1/4\lambda$ , where  $\lambda$  is the wavelength of the operating frequency [BU3]. From this statement the optimum relation between the tape length and the operating frequency can be obtained as:

$$h = \frac{1}{4} \frac{c}{f\sqrt{\epsilon_r}} \quad (7.4.4)$$

One more consideration is the effect of surrounding dielectric materials around the tape surfaces. When two different types of dielectric materials are used for the upper and lower surfaces of the tape-line for insulation, the effective dielectric constant can be defined by:

$$\epsilon_r = \sqrt{\epsilon_{1r} \cdot \epsilon_{3r}} \quad (7.4.5)$$

The above relation holds provided the dielectric deposition of finite regions is treated.

The connecting devices between rf connectors and the tape-line use an exponentially or linearly increasing tape until the final width of the increased sides equals that of the microstrip line.

The meander-tape line is designed in accordance with the above criteria. A design example of the meander line is given as:

Parameter	Design value
conductor thickness	$t = 2 \sim 10 \mu$
conductor width	$s = 15 \mu$
conductor spacing	$d = 15 \mu$
pitch	$p = 60 \mu$
conductor length	$h = 7500 \mu$
total width of conductor	$\ell = 1200 \mu$
material used	InSb
optimum frequency	2.5 GHZ

The above example was calculated on the basis that  $u_0 = 6 \times 10^7$  cm/sec,  $f_s = 2$ ,  $\epsilon_r = 15.7$ . Similar calculations will be done when different semiconductors are used.

### 7.5 Fabrication Considerations of Devices

The first step of constructing the slow-wave circuit consists of drafting a large scale version of the desired circuit, reducing it to a proper size by a reduction camera and etching an image of the circuit onto a piece of glass. For constructing a capacitively coupled slow-wave circuit, one side of the fingers of the meander-line is required for the first layer of deposition on the semiconductor, and then the other side of the fingers can be deposited by turning the mask glass upside down — making a complete slow-wave structure.



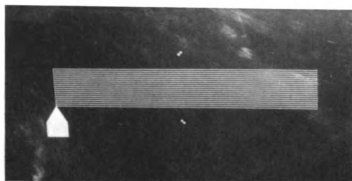
The semiconductors are cut in a (111) crystal surface orientation and polished by several grades of sandpaper on rotating disc. The possible size of the semiconductor slab of InSb is  $9 \times 3 \times 0.1 \text{ mm}^3$ . The surface damage layer is also removed by an ordinary etching technique with the solution of CP4a ( $\text{HNO}_3$ ;  $\text{CH}_3\text{CO}_2\text{H}$ ;  $\text{HF} = 5:3:3$ ).

The wafers are evaporated with gold of  $2 \sim 5 \mu$  thickness in a vacuum chamber. Then a uniform photoresist pattern is formed on them with Kodak Shirpley 1350. The photoresist pattern is uniformly deposited when the disc is rotating at a rate of about 3000 rpm. First meander type of circuit is manufactured by the photo etching process. To make a capacitively coupled meander circuit, some dielectric material (mica,  $\text{SiO}_2$  or Kmer) is deposited on the first type of fingers. The thickness of the dielectric material is approximately one-half to one micron, which gives  $C = .02 \sim .05 \text{ PF/sq.mil}$ .

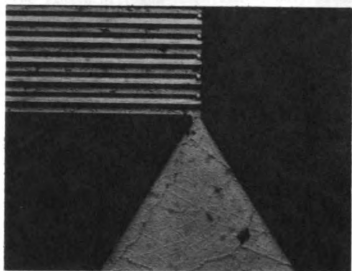
Another gold evaporation is made to form the other side of the meander circuit. Such structure can be made from two metal layers of overlapping bars separated by the dielectric material. Actually three layers are deposited successively with the metal layers being etched after deposition. One side of the circuit pattern is shown in Figure 7.5.1a and the small portion of the complete circuit is taken by the enlargement of a microscope as shown in Figure 7.5.1b.

A final assembly of the wafer is connected through a commercial microstrip line with  $50 \Omega$  OSM fixture. The circuit is then placed onto the middle part of the wafer to make carriers flow parallel to the direction of slow-wave propagation. The substrate under the wafer is made by alumina. One of the final test structures is presented in Figure 7.5.1c.

(a)



(b)



(c)

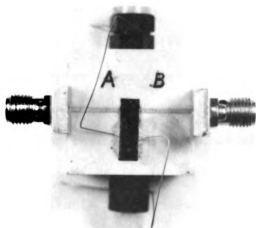


Fig 7.5.1 Slow-wave circuit and test structure of a solid-state traveling-wave amplifier. (a) One side of the meander circuit. (b) A small portion of the complete circuit after fabrication. (c) A final assembly of the test structure.

To establish the optimum drift field ohmic contacts at both ends of the wafer are formed by evaporating a film of silver tin which is alloyed in at 600 degrees celsius. Indium ohmic contacts may be substituted at both ends of semiconductor.

Unfortunately fabricated samples of the InSb, Ge and Si did not give qualitatively reasonable results as anticipated from the theoretical analysis. Under the liquid nitrogen temperature, only several dbs of electronic gain have been recorded. Physically, the result showed the evidence of coupling between rf circuit waves and carrier waves in the circuit. For better results several carefullness should be taken into account and they will be outlined..

Sandpaper polishing is not adequate for this type of device which requires a high degree of precision. The rough surfaces might be resulted in non-uniform circuit and be broken at several places. The input impedance will be high at most frequencies — making a highly mismatched circuit. However, minor circuit imperfections are unavoidable. The other factor comes from point contacts for the drift field, which make a weak coupling of a carrier stream with the rf wave, since the point contact induces the carrier waves along a thin line between two contacts. For a stronger coupling the contacts of dc potential would be better extended — covering the contact surfaces with silver plates.

Practically, regardless of design or preciseness of fabrication technique, it is almost inevitable in the laboratory to expect a flat and ideal characteristics without the accompanying reactive component. Reactive effects are largely associated with the gap and tape widths, connections of the system and discontinuity at the junction, with additional reactance being due to the capacitively coupling of the

meander-tape line in the original design. However, some reactive elements can be eliminated by adjusting the input and output double-stub tuners. To improve the mismatch, an additional modification of the device circuit is suggested. The modification might be made by utilizing a tapered region at each end of the meander line. The tapering raises the impedance of the line to a nominal value close to 50 ohms and further reduces the dispersion in the end regions; thus the impedance is nearly constant over the operating frequency. This technique can be employed empirically.

## CHAPTER VIII

### CONCLUSIONS AND SUGGESTIONS FOR FURTHER DEVELOPMENT

The purpose of this study is to investigate the carrier wave interactions in solids. Two types of interactions are considered: the first type of interaction is between the carrier wave in solids and the circuit wave propagating along the surface of the solids, and the second type of interaction is due to carrier waves in two adjacent streams propagated in the same direction.

In these analyses, the effect of lattice vibrations in solids are taken into account by introducing carrier effective mass and thermal diffusion. The main work embodied here can be divided into three parts: theoretical analysis, computer simulation, design and fabrication considerations.

The general theory of two stream instability was developed — leading to a clearer description of Gunn devices. The dispersion and attenuation curves are presented. This two stream analysis given here was checked closely with the experimental results published recently. The results show that the gain of the interaction is proportional to the doping level of the semiconductor, which was expected since a higher power output is possible with more charged carriers taking part in the interaction. However, it is also expected that the gain will level off as the doping reaches a high level, which means the collision effect will be dominated.

Also, investigated was the second type of wave interaction due to the coupling of a drifting stream of carriers with the rf circuit

attained by evaporating gold on the solid-state materials. The slow wave circuit used was a capacitively coupled meander-tape line. Such a complicated structure is advantageous because the dc drift field will not be disturbed by the presence of the slow-wave circuit. As a result, the drift velocity of the carriers will be reasonably uniform.

A two dimensional boundary problem of slow-wave circuit has been carried out. Numerical solutions for commonly used materials such as Si, Ge, GaAs and InSb were obtained. Based upon dispersion equations, derived from the two dimensional boundary conditions, instability characteristics of carrier waves propagating along the semiconductor were obtained for continuous type of tape circuit model and capacitively coupled tape circuit model. It has been demonstrated that an optimum gain of the device is a strong function of insulating layer thickness, circuit velocity, collision frequency and carrier drift velocity. The insulating layer impairs operation drastically because the electromagnetic field of the tape line decreases rapidly in the transverse direction. The variation of the net gain as a function of circuit velocity was anticipated. It was also found that the ratio of carrier drift to thermal velocity is 3.0 for the highest attainable gain. The collision frequency dependence of the gain confirmed the Vural's hypothesis which collisions tend only to decrease the amplification.

Theoretically, traveling-wave interaction in solids shows good gain-frequency characteristics, compared to most of the classical microwave active device. This is an attractive feature for the solid-state traveling-wave amplifier device, which may be a potential application for space communication. In reality, however, the inevitable circuit loss, fabrication loss and the reduction of carrier mobility in the surface will reduce the gain significantly. Under optimum conditions, both InSb and

Ge give highest gain. Furthermore, InSb has the best velocity vs. field characteristic which is crucial in design criterion concerning device fabrication.

As has been mentioned, the device has potential possibilities in broad band high frequency operation. Therefore, solid-state devices appear promising as a means of improving the operation efficiency when considering its future applicability.

At the present stage of development a few outlines are suggested for further improvement based upon the analysis. Primarily the best result of this type of device will heavily depend upon proper design and fabrication. Further work in fabricating comparatively perfect meander circuit lines may be developed with electron-beam scanning techniques. This method will reduce the tape size in length and width, and then increase the optimum operating frequencies of the device up to nearly 40 GHz. It is also desirable to have a smoothly lapped semiconductor surface before evaporating gold for making fine circuit structure. Matching the device structure to the external circuit system is also a serious problem.

The gold bond wire technique presently used is definitely not an ideal method. The ohmic contact for the dc supply should be made as broad as the wafer in a vacuum chamber so that a uniform dc field can be established across the sample. If such a contact can be made, then a broader active region will result, which in turn will give better interaction. The group velocity of propagating carrier waves varies with operating frequencies, which means the slowing factor should be adjusted with frequencies. Therefore, a modification on the circuit part should be also developed to represent a close correlation between wave propagation and slowing factor of the circuit.

## BIBLIOGRAPHY



## BIBLIOGRAPHY

- [AI1] Aigrain, P. "Proceedings of the international conference on semiconductor physics, Prague, 1960," Czechoslovak Academy of Sciences, p. 224.
- [BA1] Bartelink, D.J. "Amplification of transverse plasma waves in bismuth," Phys. Rev. Letts., Vol. 16, No. 12, January 15, 1967, pp. 510-513.
- [BE1] Bevensee, R.M. "Electromagnetic slow wave systems," John Wiley & Sons, Inc., New York, 1964.
- [BE2] Betjemann, A.G. "On the mobility of photoexcited carriers in silicon at low temperatures," Proc. Phys. Soc., Vol. 85, 1962, pp. 149-152.
- [BI1] Birdsall, C.K. and Whinnery, J.R. "Waves in an electric stream with general admittance walls," Jour. Appl. Phys., Vol. 24, 1953, pp. 314-323.
- [BI2] Birdsall, C.K.; Brewy, G.R. and Haeff, A.V. "The resistive-wall amplifier," Proc. IRE, Vol. 41, 1953, pp. 865-875.
- [BL1] Blotekjaer, K., and Quate, C.F. "The coupled modes of acoustic waves and drifting carriers in piezoelectric crystals," Proc. IEEE, Vol. 52, 4, April, 1964, pp. 360-377.
- [BL2] Blotekjaer, K.R. "Waves in semiconductor with nonconstant mobility," Elec. Letts., Vol. 4, No. 17, August 23, 1968, pp. 347-358.
- [BL3] Blotekjaer, K.R. "Temperature effect in wave propagation on drifting carriers in semiconductors," Proc. IEEE, Vol. 55, No. 3, March, 1967, pp. 432-434.
- [BL4] Blotekjaer, K.R. "Transport equations for electrons in two valley semiconductors," IEEE trans. on Electron Devices, Vol. ED-17, No. 1, January 1970, pp. 39-47.
- [BO1] Bowers, R; Legendy, C and Rose, F. "Oscillating galvanomagnetic effect in metallic sodium," Phys. Rev. Letts., Vol. 7, No. 7, November 1961, pp. 339-341.
- [BO2] Bok, J., and Nozières, P., "Instabilities of transverse waves in a drifted plasma," J. Phys. Chem. Solids, Pergamon Press, Vol. 24, 1963, pp. 709-714.
- [BO3] Bobroff, D.L. "Independent space variables for small signal electron beam analyses," IRE Trans. Electron Devices, Vol. ED-6, January 1959, pp. 68-68.



- [BU1] Budden, K.G. "The wave-guide mode theory of wave propagation," Prentice-Hall, Inc., New Jersey, 1961.
- [BU2] Butcher, P.N., and Faucett, W. "Calculation of the velocity-field characteristic for gallium arsenide," Phys. Letts., Vol. 21, No. 5, June 15, 1966, pp. 489-490.
- [BU3] Butcher, P.N. "The coupling impedance of tape structures, Proc. IEE, Vol. 104, March 1957, pp. 177-187.
- [BU4] Burnsweig, J.; Gregory, E.H., and Wagner, R.J. "Surface wave devices applications and component developments," IEEE J. Solid State Circuits, Vol, sc-5, No. 6, December 1970, pp. 310-319.
- [CH1] Chu, L.J. and Jackson, J.D. "Field theory of traveling-wave tubes," Proc. I.R.E., Vol. 37, No. 7, July 1948, pp. 853-863.
- [CO1] Coldren, L.A., and Kino, G.S. "Monolithic acoustic surface-wave amplifier," Appl. Phys. Letts., Vol. 18, No. 8, April 15, 1971.
- [CO2] Collin, R.E. "Foundations for microwave engineering," McGraw-Hill Pub. Co., New York, 1966.
- [DE1] Dean, R.H.; Dreeben, A.B.; Kamiski, and Triano, A. "Traveling-wave amplifier using thin epitaxial GaAs layer," Elec. Letts., Vol. 6, No. 24, November 1970.
- [DE2] Dean, R.H. "Optimum design of thin-layer GaAs amplifiers," Proc. IEEE, Vol. 57, No. 7, July 1969, pp. 1327-1328
- [ED1] Edelman, Sheldon. "EBS amplifiers debut," The Elec. Engr., February 1971, pp. 52-53.
- [EN1] Engelmann, R.W.H., and Quate, C.F. "Linear or small signal theory for the Gunn effect," IEEE Trans., ED., Vol. Ed-13, No. 1, January 1966, pp. 44-52.
- [ET1] Ettenberg, M. "Gain in solid-state traveling-wave amplifiers," Proc. IEEE, Vol. 56, No. 4, April 1968, pp. 741-742.
- [FO1] Foyt, A.G., and McWhorter, A.L. "The Gunn effect in polar semiconductors," IEEE, Trans. Electron Devices, Vol. ED-13, January 1966, pp. 79-87.
- [FR1] Freeman, J.C. "Traveling-wave amplification in semiconductors, Purdue University, 1972.
- [FU1] Fujisawa, K. "Transmission line analogs and kinetic power theorems for space charge waves in semiconductors," Elect. & Comm. J., Vol 51-C, No. 5, 1968, pp. 120-127.
- [FU2] Fujisawa, K. "Wave amplification due to the coupling between space charge waves in semiconductors and a forward circuit wave," Elec. & Comm. J., Vol. 51-C, No. 5, 1968, pp. 128-133.
- [GA1] Gandhi, O.P. "A slow-wave structure at ultramicrowaves," Proc. IEEE, Vol. 51, No. 2, February 1963, p. 72.

- [GI1] Giannini, F., Ottavi, C.M., and Salsano, A. "Wave propagation in negative-conductivity media," Elec. Letts., Vol. 7, No. 3, February 11, 1971, pp. 65-66.
- [GL1] Glickman, M. and Hicinbotham, W.A. "Hot electrons in indium antimonide," Phys. Rev., Vol. 129, No. 4, February 1963, pp. 1572-1577.
- [GU1] Gunn, J.B. "Microwave oscillations of current in III-V semiconductors," Solid-State Comm., Vol. 1, September 1963, pp. 88-91.
- [GU2] Gunn, J.B. "Instabilities of current in III-V semiconductors," IBM Journal of Research and Development, Vol. 8, April 1964, pp. 141-159.
- [HA1] Harvey, A.F. "Periodic and guiding structures at microwave frequencies," IRE, Trans. MTT. Vol. MTT-8, No. 1, pp. 30-61, January 1960.
- [HA2] Haddard, G.I.; Greiling, P.T. and Schroeder, W.E. "Basic principles and properties of avalanche transit-time devices," IEEE Trans. MTT, Vol. MTT-18, No. 11, November 1970, pp. 752-772.
- [HA4] Hahn, W.C. "Small signal theory of velocity-modulated electron beams," General Elec. Rev., Vol. 33, 1939, pp. 591-596.
- [HA5] Hammer, J.M. "Coupling between slow waves and convective instabilities in solids," App. Phys. Letts., Vol. 10, No. 12, June 1967, pp. 358-360.
- [HE1] Heeks, J.S.; King, G., and Sandbank, C.P. "Transferred electron bulk effects in gallium arsenide," Elec. Comm., Vol. 43, No. 4, April 1968, pp. 334-344.
- [HI1] Hines, M.E. "Theory of space-harmonic traveling-wave interaction in semiconductors," IEEE, Trans. ED., Vol. ED-16, No. 1, January 1969, pp. 88-97.
- [HI2] Hilsum, C. "Transferred electron amplifiers and oscillators," Proc. IRE, Vol. 50, No. 2, February 1962, pp. 185-189.
- [HO1] Ho, B. "Coupled-mode description of beam-plasma interaction," Elec. Letts, Vol. 5, No. 26, December 27, 1969.
- [HO2] Ho, B., and Fanson, L. "Transmission line analogue of carrier waves in solids," Elec. Letts., Vol. 6, No. 13, June 25, 1970.
- [HO3] Ho, B. "Transmission line analogue of electron stream in solid-state plasmas," IEEE Trans. on Electron Devices, Vol. ED-17, No. 11, November 1970, pp. 1011-1013.
- [HU1] Hutson, A.R. and McFee, J.H. "Ultrasonic amplification in CdS," Phys. Rev. Letts., Vol. 7, No. 6, September 1961, pp. 237-239.

- [HU2] Hutson, A.R., and White, D.L. "Elastic wave propagation in piezoelectric semiconductors," J. Appl. Phys., Vol. 33, No. 1, January 1962, pp. 40-47.
- [HU3] Hurwitz, C.E. and McWhorter, A.L. "Growing Helical density waves in semiconductor plasmas," Phys. Rev., Vol. 134, No. 4A, May 1964, pp. 1033-1050.
- [HU4] Hutson, A.R., et. al. "Mechanics of the Gunn effect from a pressure experiment," Phys. Rev. Letts., Vol. 14, No. 16, April 19, 1965, pp. 639-641.
- [HU5] Hutter, R.G.E. "Beam and Wave electronics in microwave tubes," VanNostrand Book Co., New Jersey, 1960.
- [KI1] Kino, G.S. "Carrier waves in semiconductors I, zero temperatures theory," IEEE Trans. on Electron Devices, Vol. ED-17, No. 3, March 1970, pp. 178-191.
- [K01] Kodali, V.P. "Fundamental power/frequency limitations of microwave semiconductor devices," Elec. Letts., Vol. 4, No. 15, July 26, 1968, pp. 311-312.
- [K02] Konstantinov, O.K., and Perel, V.I. "Possible transmission of electromagnetic waves through a metal in a strong magnetic fields," Soviet Phys. JETP, Vol. 11, 1960, p. 117.
- [K03] Koechner, W. "Investigation of the two stream instability in InSb," Proc. IEEE, Vol. 53, No. 9, September 1965, pp. 1234-1235.
- [KR1] Krimholtz, R. and Matthael, G.L. "Amplification of Acoustic surface waves by means of a broad band hybrid-junction transducer and negative-resistance circuits," Elec. Letts., Vol. 7, No. 9, pp. 233-235, May 6, 1971.
- [KR2] Kromer, H. "Proposed negative mass microwave amplifier," Phys. Rev., Vol. 109, March 1958, p. 1856.
- [KR3] Kromer, H. "The physical principles of a negative mass amplifier, Proc. IRE, March 1959, pp. 397-406.
- [KR4] Kromer, H. "Theory of the Gunn effect," Proc. IEEE, Vol. 52, No. 12, December 1964, p. 1736.
- [KR5] Kromer, H. "Nonlinear space-charge domain dynamics in a semiconductor with negative differential mobility," IEEE Trans. on Electron Devices, Vol. ED-13, No. 1, January 1966, pp. 27-40.
- [LA1] Law, H.C., and Kao, K.C. "Negative differential resistance produced by joule heating in semiconductors," IEEE Trans. on Electron Devices, Vol. 17, No. 7, July 1970, pp. 562-564.

- [L01] Lonngren, K.E. "An energy relation for acoustic modes in a plasma," Proc. IEEE, Vol. 54, No. 8, August 1966, pp. 1101-1102.
- [LU1] Luukkala, M. and Kino, G.S. "Convolution and time inversion using parametric interactions of acoustic surface waves," Appl. Phys. Letts., Vol. 18, No. 9, May 1, 1971, pp. 393-394.
- [MA1] Mantena, N.R. and Wright, M.L. "Circuit model simulation of Gunn effect devices," IEEE Trans. on MTT, Vol. MTT-17, No. 7, July 1969, pp. 363-373.
- [MC1] McCumber, D.E. and Chynoweth, A.G. "Theory of negative conductance amplification and of Gunn instabilities in two valley semiconductors," IEEE Trans. on Electron Devices, Vol. ED-13, No. 1, pp. 4-21, January 1966.
- [MI1] Mizushima, Y. and Sudo, T. "Surface-wave amplification between parallel semiconductors," IEEE Trans. on Electron Devices, Vol. ED-17, pp. 541-549, July 1970.
- [MU1] Mush, T. "Amplification of waves due to electron streams," J. Phys. Soc. of Japan, Vol. 18, No. 9, September 1963, pp. 1326-1334.
- [NA1] Narayan, S.Y. and Sterzer, F. "Transferred electron amplifiers and oscillator," IEEE Trans. on MTT, Vol. MTT-18, No. 11, November, 1970, pp. 773-783.
- [NE1] Newhouse, V.L. and Freeman, J.C. "A capacity coupled meander-line for solid-state traveling-wave amplification," IEEE Trans. on Electron Devices, Vol. ED-17, No. 4, April 1970, pp. 383-384.
- [NE2] Neukermans, A. and Kino, G.S. "Measurements of velocity-field characteristics of electrons in InSb at high fields," Appl. Phys. Letts., Vol. 17, No. 3, August 1970, pp. 102-104.
- [PE1] Perlman, B.S. "CW microwave amplification from circuit-stabilized epitaxial GaAs transferred electron devices," IEEE J. Solid-State Circuits, Vol. Sc-5, No. 6, December 1970, pp. 331-337.
- [PI1] Pines, D. and Schrieffer, J.R. "Collective behavior in solid-state plasmas," Phys. Rev., Vol. 124, No. 5, December 1961, pp. 1387-1400.
- [PI2] Pierce, J.R. "Traveling-wave tubes," D. VanNostrand Co., Inc., New York, 1950.
- [RA1] Ramo, S. "Space charge waves and field waves in an electron beam," Phys. Rev., Vol. 56, 1939, pp. 276-283.
- [RE1] Reeder, T.M.; Kino, G.S., and Adams, P.L. "Enhancement of piezoelectric surface-wave coupling by thin film perturbation," Appl. Phys. Letts., Vol. 19, No. 8, October 15, 1971, pp. 179-180.
- [RI1] Ridley, B.K. and Watkins, T.B. "The possibility of negative resistance effects in semiconductors," Proc. Phys. Soc. (London) Vol. 79, August 1961, pp. 293-304.

1

- [RI2] Ridley, B.K. "Specific negative resistance in solids," Proc. Phys. Soc. (London), Vol. 82, December 1963, pp. 954-966.
- [RI3] Ridley, B.K. "The inhibition of negative resistance dipole waves and domains in n-GaAs," IEEE, Trans. on Electron Devices, Vol. ED-13, No. 1, January 1966, pp. 41-43.
- [RO1] Robson, P.N.; Kino, G.S. and Fay, B. "Two port microwave amplification in long samples of gallium arsenide," IEEE Trans. on Electron Devices, Vol. ED-14, No. 9, September 1967, pp. 612-615.
- [RU1] Ruch, J.C. and Kino, G.S. "Measurements of the velocity field characteristics of gallium arsenide," Appl. Phys. Letts., Vol. 10, No. 2, January 15, 1967.
- [SA1] Sakurai, T.; Suzuki, T., and Noguchi, Y. "Formation and properties of anodic oxide films on indium antimonide," Jap. J. Appl. Phys., Vol. 7, No. 12, December 1968, pp. 1491-1496.
- [SA2] Sasaki, A. and Takagi, T. "Conditions for amplification, oscillation in GaAs bulk semiconductors," Proc. IEEE, Vol. 54, No. 12, December 1966, pp. 2027-2028.
- [SE1] Self, S.A. "Waves on an electron beam in vacuo and in a plasma," IEEE Trans. on Electron Devices, Vol ED-15, No. 11, November 1968 pp. 889-895.
- [SO1] Solymar, L. and Ash, E.A. "Some traveling-wave interactions in semiconductors, theory and design considerations," Int. J. Electronics, Vol: 20, No. 2., 1966, pp. 127-148.
- [ST1] Sturrock, P.A. "Kinematics of growing waves," Phys. Rev., Vol. 112, No. 5, December 1958, pp. 1488-1503.
- [ST2] Steele, M.C. and Vural, B. "Wave interactions in solid-state plasmas," McGraw-Hill Book Co., New York, 1969.
- [SU1] Sumi, M. "Traveling wave amplification by drifting carriers in semiconductors," Jap. J. Appl. Phys., Vol. 6, No. 6, June 1967, p. 688.
- [SU2] Sumi, M. and Susuki, T. "Evidence for directional coupling between semiconductor carriers and slow circuit waves," Appl. Phys. Letts., Vol. 13, No. 9, November 1968, pp. 326-327.
- [TH1] Thim, H.W.; Barber, M.R.; Hakki, B.W., Knight, S. and Uenokara, M. "Microwave amplification in a dc-biased bulk semiconductor," Appl. Phys. Letts., Vol. 7, No. 6, pp. 167-168, September 15, 1965.
- [TO1] Tosima, S. and Hirota, R. "New type of two-stream plasma instability," J. Appl. Phys., Vol. 34, No. 10, October 1963, pp. 2993-2996.



- [TU1] Turner, C.W. and Weller, K.P. "DC flow considerations for cross-field acoustic amplifiers and other solid-state traveling-wave devices," IEEE Trans. on Electron Devices, Vol. ED-16, No. 9, September 1969, pp. 787-797.
- [VU1] Vural, B. "Streaming instabilities in solids and the role of collisions," IEEE Trans., ED-13, No. 1, pp. 57-63, January 1966.
- [VU2] Vural, B. and Bloom "Small-signal power flow and energy density for streaming carriers in the presence of collisions," IEEE, Trans. on Electron Devices, Vol, ED-14, No. 7, July 1967, pp. 345-349.
- [WH1] White, D.L. "Amplification of ultrasonic waves in piezoelectric semiconductors," J. Appl. Phys., Vol. 33, No. 8, August 1962, pp. 2547-2554.
- [WH2] White, R.M. and Voltmer, F.W. "Direct piezoelectric coupling to surface elastic waves, Appl. Phys. Letts, Vol. 7, No. 12, December 15, 1965, pp. 314-136.

## APPENDICES

## APPENDIX A

### PROOFS OF WAVE THEOREMS IN THE PERIODIC STRUCTURE

#### A.1 Floquet's theorem

The theorem is true whether or not the structure contains losses as long as it is periodic. If the wave function  $e^{j(\omega t - kz)}$  is assumed for the solution of wave propagation, the electric or magnetic field is written as

$$\vec{A}(x, y, z, t) = \vec{A}(x, y, z) e^{j(\omega t - kz)} \quad (A.1)$$

where the  $z$ -dependence in the factor  $\vec{A}(x, y, z)$  is restricted to a function with periodic translational symmetry of a period. Suppose the field at the starting point  $z_1$  is  $\vec{A}_1$ . The wave moves to  $z_2 = z_1 + p$  where  $p$  is pitch of the periodic structure such that  $fp = 1$ . Then, if  $\vec{A}_2$  is the field at  $z_2$ ,  $\vec{A}_1$  and  $\vec{A}_2$  become

$$\vec{A}_1(x, y, z, t) = \vec{A}_1(x, y, z) e^{j(\omega t - kz_1)} \quad (A.2)$$

$$\vec{A}_2(x, y, z_1 + np, t) = \vec{A}_2(x, y, z_1 + np) e^{j\{\omega t - k(z_1 + np)\}}$$

where  $n = 0, \pm 1, \pm 2, \pm 3, \dots$

From the periodic translation symmetry condition,  $\vec{A}(x, y, z_1) = \vec{A}(x, y, z_1 + np)$  which implies that:

$$\vec{A}_2(x, y, z_1 + np) = \vec{A}_1(x, y, z_1) e^{-jknp} \quad (A.4)$$

The field vector  $\vec{A}$  at two points on a periodic transmission line separated by  $n$  periods differs by the complex constant  $e^{-jkz}$ .

q.e.d.

## A.2 Power flow theorem

Consider the structure to be divided by a series of planes perpendicular to the axis spaced by the periodic distance  $p$ . These surfaces extend perpendicular to the axis to infinity for an unbounded structure or terminate on perfectly conduction boundaries if the structure is so bounded. Over these surfaces

$$\int_S \vec{E} \times \vec{H}^* \cdot d\vec{s} = 0 \quad (A.5)$$

where the superscript  $*$  denotes complex conjugate. The integral is zero on any metal boundaries where the tangential component of  $\vec{E}$  is zero or at infinity the fields fall off at least as fast as  $\frac{1}{r}$ .

Substituting Eq. (2.5.9) into Eq. (A.5), and applying the divergence theorem, one obtains

$$\begin{aligned} 0 &= \int_S \vec{E} \times (\nabla \times \vec{E}^*) \cdot d\vec{s} = \int_V \nabla \cdot [\vec{E} \times (\nabla \times \vec{E}^*)] dv \\ &= \int_V [(\nabla \times \vec{E}^*) \cdot (\nabla \times \vec{E}) - \vec{E} \cdot (\nabla \times \nabla \times \vec{E}^*)] dv \\ &= \int_V [-j\omega\mu\vec{H} \cdot (j\omega\mu\vec{H}^*) - \vec{E} \cdot (\omega^2\mu\epsilon\vec{E}^*)] dv \end{aligned} \quad (A.6)$$

Dividing the above equation by  $\omega^2\mu$  gives

$$\frac{1}{2} \int_V \frac{1}{2} \mu \vec{H} \cdot \vec{H}^* dv = \frac{1}{2} \int_V \epsilon \vec{E} \cdot \vec{E}^* dv \quad (A.7)$$

It can be seen that in the pass band the time average stored electrical energy per period is equal to the time average stored magnetic energy per period, from Eq. (A.7). Based on the statement, the wave theorem will be shown. Applying Maxwell's equations, Eq. (A.7) is rewritten as,

$$\int_V [(\nabla \times \vec{E}^*) \cdot (\nabla \times \vec{E}) - \epsilon \vec{E} \cdot (\omega^2\mu\epsilon\vec{E}^*)] dv = 0 \quad (A.8)$$

Differentiate Eq. (A.8) with respect to  $\omega$ .

$$\int_V (\nabla \times \vec{E}^*) \cdot (\nabla \times \frac{\partial \vec{E}}{\partial \omega}) dv + \int_V (\nabla \times \frac{\partial \vec{E}^*}{\partial \omega}) \cdot (\nabla \times \vec{E}) dv - \omega^2\mu\epsilon \int_V \frac{\partial \vec{E}}{\partial \omega} \cdot \vec{E}^* dv \quad (A.9)$$

Rewriting Eq. (A.9) gives

$$2 \operatorname{Re} \left\{ \int_V (\nabla \times \frac{\partial \vec{E}}{\partial \omega}) \cdot (\nabla \times \vec{E}^*) dv - \int_V \frac{\partial \vec{E}}{\partial \omega} \cdot (\nabla \times \nabla \times \vec{E}^*) dv \right\}$$

$$-2\omega\mu\epsilon \int_V \vec{E} \cdot \vec{E}^* dv = 0$$

Using vector identity  $\vec{B} \cdot \nabla \vec{A} - \vec{A} \cdot \nabla \vec{B} = \nabla \cdot (\vec{A} \times \vec{B})$ ,  $2\text{Re}\left\{\int_V \nabla \cdot \left[\frac{\partial \vec{E}}{\partial \omega} \times (\nabla \times \vec{E}^*)\right] dv\right\}$   
 $- 2\omega\mu\epsilon \int_V \vec{E} \cdot \vec{E}^* dv = 0$

and using the divergence theorem on the first term,

$$2\text{Re}\left\{\int_S \frac{\partial \vec{E}}{\partial \omega} \times (\nabla \times \vec{E}^*) \cdot d\vec{S} - 2\omega\mu\epsilon \int_V \vec{E} \cdot \vec{E}^* dv\right\} = 0 \quad (\text{A.10})$$

Neither metal walls nor surface at infinity contribute to the surface integral term, so only consider the surface integral over the two surfaces perpendicular to the axis bounding one cell of the structure.

Let subscript 1 and 2 designate the quantities at these two surfaces.

From the Floquet theorem the following relations hold:

$$\vec{E}_2 = \vec{E}_1 e^{-j\beta p} \quad (\text{A.11})$$

$$\frac{\partial \vec{E}_2}{\partial \omega} = \frac{\partial \vec{E}_1}{\partial \omega} e^{-j\beta p} - j p \frac{d\beta}{d\omega} \vec{E}_1 e^{-j\beta p} \quad (\text{A.12})$$

Separating the surface integral of Eq. (A.10) and using Eqs. (A.11)

and (A.12).

$$2\text{Re}\left\{\int_{S_1} \frac{\partial \vec{E}_1}{\partial \omega} \times (\nabla \times \vec{E}_1^*) \cdot d\vec{S}_1 + \int_{S_2} \frac{\partial \vec{E}_2}{\partial \omega} \times (\nabla \times \vec{E}_2^*) \cdot d\vec{S}_2 - 2\omega\mu\epsilon \int_V \vec{E} \cdot \vec{E}^* dv\right\} = 0$$

or

$$2\text{Re}\left\{\int_{S_1} \frac{\partial \vec{E}_1}{\partial \omega} \times (\nabla \times \vec{E}_1^*) \cdot d\vec{S}_1 + \int_{S_2} \frac{\partial \vec{E}_1}{\partial \omega} \times (\nabla \times \vec{E}_1^*) \cdot d\vec{S}_2 - j p \frac{d\beta}{d\omega} \int_{S_2} \vec{E}_1 \times (\nabla \times \vec{E}_1^*) \cdot d\vec{S}_2 - 2\omega\mu\epsilon \int_V \vec{E} \cdot \vec{E}^* dv\right\} = 0 \quad (\text{A.13})$$

Since  $\vec{S}_1$  and  $\vec{S}_2$  are in opposite directions, the first two integrals cancel

out. From Eqs. (A.11) and (A.12)  $\vec{E}_1 \times (\nabla \times \vec{E}_1^*) = \vec{E}_2 e^{j\beta p} \times (\nabla \times \vec{E}_2^*)$

$$e^{-j\beta p} = \vec{E}_2 \times (\nabla \times \vec{E}_2^*)$$

Then Eq. (A.13) is rewritten as:

$$2\text{Re}\left\{-j p \frac{d\beta}{d\omega} \int_S \vec{E}_2 \times (j\omega\mu\vec{H}_2^*) \cdot d\vec{S}_2\right\} = 2\omega\mu\epsilon \int_V \vec{E} \cdot \vec{E}^* dv$$

$$2\omega\mu\epsilon \int_V \vec{E} \cdot \vec{E}^* dv \quad (\text{A.14})$$

1

Multiplying Eq. (A.14) by  $\frac{1}{4\omega\mu} \frac{d\beta}{d\omega}$  and applying Eq. (A.7) leads to:

$$\frac{1}{2} \operatorname{Re} \int_{S_2} \vec{E} \times \vec{H}^* \cdot d\vec{S}_2 = \frac{1}{2} \frac{1}{p} v_g \int_v \left( \frac{1}{2} \epsilon \vec{E} \cdot \vec{E}^* + \frac{1}{2} \mu \vec{H} \cdot \vec{H}^* \right) dv \quad (\text{A.15})$$

where

$$v_g = \frac{d\omega}{d\beta} = \text{group velocity} \quad (\text{A.16})$$

which shows the main wave theorem.

q.e.d.

APPENDIX B

TABLE OF ELECTROMAGNETIC FIELD SOLUTIONS FOR ALL REGIONS

Region	Cases	TM Modes	TE Modes
Solid-state Region	General	$E_{1z} = A(e^{ax} + e^{-bx})e^{j(\omega t - kz)}$ $E_{1x} = \frac{jk}{a} \left[ e^{ax} + \frac{(ab(1-j\frac{1}{q}) - \frac{1}{2})}{a^2 - j\frac{b}{q}} e^{bx} \right] e^{j(\omega t - kz)}$ $H_{1y} = \frac{j\omega\epsilon_0}{\omega - \omega_p} \left[ \frac{(a^2 - k^2) - \frac{1}{2}(b^2 - k^2)}{a^2 - j\frac{b}{q}} e^{ax} + \frac{1}{2} e^{bx} \right] e^{j(\omega t - kz)}$	$E_{1y} = [C e^{ax}] e^{j(\omega t - kz)}$ $H_{1x} = \left[ -\frac{C}{k} \frac{a^2}{\omega} e^{ax} \right] e^{j(\omega t - kz)}$ $H_{1z} = \left[ \frac{jC}{\omega} \frac{a^2}{\omega} e^{ax} \right] e^{j(\omega t - kz)}$
	$\omega = \omega_0$	$E_{1z} = A_1 (e^{a_1 x} + e^{-b_1 x}) e^{j(\omega t - kz)}$ $E_{1x} = \frac{jk}{a_1} \left[ e^{a_1 x} + \frac{a_1 b_1 (1-j\frac{1}{q_1}) - \frac{1}{2}}{a_1^2 - j\frac{b_1}{q_1}} e^{-b_1 x} \right] e^{j(\omega t - kz)}$ $H_{1y} = \frac{j\omega A_1}{a_1} \left[ \frac{\omega^2}{\omega - \omega_0} e^{a_1 x} - \frac{j\omega \omega_0}{\omega(\omega - \omega_0 - j\frac{\omega_0^2}{2D})} e^{-b_1 x} \right] e^{j(\omega t - kz)}$	$E_{1y} = [C_1 e^{a_1 x}] e^{j(\omega t - kz)}$ $H_{1x} = \left[ -\frac{C_1}{k} \frac{a_1^2}{\omega} e^{a_1 x} \right] e^{j(\omega t - kz)}$ $H_{1z} = \left[ \frac{jC_1}{\omega} \frac{a_1^2}{\omega} e^{a_1 x} \right] e^{j(\omega t - kz)}$
	Collisionless ( $\nu=0$ )	$E_{1z} = [A_2 e^{a_2 x}] e^{j(\omega t - kz)}$ $E_{1x} = \left[ \frac{jk}{a_2} e^{a_2 x} \right] e^{j(\omega t - kz)}$ $H_{1y} = \left[ \frac{j\omega A_2}{a_2} \left( 1 - \frac{\omega^2}{\omega(\omega - \omega_0)} \right) e^{a_2 x} \right] e^{j(\omega t - kz)}$	$E_{1y} = [C_2 e^{a_2 x}] e^{j(\omega t - kz)}$ $H_{1x} = \left[ -\frac{C_2}{k} \frac{a_2^2}{\omega} e^{a_2 x} \right] e^{j(\omega t - kz)}$ $H_{1z} = \left[ \frac{jC_2}{\omega} \frac{a_2^2}{\omega} e^{a_2 x} \right] e^{j(\omega t - kz)}$
Circuit Region	General	$E_{1z} = [F_2 e^{-\gamma_1 x} + F_3 e^{\gamma_1 x}] e^{j(\omega t - kz)}$ $E_{1x} = \left[ -\frac{jk}{\gamma_1} F_2 e^{-\gamma_1 x} - F_3 e^{\gamma_1 x} \right] e^{j(\omega t - kz)}$ $H_{1y} = \left[ -\frac{j\omega\epsilon_1}{\gamma_1} F_2 e^{-\gamma_1 x} - F_3 e^{\gamma_1 x} \right] e^{j(\omega t - kz)}$	$E_{1y} = [G_2 e^{-\gamma_1 x} + G_3 e^{\gamma_1 x}] e^{j(\omega t - kz)}$ $H_{1x} = \left[ -\frac{\omega_1}{2} k [G_2 e^{-\gamma_1 x} + G_3 e^{\gamma_1 x}] \right] e^{j(\omega t - kz)}$ $H_{1z} = \left[ -\frac{j\omega_1 \gamma_1}{2} (G_2 e^{-\gamma_1 x} - G_3 e^{\gamma_1 x}) \right] e^{j(\omega t - kz)}$
Circuit Region	General	$E_{1z} = [F_1 e^{-\gamma_3 x}] e^{j(\omega t - kz)}$ $E_{1x} = \left[ -\frac{jk}{\gamma_3} F_1 e^{-\gamma_3 x} \right] e^{j(\omega t - kz)}$ $H_{1y} = \left[ -\frac{j\omega\epsilon_3}{\gamma_3} F_1 e^{-\gamma_3 x} \right] e^{j(\omega t - kz)}$	$E_{1y} = [G_1 e^{-\gamma_3 x}] e^{j(\omega t - kz)}$ $H_{1x} = \left[ -\frac{\omega_3 k}{2} G_1 e^{-\gamma_3 x} \right] e^{j(\omega t - kz)}$ $H_{1z} = \left[ -\frac{j\omega_3 \gamma_3}{2} G_1 e^{-\gamma_3 x} \right] e^{j(\omega t - kz)}$

NOTE: Field solutions in solid-state region are obtained under the assumption of the thick semiconductor slab for convenience. However, these solutions are not used in the numerical analysis.



## APPENDIX C

### DERIVATION OF DISPERSION RELATION BY ADMITTANCE MATCHING METHOD

First, the admittance functions in the solid-state and the circuit regions will be obtained from solutions of coefficients inter-related in Section 4.5. The admittance functions in both spaces are connected on the boundary surface  $x = 0$  and will determine a dispersion characteristic equation of the complete coupled system.

By manipulating Eq. (4.5.11), one can find the ratio of  $B_2$  to  $B_1$ ,

$$\frac{B_2}{B_1} = \frac{a - \gamma_4}{a + \gamma_4} e^{-2a\delta} \quad (C.1)$$

In the solid-state region the general admittance function for the TE waves evaluated at the semiconductor surface  $x=0^-$  is, as the ratio of  $H_{1z}$  to  $E_{1y}$

$$Y_{TE}^S = j \frac{a}{\omega \mu_0} \cdot \frac{a \tanh a\delta + \gamma_4}{a + \gamma_4 \tanh a\delta} \quad (C.2)$$

By using Eq. (4.5.12) the corresponding admittance function for the TM waves is then, as the ratio of  $H_{1y}$  to  $E_{1z}$

$$Y^S = \frac{\epsilon_2 c_2^2}{j\omega} \cdot \frac{\frac{a^2 - k^2}{a} (1 - \Pi_2) + \frac{(a^2 - k^2) - j \frac{b^2 - k^2}{g}}{a^2 - j \frac{b^2}{g}}}{1 + \Pi_2 + \Pi_3 + \Pi_4} \quad (C.3)$$

and by simplifying

$$Y^S = \frac{j\omega \epsilon_4}{\gamma_4} \frac{N}{D} \quad (C.4)$$

where

$$N = (e^{-2a\delta} - 1) \left[ \left( h_1 + \frac{h_2}{R} \right) \cosh b\delta + \left( 2h_1 h_2 + R h_1^2 + \frac{h_2^2}{R} \right) \sinh b\delta \right] - \\ (1 + e^{-2a\delta}) (R h_1 + h_2) \sinh b\delta$$

$$D = e^{-a\delta} + (2e^{-2a\delta} - 1) \left[ \left( h_1 + \frac{h_2}{R} \right) \cosh b\delta + \left( R + \frac{1}{R} \right) \sinh b\delta \right] - (2e^{-2a\delta} + 1) [2 \cosh b\delta + (Rh_1 + h_2) \sinh b\delta]$$

Eq. (C.3) may be reduced to

$$Y^S = \frac{j\omega\epsilon_4}{Y_4} \cdot \frac{\left( h_1 + \frac{h_2}{R} \right) \cosh b\delta + R \left( h_1 + \frac{h_2}{R} + 1 \right) \sinh b\delta}{-e^{-a\delta} + \left( h_1 + \frac{h_2}{R} + 2 \right) \cosh b\delta + \left[ \left( R + \frac{1}{R} \right) + R \left( h_1 + \frac{h_2}{R} \right) \right] \sinh b\delta} \quad (C.4)$$

provided that  $a\delta \gg 1$  which is practically true.

Similarly, the admittance function of the circuit region at the boundary  $x = 0^+$  can be obtained. Accordingly, from Eqs. (4.5.33) and (4.5.34) the admittance of the circuit region is, for the TE waves,

$$Y_{TE}^C = \frac{jY_1}{\omega\mu_0} \left( \frac{a}{Y_1} \right) \frac{1 - \left( \frac{a - Y_4}{a + Y_4} \right) e^{-2a\delta}}{1 + \left( \frac{a - Y_4}{a + Y_4} \right) e^{-2a\delta}} \quad (C.5)$$

The circuit propagation constants are simplified by  $\gamma_1 \doteq \gamma_3 \doteq \gamma_4 \doteq k$  since for slow waves  $k^2 \gg \beta_1^2$ ,  $k^2 \gg \beta_3^2$  and  $k^2 \gg \beta_4^2$ . From definitions of  $a^2$  and  $b^2$  they may be approximated by  $a \doteq k$  and  $b \doteq \omega_p/v_t$  where

$$a^2 = k^2 \left[ 1 - \left( \frac{\omega}{kc_2} \right)^2 \left( 1 - j \frac{\omega_p}{\omega\omega_v} \right) \right]$$

$$b^2 = \left( \frac{\omega_p}{v_t} \right)^2 \left[ 1 + k^2 / \left( \frac{\omega_p}{v_t} \right)^2 \right]$$

The last statement can be justified as:

$$\left| \frac{\omega_p + k^2 v_t}{\omega_v} \right| \gg \left| -\omega + k u_0 \right|$$

$$\frac{\omega}{kc_2} \doteq \frac{v_{ph}}{c_2} \approx 10^{-3} \sim 10^{-4}$$

and

$$\frac{k}{\omega_p/v_t} \ll 1 \quad \text{for high doping materials}$$

With these assumptions, notice that the TE admittance in the solid-state region and circuit region are exactly the same and are not affected by the presence of either the circuit or the semiconductor, hence there is no discontinuity of the TE fields at  $x = 0$ .

The corresponding admittance function for the TM waves in the circuit region is, in straightforward manner, calculated with the coefficients solutions. At the boundary surface the admittance  $Y^c$  is

$$Y^c = \frac{j\omega\epsilon_1}{\gamma_1} \cdot \frac{\kappa_3(\Gamma_1 + \tanh \gamma_1 d) - \kappa_4(\Gamma_2 - \tanh \gamma_1 d)}{-\kappa_3(\Gamma_1 \tanh \gamma_1 d + 1) + \kappa_4(\Gamma_2 \tanh \gamma_1 d)} \quad (C.6)$$

The admittance, where the same dielectric materials surrounding the meander line are used, can be obtained from a special case of the general solution with  $\epsilon_1 = \epsilon_3$  and  $\gamma_1 = \gamma_3$ , which are reduced to

$$Y^c = \frac{j\omega\epsilon_1}{\gamma_1} \cdot \frac{-\kappa_3^0 + \kappa_4^0[(1 + e^{2\gamma_1 d})\gamma_1^2/\beta_{s1}^2 - e^{2\gamma_1 d}]}{-\kappa_3^0 + \kappa_4^0[(1 - e^{2\gamma_1 d})\gamma_1^2/\beta_{s1}^2 + e^{2\gamma_1 d}]} \quad (C.7)$$

where

$$\kappa_3^0 = \frac{\gamma_1 - a}{\gamma_1 + a} (1 - e^{-2a\delta}) \quad (C.8)$$

$$\kappa_4^0 = 1 - \left(\frac{\gamma_1 - a}{\gamma_1 + a}\right)^2 e^{-2a\delta} \quad (C.9)$$

In practice, when the device sample is fabricated it is easier either to choose a single material for the insulating layers or to leave the top region as a free space.

Eq. (C.13) can be more simplified, depending upon the following situations:

(1) Case 1:  $d = 0$

$$Y^c = \frac{j\omega\epsilon_1}{k} \cdot \left[ 2 \left(\frac{k}{\beta_{s1}}\right)^2 - 1 \right] \quad (C.10)$$

(2) Case 2:  $|\gamma_1 d| \ll 1$

For small  $x$ ,  $\exp(x) \doteq 1+x$ , then the admittance becomes

$$Y^c = \frac{j\omega\epsilon_1}{k} \cdot \frac{\beta_{s1}^2 - 2k^2(1-kd)}{2k^3d - \beta_{s1}^2} \quad (C.11)$$

(3) Case 3:  $|\gamma_1 d| \leq 1$

This case may be better approximated  $\exp(x)$  by

$$\frac{1 + \frac{1}{2}x + \frac{x^2}{12}}{1 - \frac{1}{2}x + \frac{x^2}{12}}$$

Hence the admittance is

$$Y^c = \frac{j\omega\epsilon_1}{k} \cdot \frac{2d^2k^4 + (6 - d^2\beta_{s1}^2)k^2 - 3d\beta_{s1}k - 3\beta_{s1}^2}{-6dk^3 + d^2\beta_{s1}^2k^2 + 3d\beta_{s1}k + 3\beta_{s1}^2}$$

(4) Case 4: extremely large  $\gamma_1 d$  such that  $e^{-2\gamma_1 d} \ll 1$

$$Y^c = -\frac{j\omega\epsilon_1}{k} \quad (C.13)$$

The case 4 implies that very thick thickness of insulating layer are involved, and hence there is no chance for the carriers to interact with the circuit.

The admittance of the slow-wave circuit space and the solid-state space must be connected at the interface of  $x=0$ , and thus Eqs. (C.3) and (C.6) yield the general dispersion relation.

## APPENDIX C

### THE COMPUTING METHOD FOR THE COMPLEX ROOTS OF A DISPERSION EQUATION WITH COMPLEX COEFFICIENTS

As a matter of fact, all classical methods require a large amount of skill and judgement for isolation and separation of complex roots of a polynomial equation. Quite often one encounters an unexpected difficulty in taking a root as a starting interaction solution. With these difficulties in mind Lehmer has constructed a method which can easily capture approximate locations of roots. Therefore, Lehmer's method is used to find approximate values of the roots and then the faster successive interaction by Newton - Raphson method is used to locate the roots within the specified convergence criterion.

Let a function  $P(k)$  be analytic inside and on a closed contour  $C$  except for at most a finite number of poles interior to  $C$ . Also, let  $P(k)$  have no zeros on  $C$  and at most a finite number of zeros interior to  $C$ . Then, if  $C$  is described in the positive sense, it is a well-known fact that

$$\frac{1}{2\pi j} \int_C \frac{P'(k)}{P(k)} dk = N_o - N_p \quad (D.1)$$

where  $N_o$  is the total number of zeros of  $P(k)$  inside  $C$ , a zero of order  $m_o$  being times, and  $N_p$  is the total number of poles inside  $C$  if a pole of order  $m_p$  is counted  $m_p$  times. As shown in the dispersion equation,  $N_p = 0$  and then the integral gives the number or roots for the polynomial function.

To capture a root of the polynomial  $P(k) = 0$  by Lehmer's method, first remove zero roots, c.f. flow chart,  $P(0) = 0$ . One starts with the unit circle and begin to process in double (or having) the radius at each step. Since the roots are bounded, one soon finds an annulus  $R < |k| < 2R$  where the circle of radius  $2R$  contains a root of  $P(k)$  while the inner circle is free of roots. This annulus can be completely covered by eight overlapping circles each of radius  $R_1 = 5R/6$  with centers at  $\frac{5\pi R}{3} e^{2\pi i n/7}$ ,  $(n=0(1)7)$ . Repeating the process on these circles in turn, one soon finds a circle containing a root of  $P(k)$ . This completes step 1. Calling the center of this circle  $C_1$ , one finds as before, an annulus  $R_2 < |k - C_1| < 2R_2$ , such that  $2R_2$  contains a root of  $P(k)$  but whose inner circle is free of roots. Eight smaller circles of radius  $5R_2/6$  at center  $C_2$  cover this annulus and find a circle containing a root. This completes second step.

After  $n$  steps one has a circle of radius not exceeding  $2R (5/12)^n$ , and probably smaller containing a root. This procedure gives the small roots first. In this routine one obtains roots as a first approximation, upon completion of 8 steps with Lehmer's method.

Newton-Raphson's method is applied to improve our estimation of the root obtained by Lehmer's method, Taylor series expansion is then used to a polynomial.

$$P(k+h) = P(k) + P'(k)\frac{h}{1!} + P''(k)\frac{h^2}{2!} + \dots \quad (D.2)$$

Let a root of the polynomial be  $k = k_1$ , which can be obtained by the Lehmer method. Suppose, however, that the root is actually  $k_1 + h$ . Then, in the Taylor expansion of  $P(k)$  becomes  $P(k_1+h) = P(k_1) + hP'(k_1) + \dots$  (D.3)

1000

1000

The deviation in the real root is  $h$ . If  $h$  is small,  $h$  can be written as

$$h = \frac{P(k_1)}{P^1(k_1)} \quad (D.4)$$

Then the iterated approximation to the actual root gives the general formula

$$k_{i+1} = k_i - \frac{P(k_i)}{P^1(k_i)} \quad (D.5)$$

Iteration steps will be continued until  $\text{Re}|k_2 - k_{i-1}| \leq \text{DELTA } 2$  and  $\text{Im}|k_i - k_{i-1}| \leq \text{DELTA } 2$  where  $\text{DELTA } 2$  is a permissible error which is taken  $10^{-7}$  in our computer program.

This new approximation determines one root of the polynomial and a reduced polynomial  $P_1(k) = \frac{P(k)}{k - k^1}$  is then computed and solved in the same fashion where  $k^1$  is a first root of  $p(k)$ . Continuing the procedure, all roots are finally obtained. The flow chart explaining the procedure is illustrated in Figure D.1.



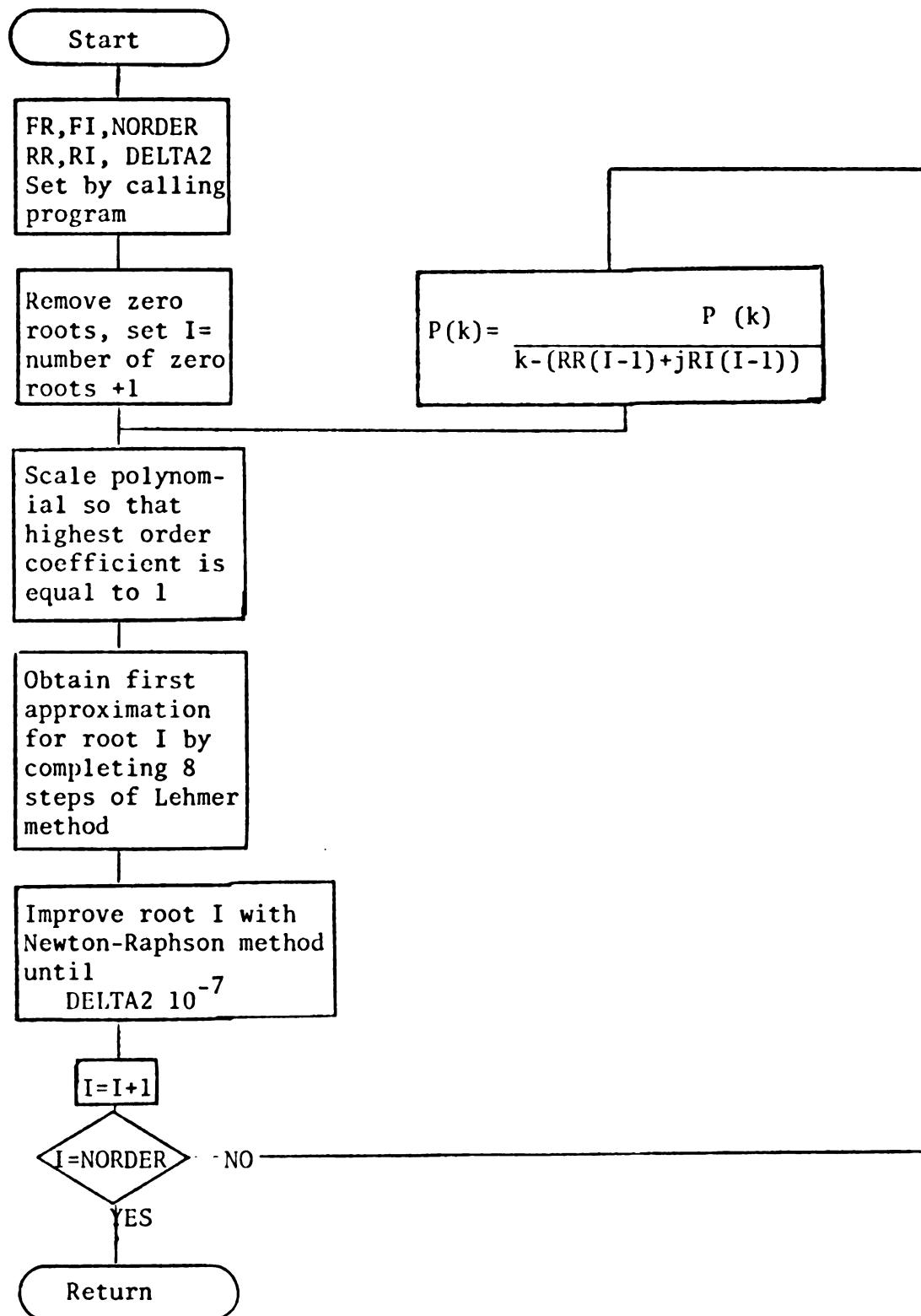


Figure D.1 Flow chart for computer solutions of a polynomial.

MICHIGAN STATE UNIVERSITY LIBRARIES



3 1293 03083 1063